Università degli Studi di Napoli Federico II

Doctoral Degree in Industrial Engineering

XXXV Cycle

PhD Thesis

ENERGY EFFICIENCY OF THE BUILDING ENVELOPE: MODELING, SIMULATION AND PERFORMANCE OF PASSIVE-ACTIVE TECHNOLOGIES FOR DOUBLE SKIN AND RESPONSIVE COMPONENTS

Doctorate Program Coordinator

Prof. Michele Grassi

Tutor

Prof. Fabrizio Ascione

Prof. Nicola Bianco

Candidate

Teresa IOVANE

Student ID: DR993904

Academic year 2021/2022

Index

Abstract

Climate change and its impacts represent the challenges of our day. Really, the climate has always changed in the history of our planet. However, the way in which it has been changing in recent decades puts us in front of a real climate crisis. Arctic sea ice reduction, sea level rise, intensification of extreme weather events, and global surface temperature rise are some of the contributing factors to the climate crisis. To date, it can be said that the anthropic greenhouse effect, which is caused by human activities, is responsible for these factors. The COVID-19 pandemic, the greatest shock of the last decades, has dispelled all doubts. The global electricity demand and the Global CO_2 emission fell due to the restrictions adopted. Nevertheless, the past showed us that the rebound in emissions may be larger than the decline with the improvement of economic conditions. For this reason, it is necessary to think more to save energy, to have circular economy and to use sources with low environmental impacts. It is necessary to implement an energy transition by moving from an energy mix based on fossil fuels to one based on renewable energies in order to achieve the goal of decarbonization and climate neutrality.

The construction sector, being energy-intensive, plays a key role in this context. To achieve the targets set at the European level, most of the built environment needs to be energetically redeveloped. Chapter 1 of this Thesis provides an excursus on the regulations adopted at International and European levels on environmental matters, highlighting the role played by the built environment and the consequent regulations issued in the field of energy efficiency in buildings.

The focus of the Thesis concerns the analysis of strategies for improving the energy performance of existing buildings. To this end, the methods for

the modeling and the simulation of the building energy performance are first described in Chapter 2 and then applied to different building types in Chapter 3. The complexity of these methods exposed first theoretically and then through examples has highlighted two aspects that have been discussed in Chapter 3. In detail, the influence of the effect of the urban context on the energy consumption of a single building is first investigated. The objective is to understand when and if it is possible to simplify the modeling phase while ensuring a high degree of reliability of the energy performance of the building obtained through dynamic simulation. Subsequently, it is proposed a novel, accurate but user-friendly tool for building modeling and energy simulation, called EMAR. This tool is aimed at professionals in the sector with the objective of simplifying the building modeling and characterization phase, carried out by defining only 63 inputs. This would avoid the use of simplified tools based on stationary/semi-stationary analyzes that compromise the accuracy of the results.

Once the context and the methods necessary for the analysis of the energy performance of a building are known, technologies for the energy renewal of the existing building environment are investigated in Chapter 4. An effective way to reduce the energy consumption of buildings, while ensuring the comfort of the occupants, is the reduction of heat transfer and losses through the building envelope and therefore the reduction of heating/cooling loads. Attention was focused on the building envelope, as it is the primary subsystem through which energy losses between internal and external environments occur. In recent years, the concept of building envelope has undergone a transformation process: from a passive element, a protective barrier to a dynamic/adaptive element capable of varying its performance as the external environmental conditions vary and at the same time able to accommodate various types of plant engineering devices and equipment. In this context, the following topics have been addressed in Chapter 4:

- a review and discussion of the most recent research on double skin facades and responsive elements for building retrofit;
- the application of passive and active technologies based on double skin facades (DSF) for the energy retrofit of existing buildings with the analysis of the obtainable advantages.

The aim of the review work is to identify recurring potentials and benefits related to the retrofit solutions discussed - such as reducing energy consumption and $CO_{2\text{-eq}}$ emissions, exploitation of renewables, and conceptual transformation of the building envelope - but also barriers and critical issues - as a risk of overheating, lower efficiency of transparent photovoltaics compared to traditional ones, high cost of reactive elements - which must be addressed and solved in the future.

With this background, the use of double skin facades as a retrofit intervention for buildings typical of the Mediterranean area is proposed and investigated in terms of energy performance. A passive configuration is first analyzed. It consists of a second skin (entirely closed, without ventilation) that wraps the building, which is usually completely glazed. Secondly, to increase the energy advantages and reduce the problems of overheating in the cavity of the DSF, a system is proposed that makes the facade itself dynamic, by means of the controlled opening of the windows of the external layer. This active/dynamic configuration is described, and the energy benefits achieved through it are evaluated.

Finally, a further aspect is discussed, which has recently become more significant in relation to energy renewal interventions. That is the importance of assessing the environmental impact of the materials used for energy renovation throughout their entire life cycle. The attention to this issue arises from a change in the relationship between the energy attributed to the operational and construction phases, following the increase in energy efficiency required by current regulations. The energy impact of different materials used for energy efficiency interventions for the building envelope, both opaque and transparent was then assessed, starting from the phase of extraction of the raw materials, to the realization of the product, to the implementation and use in the building.

CHAPTER 1

Energy and environmental issues and the role of the building sector

“Energy sector is central to efforts to combat climate change” with this incipit, the IEA (International Energy Agency) opens the report on climate change published in 2021 [1]. The increase in global surface temperature, increase in CO_2 and greenhouse gases in the atmosphere, reduction of Arctic Sea ice, loss of mass for the ice caps in Antarctica and Greenland, and rise in sea level are all related factors that contribute to global climate change [2]. The Earth's average surface temperature has increased by about 1°C since the 19th century [3]. Figure 1.1 shows the progression of changes in global surface temperature anomalies - in 5-year increments – with reference to the 1880-1884 and 2017-2021. The base period against which the changes are evaluated is that of 1951-1980.

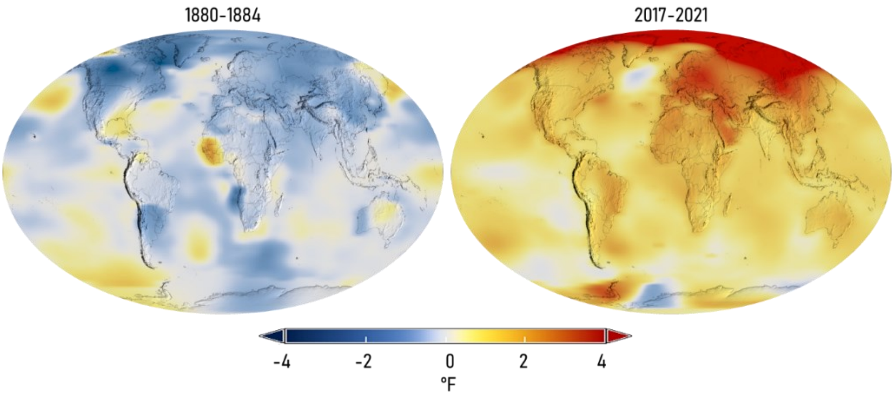

Figure 1.1: Progression of changes in global surface temperature anomalies from 1880-1884 to 2017-2021. Data from NASA Scientific Visualization Studio [4]

Considering that the temperature of the Earth's surface depends on the energy received from the Sun and on that which the planet itself radiates into space, it is deduced the direct influence of human activities on the warming of the planet. The radiated energy depends on the amount of heat-retaining greenhouse gases (GHGs) in the atmosphere. Energy use, industrial processes, agriculture, and waste treatment are responsible for releasing these gases into the atmosphere [5]. In Europe, about 77% of greenhouse gas emissions are due to energy use, and carbon dioxide accounts for about 80% of the greenhouse gases present in the atmosphere [5].

The irreversibility of the phenomena that have occurred in recent decades is pushing States, especially Europeans, to implement policies to protect the environment. The main objective is the containment of the global average temperature rise, and therefore the reduction of greenhouse gas emissions and the reduction of energy consumption from non-renewable sources.

1.1 The International and European framework

It was 1972 when an intense link between man and the environment was recognized for the first time. With the United Nations Conference on the Human Environment [6], held in Stockholm, it was recognized the need to undertake common actions to safeguard and enhance the environment and natural resources. In 1988 the Intergovernmental Panel on Climate Change (IPCC) was founded. This body periodically publishes assessment reports to understand and assess climate change, and they represent an important contribution to the adoption of global agreements. On the occasion of the 20th anniversary of the conference held in Stockholm, the United Nations Conference on Environment and Development was held in Rio de Janeiro [7], in which the rights and responsibilities of nations were defined to guarantee sustainable development. The United Nations Framework Convention on Climate

Change, defined during this conference, recognized the need to reduce greenhouse gas emissions but delegated to special conferences the possibility of setting mandatory limits for this purpose. The Kyoto Protocol of 1997 implemented this treaty and is based on the second IPCC report from 1995. This protocol set the goal of reducing polluting emissions by 5% compared to 1990 and also defined three types of countries with different responsibilities depending on the economy (developing, transition, and economically advanced). The commitments made by the post-Kyoto European States led the European Commission to approve the first strategy for climate and energy "20 20 by 2020: Europe's Climate Change Opportunity" in 2008. According to the European Environment Agency (EEA), the objectives - set a 20% reduction in greenhouse gas emissions (compared to 1990 levels), an increase in energy efficiency by 20%, and energy production from renewable sources by 20% - have been achieved [8]. To achieve the objective of reducing CO_2 emissions, Europe has introduced the Emission Trading System (ETS) tool. It is a system for the trading of emission allowances based on the "cap and trade" principle. A maximum limit is set for the emissions of pollutants, and the companies that emit these pollutants receive emission quotas (one quota is equivalent to one ton of CO_2). The recipients of this instrument are alone responsible for around 40% of the total emissions [9]. These are the sectors of industry, energy, and aviation.

In 2015, 195 countries took part in the conference of the parties (COP 21) in Paris and signed an agreement in which they commit to "Holding the increase in the global average temperature to well below 2 °C above pre-industrial levels and pursuing efforts to limit the temperature increase to 1,5 °C above pre-industrial levels" [10]. To achieve this, each party must prepare and communicate Nationally Determined Contribution (Ndc). At the same time, the 2030 climate and energy framework indicated the following objectives [11]:

- a 40% reduction in greenhouse gas emissions (compared to 1990 levels);
- energy production from renewable sources by 32%;
- an increase in energy efficiency by 32,5%.

In December 2019, the threshold for reducing emissions has raised from 40% to 55% by 2030. Indeed, the European Commission proposed a set of policy initiatives to make Europe climate neutral by 2050: the so-called “European Green Deal”. The goal is a net greenhouse gas emissions by 2050, i.e., a balance between carbon emissions and their absorption. To make this objective legally binding, the European climate law has been proposed. Subsequently a package, known as "Fit for 55", was adopted by the Commission in July 2021. It contains proposals to achieve the objectives of the Green Deal.

The International Energy Agency (IEA) has published the World Energy Outlook every year since 1998, with global energy projections and analyses by considering different scenarios. From the latest report, published in November 2021, it emerges that with the announced policy scenario, updated to the commitments established at COP 26, it would be possible to maintain the temperature increase at 1,8 °C (Figure 1.2). At the same time, however, it emerges that only with the Net Zero scenario is it possible to keep the temperature well below 2 °C, respecting the Paris agreement, and reach the goal of zero net CO_2 emissions by 2050 (Figure 1.3). The distance between the stated and announced policies and the net zero scenarios, both in terms of CO_2 emissions and temperature, highlights the need to implement stronger policies.

Figure 1.2: Temperature rise in 2100 for different scenarios [12]

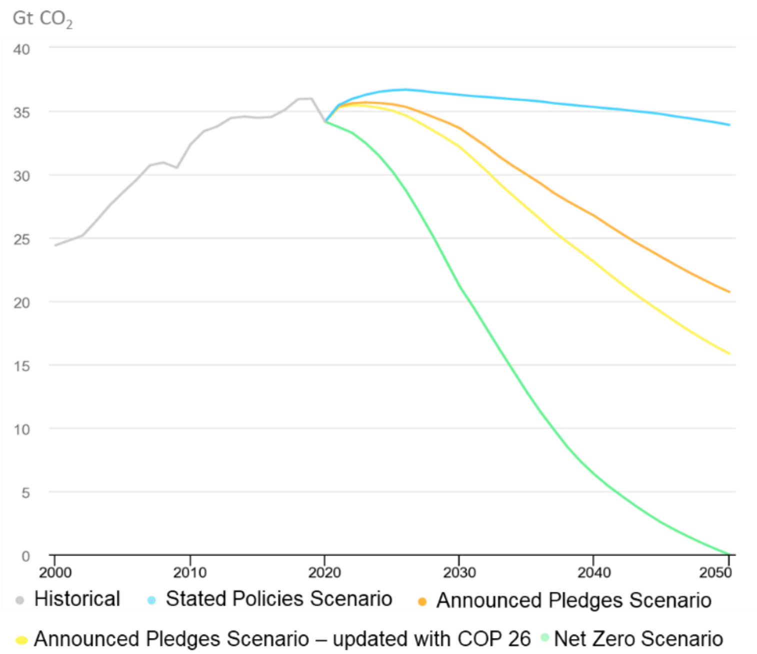

Figure 1.3: CO_2 trend for different scenarios [13]

The energy transition and decarbonization processes concern different sectors: transport, industry, construction, and agriculture. For this reason, the European Green Deal provides for initiatives aimed at each sector (Figure 1.4) in order to achieve the common objectives of sustainable development in the economic, social, and environmental fields. What is hoped for is an inclusive, "no person and no place left behind" transition, towards a clean and circular economy.

Figure 1.4: The European Green Deal [14]

This Ph.D. Thesis investigated criticalities, limits, issues and potentialities of the construction sector. In the following sections, the energy consumption, the CO_2 emissions of this sector, and the evolution of the regulatory framework in the matter of energy efficiency will be discussed.

1.2 The role of the built environment

The building sector is highly energy intensive. According to the Global Status Report for Buildings and Construction of 2021, buildings provide for 36% of global energy demand and 37% of energy-related CO_2 emissions [15].

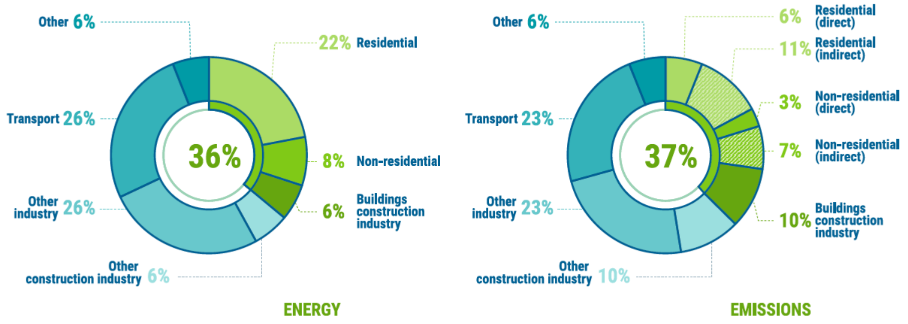

Figure 1.5: Energy consumption and emissions accounted to the construction sector [15]

The built environment features ancient and inefficient from both energy and well-being points of view. About 40% of the existing building stock was built before the adoption of any regulation in the field of energy efficiency, therefore without any thermal insulation and without complying with any energy performance obligation [16]. Considering that in 2050 about 85-95% of the present buildings will continue to exist [16], it is necessary to enhance their energy redevelopment.

Given the role played by buildings, the international and European agreements have promoted Directives to regulate the performance and the energy efficiency of buildings.

1.2.1 The evolution of the regulatory framework on the energy efficiency of buildings

The Directive 2002/91/CE, called EPBD (Energy Performance of Building Directive) was published to comply with the agreements established with the Kyoto Protocol. It was the first directive in Europe whose main objective was to improve the energy performance of buildings [17]. For this purpose, it was necessary to define a methodology for calculating the energy performance. The need to define minimum requirements for new buildings or buildings subject to major renovations was therefore indicated. In addition, Member States had to introduce energy certification for buildings and periodically inspect boilers and air conditioning systems. Then, taking into account the provisions deriving from the objectives of the package known as "20-20-20", the Directive of 2002 has been repealed and replaced by the Directive 31/2010/CE on the energy performance of buildings (EPBD Recast). The definition of minimum requirements for energy performance was extended from buildings as a whole to building elements and installed systems. It also introduced the definition of nearly zero energy building (nZEB) [18], that is a building with " nearly zero or very low amount of energy required should be covered to a very significant extent by energy from renewable sources, including energy from renewable sources produced on-site or nearby", and of an optimal level in relation to costs. In compliance with this directive, from 1 January 2021 new buildings must be nZEB. This data has been anticipated of two years for public buildings and new buildings owned or occupied by public authorities.

To ensure the achievement of the energy efficiency improvement target of 20% by 2020, the Directive 2012/27/UE on energy efficiency was published [19]. A novelty introduced by this Directive concerns buildings occupied by public bodies. According to article 5, member states must undertake to renovate 3% of the total occupied area annually.

To comply with the objectives set by the 2030 climate and energy framework, the EU Directive 2018/844 was published, amending the Directives of 2010 and 2012. This directive has set even higher objectives giving a higher priority to the energy refurbishment of the existing buildings. The average annual renewal rate of the built environment should be equal to 3%.

As part of the package of European policy initiatives, Green Deal [14] (Figure 1.4), one point is dedicated to the construction sector, "Building and renovating in an energy and resource efficient way". The different initiatives have the common goal of reducing emissions by 55% by 2030 and achieving decarbonisation by 2050. According to the IEA report "Net Zero by 2050", by 2040, 50% of existing buildings will have to be zero emissions, by 2045, 50% of the energy demand for heating will have to be met with heat pumps, and, by 2050, 85% of the built environment will have to be zero emissions [20]. This implies an enormous effort to renovate both public and private buildings. The "A Renovation Wave for Europe" strategy provides guidelines for building renovation. The goal is to at least double the annual rate of energy renewal [21]. To this end it is necessary to guarantee funding to renew in a sustainable way by integrating renewable energies and obtaining smart buildings. The European Commission has presented a recovery and resilience plan: Next Generation EU, in which a large part of the resources is reserved for the mission of green revolution and ecological transition.
The "Fit for 55" package, adopted by the European Commission in July 2021, contains proposals to achieve the 2030 goals in a fair, competitive, and environmentally friendly way [22]. Furthermore, in December 2021 the European Commission proposed a revision of the directive on the energy performance of buildings [23]. This review is necessary to align with the objectives set by the European Green Deal and the Renovation Wave strategy. It is proposed that residential buildings with the worst energy performance be brought at least to class F by 2030 and at least to class E by 2033. The "renovation passport" is introduced to plan interventions in order to increase the energy performance of buildings. New minimum performance standards are proposed for the renovation of

existing buildings, and each Member State must prepare national plans with objectives set for 2040 and 2050.
All the introduced directives have the common goal of renovating and decarbonising buildings to have a climate-neutral Europe by 2050.

1.2.2 The Italian framework

Italy, like all states belonging to the European Union, has followed EU directives, sometimes anticipating them. Indeed, it was 1976, about 25 years before the first EPBD, that Italy introduced Law 373/76 "Rules for the containment of energy consumption for thermal use in buildings". This law was upgraded by the worth L. 10/1991 and related decrees. Subsequently, Italy adapts and follows the European regulations starting from Legislative Decree 192/2005 which transposes the EPBD of 2002. Then with the Decree n.63 of 2013, the EPBD of 2010 was implemented, then converted into law by L. n.90 of 2013. In 2015, the 3 Ministerial decrees were published. These decrees define the methods for calculating energy performance and the minimum energy efficiency requirements for new buildings and those undergoing renovation. New regulations are also defined for the drafting of the energy performance certificate. Finally, the implementation of the European directive 2018/844 took place through the legislative decree n.48 of June 2020.
As part of the recovery plan envisaged by Europe to combat the economic and social crisis caused by the coronavirus pandemic, Italy has allocated 15.3 billion to energy efficiency for residential and public buildings. In 2020, Italy approved decree n.34, known as the "Recovery Decree" which introduces and regulates the subsidy known as "Superbonus 110%". With this facility, a 110% deduction of the expenses incurred for the implementation of energy efficiency interventions is obtained. The feasible interventions are divided into two categories:

- *Driving interventions*: thermal insulation of the opaque envelope, replacement of winter air conditioning systems and anti-seismic interventions.
- *driven interventions*: these are complementary to achieve e full energy efficiency and are, for instance, installation of photovoltaic systems and storage, installation of devices for recharging electric vehicles, novel windows, solar shadings and other thermal conservation and protection measures.

In order to access this tax advantage, the proposed interventions must improve the energy performance of the building by at least two energy classes.

To ensure sustainable development, in the construction sector, there are two ways to go:

- new buildings must be highly efficient, with very low energy consumption.
- existing buildings should be energy renovated.

In this Thesis the attention will be focused on the existing building stock. As previously said it is not only energetically inefficient, but also inadequate to the current requirements of thermal and acoustic comfort, healthiness and accessibility. As these buildings will continue to exist in 2050, the year by which Europe expects to achieve climate neutrality, their energy renewal is essential, also by taking into account the very poor turn-over rate of buildings in Europe (lower than 1%/yearly, about 0.6%/yearly).

CHAPTER 1 - Nomenclature

Acronyms	
CO_2	Carbon Dioxide
COP	Conference of Parties
EEA	European Environment Agency
EPBD	Energy Performance of Building Directive
ETS	Emission Trading System
EU	European Union
GHG	Greenhouse gas
IEA	International Energy Agency
IPCC	Intergovernmental Panel on Climate Change
Ndc	Nationally Determined Contribution
nZEB	nearly Zero Energy Building

CHAPTER 1 - References

[1] Climate change: https://www.iea.org/topics/climate-change. Accessed in August 2022

[2] Understanding our planet to benefit humankind: https://climate.nasa.gov/. Accessed in August 2022

[3] Global climate change: https://climate.nasa.gov/evidence/. Accessed in August 2022

[4] Global Temperature Anomalies from 1880 to 2021: https://svs.gsfc.nasa.gov/4964. Accessed in August 2022

[5] Greenhouse gas emissions by country and sector (infographic): https://www.europarl.europa.eu/. Accessed in August 2022

[6] United Nations Conference on the Human Environment, 5-16 June 1972, Stockholm: https://www.un.org/en/. Accessed in August 2022

[7] United Nations Conference on Environment and Development, Rio de Janeiro, Brazil, 3-14 June 1992: https://www.un.org/en/. Accessed in August 2022

[8] European Environment Agency - ‘Trends and Projections in Europe 2021’: https://www.eea.europa.eu/. Accessed in August 2022

[9] EU progress towards its 2020 climate change goals (infographic): https://www.europarl.europa.eu/. Accessed in August 2022

[10] Paris Agreement: https://eur-lex.europa.eu/. Accessed in August 2022

[11] 2030 climate & energy framework: https://ec.europa.eu/. Accessed in August 2022

[12] IEA, *Temperature rise in 2100, by scenario*, IEA, Paris https://www.iea.org/data-and-statistics/charts/temperature-rise-in-2100-by-scenario. Accessed in August 2022

[13] IEA, *CO2 emissions in World Energy Outlook scenarios over time, 2000-2050*, IEA, Paris https://www.iea.org/data-and-statistics/charts/co2-emissions-in-world-energy-outlook-scenarios-over-time-2000-2050-and-corresponding-global-temperature-rise-in-2100. Accessed in August 2022

[14] The European Green Deal: https://eur-lex.europa.eu/. Accessed in August 2022

[15] 2021 Global Status Report for Buildings and Construction: http://globalabc.org/. Accessed in August 2022

[16] A Renovation Wave for Europe - greening our buildings, creating jobs, improving lives: https://eur-lex.europa.eu/. Accessed in August 2022

[17] EU Commission and Parliament Directive 2002/91/EU of the European Parliament and of the Council of 16 December 2002 on the energy performance of buildings: https://eur-lex.europa.eu/. Accessed in August 2022.

[18] EU Commission and Parliament, Directive 2010/31/EU of the European Parliament and of the Council of 19 May 2010 on the energy performance of buildings (EPBD Recast): https://eur-lex.europa.eu/. Accessed in August 2022.
[19] Directive 2012/27/EU of the European Parliament and of the Council of 25 October 2012 on energy efficiency, amending Directives 2009/125/EC and 2010/30/EU and repealing Directives 2004/8/EC and 2006/32/EC: https://eur-lex.europa.eu/. Accessed in August 2022.
[20] IEA (2021), Net Zero by 2050, IEA, Paris https://www.iea.org/reports/net-zero-by-2050. Accessed in August 2022.
[21] A Renovation Wave for Europe - greening our buildings, creating jobs, improving lives: https://eur-lex.europa.eu/. Accessed in August 2022.
[22] 'Fit for 55': delivering the EU's 2030 Climate Target on the way to climate neutrality: https://eur-lex.europa.eu/. Accessed in August 2022.
[23] Proposal for a Directive of the European Parliament and of the Council on the energy performance of buildings (recast): https://eur-lex.europa.eu/. Accessed in September 2022.

CHAPTER 2

Methods for modeling and simulating of building energy performance

The American Society of Heating, Refrigerating and Air-Conditioning Engineers (ASHRAE) defines the building as “a structure wholly or partially enclosed within exterior walls, or within exterior and party walls, and a roof, affording shelter to persons, animals or property” [1]. Really the building is a very complex system and its properly energy modeling and simulation is crucial to promote sustainability.

For a proper and accurate energy simulation, it is necessary to have access to information relating to the geometry of the building and its thermophysical properties, to the heating, ventilation and air conditioning (HVAC) data, to weather conditions, to the intended uses of the building with the definition of the internal loads, to the typical behaviour of the occupants, to the context in which the building is located.

The time unit in which the simulation is carried out determines a classification:

- stationary and semi-stationary energy simulation: the time unit is the heating or cooling season and the month, respectively. The model is characterized through simplified inputs in which the indoor and outdoor climatic conditions and the methods of use of the building and system are constant. The energy balance, and therefore the energy transfer, takes place between the internal and external environment (identified by fixed temperature conditions) through the wall (separation element) characterized by a constant thermal transmittance over time. It is deduced that this simulation is extremely far from the real behavior of the building, but at the same time the high level of simplicity both in the characterization of the building and in the execution means that it is implemented by professionals in the sector.

- dynamic energy simulation: the time unit, for energy balances, is the hour or a sub-hour scale. Through this type of simulation, it is possible to know the response of the building-plant system to internal and external stresses. All the information necessary for a correct description of the building can be entered as variable factors and, above all, the ability of the building to store heat (thermal inertia) is considered. This takes into account the influence of climatic parameters (temperature, solar radiation, wind, humidity), internal loads and gains, the energy stored and released by the elements of the opaque envelope and the loads of the HVAC system. The high detail of the results of the building's energy performance, however, requires in-depth knowledge of all the phenomena underlying the behavior of the building itself and extremely detailed modelling.

A robust and successful design of low-energy or refurbished buildings requires a dynamic energy simulation. Only through it is it possible to accurately and reliably analyze the energy performance of the building, and this allows to optimize the choices in the design phase by reducing consumption and avoiding the oversizing of the systems (with a reduction, therefore, of construction costs).

This chapter will describe simulation methods and tools for evaluating the energy performance of the building through a dynamic simulation.

2.1 Approaches to building modeling

The evaluation of the energy performance of the building with a dynamic method can be conducted through two numerical models:

- the nodal network or multizone model: the performance of the building is evaluated through a zero-dimensional approach in the time domain. In this approach, the environments are represented by a single node characterized by uniform and homogeneous thermal and hygrometric conditions. With this method, it is therefore not possible to describe the phenomena of thermal stratification or spatial gradients of thermal and hygrometer parameters or species. In the Building Energy Performance Simulation (BEPS) code the solving method uses Conduction Transfer Functions (CTFs) and the phenomena of mass and heat transfer are described through a series of differential equations in the time domain.
- the computational fluid dynamics: the temperature and air distribution in the building are evaluated in the space domain in a single temporary moment. The environment is divided into a grid with several control volumes (cells). The choice of the number of the cells is an important parameter, the higher it is, the more reliable the simulation is. Conversely, the computational efforts increase, and the system of equations became more complex. The phenomenon is described by the Navier-Stokes equations.

2.1.1 Building energy performance simulation

To assess the energy performance of the building, the simulation engine requires a large amount of information gathered through the energy audit [2]. To date, there are numerous tools for the building performance simulation (BPS) [3]: ESP-r (Environmental Systems Performance – research), EnergyPlus, TRNSYS, IES-VE (Integrated Environmental Solutions – Virtual Environment), EDSL-Tas, and IDA ICE (Indoor Climate and Energy). The characteristic logical scheme of all these tools begins with the modeling phase, i.e., the creation of the geometrical model and its characterization through the thermophysical properties of the building component, the definition of the thermo-technical systems and the selection of the weather file. This file collects data on environmental conditions such as air temperature, relative humidity, solar radiation, atmospheric pressure, wind speed and direction.

These programs, as previously said, use calculation methods based on transfer functions, or algorithms that relate the stress on the system, therefore the cause, and the response of the system itself, or rather the effect. The CTF is used to evaluate the heat flow transmitted by conduction through the envelope and the thermal balance on the ambient air is used to calculate the load to be supplied to the environment to maintain the desired comfort conditions. The phenomenon of conduction in a dynamic regime can be expressed through the Fourier equation (2.1):

$$\alpha\left(\frac{\partial^2 T}{\partial x^2}+\frac{\partial^2 T}{\partial y^2}+\frac{\partial^2 T}{\partial z^2}\right)=\frac{\partial T}{\partial \tau}$$

(2.1)

where τ is the time, α is the thermal diffusivity of the material, defined as $\alpha=\lambda/(\rho c)$, and λ is the thermal conductivity. The above expression is valid under the assumption that $\lambda, \rho \text{ and } c$ are constant with the temperature and there are no internal heat sources. Solving this equation under realistic assumptions is somewhat complex. Therefore, there are

and are used different methods to solve the problem, that introduce approximations that affect the correctness of the results.
The mathematical equations underlying the simulation codes can be classified into two groups: the first relates to the balance for the surfaces that delimit the building (2.2); the second relates to the air inside the environment (2.3):

$$q_{i,cond} + q_{i,s-rad} = \sum_{k=1}^{N} q_{ik,rad} + q_{i,conv} \tag{2.2}$$

$$\sum_{i=1}^{N} q_{i,conv} \cdot A_i + Q_{other} - Q_{extract} = \left(\rho \cdot V_{room} \cdot c_p \cdot \Delta T_{room}\right)/\Delta t \tag{2.3}$$

where:

- $q_{i,cond}$ is the conduction thermal flow affecting the surface i;
- $q_{i,s-rad}$ is the radiative thermal flow between the surface i and an internal or solar thermal source;
- $q_{ik,rad}$ is the radiative thermal flow between the surface i and a surface k;
- $q_{i,conv}$ is the convective thermal flow affecting the surface I;
- $\sum_{i=1}^{N} q_{i,conv} \cdot A_i$ is the heat exchange by convection between the indoor air and the surface i with an area = A_i;
- Q_{other} is the thermal gain due to people, lights, equipment, etc;
- $Q_{extract}$ is the thermal load to balance;
- $(\rho \cdot V_{room} \cdot c_p \cdot \Delta T_{room})$ is the energy exchange with respect to the indoor air;
- ΔT is the indoor air temperature difference;
- Δt is the time step.

The equation (2.2) allows to evaluate the indoor surface temperatures and the energy exchanges affecting these surfaces, while the equation (2.3) allows to evaluated the mean indoor air temperature and the thermal load to be balanced. The radiative and the convective thermal flow can be written as:

$$q_{ik,rad} = h_{i,rad} \cdot (T_i - T_k) \tag{2.4}$$

$$q_{i,conv} = h_{i,conv} \cdot \left(T_i - T_{i,air}\right) \tag{2.5}$$

where:

- $h_{i,rad}$ is the linearized radiative heat transfer coefficient;
- T_i is the temperature of the internal surface i;
- T_k is the temperature of the internal surface k;
- T_{air} is the temperature of the indoor air near the surface k;
- $h_{i,conv}$ is the convective heat transfer coefficient, which is, usually, estimated by empirical equations or assumed as a constant.

Here the logical framework and the main architecture of one of programs allowing transient energy simulations are described. This is EnergyPlus [4], one of the most accredited and used calculation engines by the scientific community. The description is focuses on this because it will be the one used for many studies described in the next sections and chapters. EnergyPlus is an open-source software developed by the US Department of Energy and derives from the DOE-2 and Blast programs. Unlike the latter, it provides an integrated rather than sequential simulation. Indeed, the software is based on the integrated simulation of the ambient, built environment, HVAC (i.e., fans, pumps, terminals, pipes, ducts, generators, boilers, cooling equipment, etc.) and all energy systems (e.g., lighting, and indoor equipment) of the building facility. Figure 2.1 shows the program operation diagram.

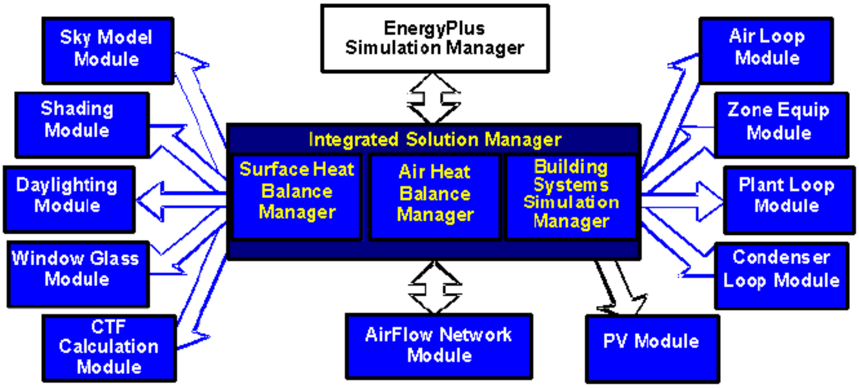

Figure 2.1: EnergyPlus operating diagram (Source: EnergyPlus Documentation)

The Integrated Solution Manager coordinates the three main modules:

- surface heat balance manager evaluates the phenomena of heat exchange through the surfaces that delimit the building;
- air heat balance manager takes into account the phenomena involving the ambient air and that of the plant;
- building systems simulation manager simulates the plant.

Figure 2.2 shows the heat balance process at the base of EnergyPlus. There are four main process:

- Outside surface heat balance;
- Conduction process through the wall;
- Inside surface heat balance;
- Air heat balance.

For each surface that delimits the building, a balance is evaluated on the internal and external surface node and the flow of heat transmitted by conduction is evaluated.

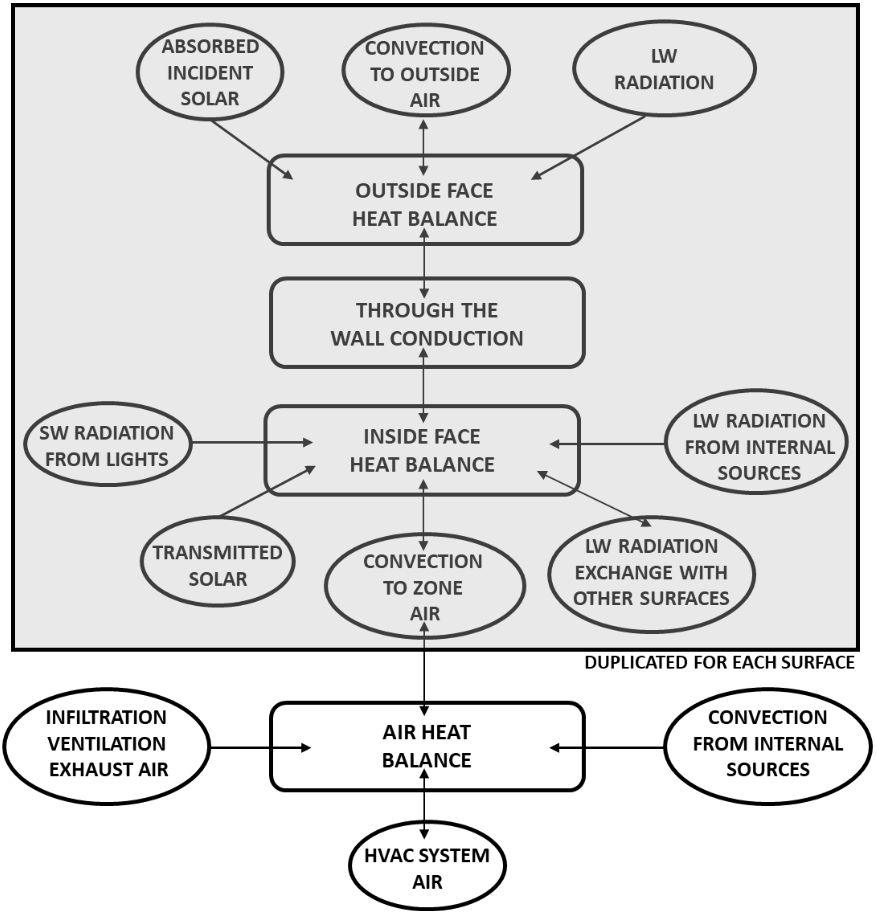

Figure 2.2: Scheme of heat balance process (source:[5])

Outside surface heat balance

The heat balance for the outside surface is:

$$q''_{\alpha sol} + q''_{LWR} + q''_{conv} - q''_{ko} = 0 \tag{2.6}$$

where:

- $q''_{\alpha sol}$ is the direct and diffuse heat flow absorbed by the sun (short wave length);
- q''_{LWR} is the long-wave radiation heat flow with air and surroundings;

- $q^{"}_{conv}$ is the convective heat exchange with the outside air;
- $q^{"}_{ko}$ is the outside conduction heat flow per unit area (q/A).

Inside surface heat balance

The heat balance for the inside surface is:

$$q^{"}_{LWX} + q^{"}_{SW} + q^{"}_{LWS} + q^{"}_{sol} + q^{"}_{conv} + q^{"}_{ki} = 0 \tag{2.7}$$

where:

- $q^{"}_{LWX}$ is the long-wave radiation heat flow between zone surfaces;
- $q^{"}_{SW}$ is the short-wave radiation heat flow from lights;
- $q^{"}_{LWS}$ is the long-wave radiation heat flow from the equipment;
- $q^{"}_{sol}$ is the solar heat flux;
- $q^{"}_{conv}$ is the convective heat flow with the inside air;
- $q^{"}_{ki}$ is the inside conduction heat flow per unit area (q/A).

Conduction process through the wall

As previously mentioned, CTFs are used to evaluate the heat flux transmitted by conduction through the building envelope. The method of transfer functions is one of the most widespread approaches to solve the conduction equation. These functions are time series that allow to evaluate the heat fluxes affecting the internal and external surfaces as a function of the current and previous surface temperatures and heat fluxes. These functions, actually, characterize the dynamic behavior of the building and allow the evaluation of the thermal storage phenomena.

For the heat flux affecting the internal and external surfaces the following equations are used :

$$q^{"}_{ki}(t) = -Z_o T_{i,t} - \sum_{j=1}^{nz} Z_j T_{i,t-j\delta} + Y_o T_{o,t} + \sum_{j=1}^{nz} Y_j T_{o,t-j\delta} + \sum_{j=1}^{nq} \Phi_j q^{"}_{ki,t-j\delta} \tag{2.8}$$

$$q^{"}_{ko}(t) = -Y_o T_{i,t} - \sum_{j=1}^{nz} Y_j T_{i,t-j\delta} + X_o T_{o,t} + \sum_{j=1}^{nz} X_j T_{o,t-j\delta} + \sum_{j=1}^{nq} \Phi_j q^{"}_{ko,t-j\delta}$$

(2.9)

where:

- T_i is the internal surface temperature;
- T_o is the external surface temperature;
- $q^{"}_{ki}$ is the heat flow on the internal side;
- $q^{"}_{ko}$ is the heat flow on the external side;
- X_j is the outside CTF coefficient;
- Y_j is the cross CTF coefficient;
- Z_j is the inside CTF coefficient;
- Φ_j is the flux CTF coefficient.

The issue is to determine the thermal flows at the previous time steps, the internal and external surface temperatures, and the coefficients of the CTFs. In EnergyPlus environment, the CTF coefficients are evaluated by the state space representation [6][7] that starts from a system of two equations:

$$\begin{cases} \dfrac{d[x]}{d\tau} = A[x] + B[u] \\ y = C[x] + D[u] \end{cases}$$

where:

- x = vector of state variables;
- u = input vector (internal and external surface temperatures);
- y = output vector (thermal flows);
- τ = time;
- A,B,C,D = matrices of constant terms.

Through matrix algebra the vector of state variables can be neglected, and the thermal flows (outputs) can be evaluated as a function of the surface temperatures (input vector). The power of this method is precisely this: the elimination of temperatures at the nodes. Once the matrices are known, the coefficient of the CTFs can be evaluated, and the heat flow on the inside and outside surface can be obtained.

<u>Heat balance on the zone air</u>

The equation for the air heat balance of the zone is as follows:

$$C_z \frac{dT_z}{dt} = \dot{Q}_{syst} + \sum_{i=1}^{N_{sl}} \dot{Q}_i + \sum_{i=1}^{N_{surface}} h_i\, A_i (T_{si} - T_z) + \sum_{i=1}^{N_{zones}} \dot{m}_i\, C_p (T_{zi} - T_z) + \dot{m}_{inf} C_p (T_\infty - T_z) \tag{2.10}$$

where:

- T_z is the indoor air temperature
- $C_z \frac{dT_z}{dt}$ is the energy stored in the zone air;
- $\sum_{i=1}^{N_{sl}} \dot{Q}_i$ is the sum of the convective internal loads;
- $\sum_{i=1}^{N_{surface}} h_i\, A_i (T_{si} - T_z)$ is the convective heat transfer from the zone surfaces;
- $\dot{m}_{inf} C_p (T_\infty - T_z)$ is the heat transfer due to infiltration of outside air;
- $\sum_{i=1}^{N_{zones}} \dot{m}_i\, C_p (T_{zi} - T_z)$ is the heat transfer due to interzone air mixing;
- $\dot{Q}_{syst}$ is the thermal energy provided by the systems.

Through an algorithm that exploits the approximation of the finite differences of the third order to solve the equation, the following equation is obtained for the evaluation of the temperature:

$$T_z = \frac{\sum_{i=1}^{N_{sl}} \dot{Q}_i + \sum_{i=1}^{N_{surface}} h_i\, A_i T_{si} + \sum_{i=1}^{N_{zones}} \dot{m}_i\, C_p T_{zi} + \dot{m}_{inf} C_p T_\infty + \dot{m}_{syst} C_p T_{supply} - \frac{C_z}{\delta t}\left(-3T_z^{t-\delta t} + \frac{3}{2} T_z^{t-2\delta t} - \frac{1}{3} T_z^{t-3\delta t}\right)}{\frac{11}{6}\frac{C_z}{\delta t} + \sum_{i=1}^{N_{surface}} h_i\, A_i + \sum_{i=1}^{N_{zones}} \dot{m}_i\, C_p + \dot{m}_{inf} C_p + \dot{m}_{syst} C_p} \tag{2.11}$$

<u>Building system simulation manager</u>

The plant management system controls three subsystems: air loop (aeraulic circuits), plant loop (hydronic circuits relating to heat transfer fluids) and the condenser loop (hydronic circuits relating to condensation fluids). For each loop, the plant components to be sized on both the demand and supply side of energy are identified.

As previously said, the three main components are solved simultaneously in order to create a simulation closer to reality.

The main difficulty of EnergyPlus is that it is a tool where the inputs are exclusively text files. For this reason, various graphic interfaces have been created. In the next chapters, EnergyPlus will be used as tool for the building dynamic energy simulation, with other suitable interface used for the creation (e.g., geometry, locations) and the characterization (all boundary conditions) of the building model.

2.1.2 Computational fluid dynamics analyses

If the interest is aimed at the knowledge of the 3D distribution of the microclimatic parameters in a building or to evaluate the indoor air quality, the methods based on the transfer functions are not enough, and CFD analysis is required. The evaluation of the parameters that define the microclimate and the thermal-hygrometric comfort takes place in the space domain in a single and fixed temporary moment. However, this analysis is characterized by a considerable computational time, due to both the creation of the model, the setting of the inputs, and mostly the resolution of the system of equations. For this reason, the CFD analysis is usually applied to single rooms under steady-state assumptions.

The Navier-Stokes equations are the basis of this analysis and describe how the temperature, pressure, velocity, and density of a moving fluid are related. Solving the system of equations, the velocity, pressure, and temperature fields are established, and one may calculate variables such as thermal comfort, indoor air quality, and pollutants distribution. For a generic variable φ the relative conservation equation is [8]:

$$\frac{\partial}{\partial t}(\rho\phi) + \frac{\partial}{\partial x_j}(\rho U_j \phi) = \frac{\partial}{\partial x_j}\left(\Gamma_\phi \frac{\partial \phi}{\partial x_j}\right) + S_\phi \tag{2.12}$$

where:

- t is the time;
- ρ is the air density;
- ϕ is the transport property;
- x_j is the distance in the direction j;
- U_j is the speed component referred to the direction j;
- Γ_ϕ is the diffusion coefficient.

The mathematical model that describes the problem is based on conservation principles and the related boundary conditions. The equations that regulate the phenomenon remain the same while the boundary conditions change relating to a specific situation. The analytical solution of these equations is feasible only in simple cases, for this reason numerical procedures are used. The equations describing the problem are applied in a region identified as the computation domain. In CFD analysis, the finite volume method is used, whereby the domain is divided into many smaller volumes (also called cells) and the equations are solved for each control volume. In order to account for turbulence effects, several models are available to solve such equations:

- Direct Numerical Simulation (DNS): model that provides the most exact solution at the cost of a high computational burden. No approximation is used to describe turbulence, and this implies a very dense mesh to be able to study even the smallest vortices that are generated;
- Reynolds Average Navier-Stokes (RANS): faster model from a computational point of view but provides an approximate solution as the quantities are time averaged - i.e. the turbulent motion is decomposed into an average motion with a fluctuation over time and a steady solution is derived;
- Large Eddy Simulation (LES): this model represents a middle way between the previous ones, it provides more accurate results than the RANS model requiring a lower computational burden than the DNS model.

The use of the CFD analysis to evaluate the building-air-conditioning performance allows a reduction of the experimental studies, the opportunity to conduct different analyses with the same model, by modifying the design conditions and the visualization of the results in a simple way.

Analysis procedure

The analysis can be divided into three phases:

- pre-processing phase in which the space domain (geometry) is defined and discretized into a certain number of elementary control volumes (cells) that create a calculation grid (also called mesh). After choosing the governing equations under the appropriate assumptions, boundary and initial conditions are defined;

- resolution phase in which the physical models are defined. The discretized equations are formulated for each point of the grid. The initial conditions are defined. The equations are solved iteratively and once the desired degree of accuracy is reached the calculation is stopped;
- post-processing phase in which the results are analyzed.

The definition of the calculation grid is the first step of the CFD, and it influences the whole analysis. A grid with too large a pitch leads to inaccurate results, and information on flows may be lost, on the contrary a too detailed grid increases the calculation time. A trade off solution is required to use the minimum number that ensure a desired accuracy. Generally, the grid can be:

- structured: the cells, that are sorted, can be quadrangular or hexahedral. In this case the matrix of the algebraic equations has a regular geometry, and this simplifies the achievement of convergence. Such meshes are less suitable for describing complex or curvilinear geometries;
- unstructured: the cells are not ordered and the elements that make up the mesh can have any geometry. This type of mesh is suitable for complex geometries.

A good quality mesh should be dense in areas with strong gradients, i.e., near the domain boundary, and less dense in areas with low gradients. Once the grid has been defined, the boundary conditions must be assigned to set the simulation inputs. These conditions are essential as they create a connection between the model and the environment in which it is inserted, and their accuracy affects the entire analysis and the resolution of the characteristic equations and the turbulence field. They concern the chemical and physical characteristics of the fluid, which can be constant or variable in the simulation time. In air conditioning problems, the boundary conditions required for a CFD analysis consist in the definition of the air diffusion terminals in the environments, of the envelope and the surfaces that delimit the environment under study, the symmetrical surfaces, and parameters related to the elements of generation or destruction.

Subsequently, it is necessary to define a turbulence model. A model commonly used is the k-ε, which is a model of two equations in which k is the kinetic turbulence energy and ε is the velocity of dissipation.

However, this model is not able to adequately describe the decreasing trend near a wall (therefore it works better away from the wall) and is less accurate for decelerating flows.

In summary, this approach allows a detailed description of the distribution of microclimatic parameters within a building. Furthermore, once the boundary conditions have been defined, it is possible to evaluate and compare different scenarios in order to improve the efficiency of the system. However, this analysis requires a high computational burden and the construction of a complex model, especially in the definition of the inputs.

2.1.3 Coupling of BEPS and CFD approaches

The information provided by the energy simulation (BEPS) and the information from the CFD simulation can be integrated. For example, building energy simulation can be used to define detailed boundary conditions (i.e., the inner surface temperatures) for the CFD analysis. On the other hand, the CFD analysis results (i.e., h_c or the indoor air temperature) can be used on the BEPS code. The logical connections for these two methods can be static or dynamic [9]. In the first case, static coupling, the transfer of information can take place in one or two steps. In

the second case, dynamic coupling, there are three cases depending on the time intervals in which the data transfer takes place between the energy simulation and the CFD one. The transfer can take place in a single time interval, this is the simplest case. The simulations exchange information until convergence is achieved in this single time interval. The second case is called almost dynamic, and the exchange takes place for different time intervals. The last case, completely dynamic, in which the exchange of information takes place until convergence is reached in each time interval. As the number of information exchanges increases, the accuracy increases, but the computation time also increases.
However, it should be emphasized that the exchange of information is not a simple process due to a different "time scale" (the BEPS is an hourly or sub-hourly analysis, while the CFD is a single-moment analysis); a computational temporal discontinuity (less than one hour for a BEPS analysis compared to at least 30 hours for a CFD analysis); and a modeling discontinuity (average data for an internal space in the BEPS analysis versus a wide spatial distribution of the data in the CFD one).

In summary, the coupling of the two approaches, BEPS and CFD, provides a complete description of the problem (investigating both the energy performance of the building and the microclimatic conditions of an internal space) offering new possibilities for evaluation.

2.2 Energy modeling of the building

The first stage to evaluate the energy performance of a building consists in the realization of the model. The building was characterized in its current state through an accurate energy audit, which requires [2]:

- general user analysis: climatic data, employment profiles, census of electrical equipment, reconstruction of energy, electrical and thermal consumption, based on supply lists and contract type;
- collection of data on the opaque and transparent building envelope;
- collection of data related to the thermo-technical systems installed.

The audit allows the user to photograph the current state of consumption and to highlight the main problems and improvements achievable with respect to the current situation of the building/plant system. As previously said, EnergyPlus software is commonly used for the dynamic energy simulation of the building, but due to a lack of a comprehensive graphical user interface DesignBuilder® [10] is used to define the building geometry. It facilitates the process of modeling for advanced building energy simulations. The inputs required by DesignBuilder® are organized in the following modules:

- location, where an annual weather data file is set;
- geometry, where the building skeleton is developed and divided into thermal zones;
- activity: where the use destination of each thermal zone is defined;
- construction: where the thermophysical characteristics of the opaque building envelope elements are assigned;
- openings: where the thermophysical characteristics of the transparent building envelope elements of the building are defined;
- HVAC (heating, ventilating and air conditioning) systems: where the technical characteristics of the air conditioning plants are modeled.

All these data can be collected both by in-situ survey and documents. Once obtained the transient energy model, it is necessary to calibrate it, where "calibration" means the process of comparing the outputs of the simulation and those deriving from experimental data, determining the deviation of the results and the degree of uncertainty, and then correcting - consequently - the measuring apparatus or the numerical model.

For the calibration of a transient energy model of a building, and so for a measure of the accuracy of the model, the two most used indices, proposed by the M&V Guidelines “Measurement and Verification for Federal Energy Projects” [11] and the ASHRAE Guidelines 14 [12], are the mean square error (Mean Bias Error, MBE) and the Coefficient of Variation of the Root Mean Square Error (CV(RMSE)), defined in the following equations (2.13), (2.14):

$$MBE\ [\%] = \frac{\sum_{period}(M-S)_{month}}{\sum_{period} M_{month}} \times 100$$

(2.13)

$$CV(RMSE_{month})[\%] = \frac{RMSE_{month}}{A_{month}} \times 100$$

(2.14)

where:

- $A_{month} = \frac{\sum_{year} M_{month}}{N_{month}}$ denotes the average value of the monitored energy consumption;
- $RMSE = \sqrt{\frac{\sum(M-S)^2_{month}}{N_{month}}}$ denotes the root-mean squared monthly error.

In order to consider an energy model properly calibrated, ASHRAE Guideline 14 and the M&V protocol identifies the following limits:

- MBE_{month} (%) ≤ ± 5%,

- CV($RMSE_{month}$) (%) ≤ + 15%.

Higher discrepancies and thresholds are allowed if the time scale of analyses in not monthly but daily or hourly. In the next chapter (Chapter 3) the methods described, for modeling, calibration, and simulation, will be applied to different case studies: buildings with different intended uses from residential to industrial, passing through the commercial up to the historic buildings.

CHAPTER 2 - Nomenclature

Acronyms		
ASHRAE	American Society of Heating, Refrigerating and Air-Conditioning Engineers	
BEPS	Building Energy Performance Simulation	
CFD	Computational fluid dynamics	
CTF	Conduction Transfer Function	
CV(RMSE)	Coeff of variation of Root Mean Square Error	
DNS	Direct Numerical Simulation	
ESP-r	Environmental Systems Performance – research	
HVAC	Heating, ventilation and Air-conditioning	
IDA-ICE	Indoor Climate and Energy	
IES-VE	Integrated Environmental Solutions – Virtual Environment	
LES	Large Eddy Simulation	
MBE	Mean Bias Error	
RANS	Reynolds Average Navier-Stokes	
Symbols		
α	Thermal diffusivity	
λ	Thermal conductivity	W/mK
ρ	Density	kg/m³
c	Specific heat	J/kgK

CHAPTER 2 - References

[1] ASHRAE Terminology: https://www.ashrae.org/. Accessed in September 2022
[2] Energy Audit for Building http://www.bdg.nus.edu.sg/BuildingEnergy/publication/papers/BCABEAud.pdf
[3] Solmaz, A. S. (2019). A critical review on building performance simulation tools. *Alam cipta*, *12*(2), 7-21.
[4] EnergyPlus 8.9.0 Available online: https://energyplus.net
[5] Jeffrey D. Spitler Load Calculation Applications Manual: https://www.ashrae.org/. Accessed in September 2022
[6] J.E. Seem, Modelling of heat transfer in buildings, Ph.D. Thesis, University of Wisconsin, Publisher University of Wisconsin-Madison, Madison, Wisconsin, 1987. Available online at: https://minds.wisconsin.edu/handle/1793/7916. Accessed in September 2022
[7] J.E. Seem, S.A. Klein, W.A. Beckman, J.W. Mitchell, Transfer function for efficient calculation of multidimensional transient heat transfer, ASME J. Heat Transfer 111 (1989) 5–12.
[8] ASHRAE 2005, ASHRAE Handbook – Fundamentals, Chapter 34 Indoor Environmental Modeling, American Society of Heating, Refrigerating and Air-Conditioning Engineers, Inc., Atlanta GA, USA, 2005
[9] Z.J. Zhai, Q. Chen, 2005, Performance of coupled building energy and CFD simulations, Energy and Buildings 37 (2005), pp. 333-344.
[10] DesignBuilder v. 6.0. Available online: https://designbuilder.co.uk/.
[11] U.S. Department of Energy, Federal Energy Management Program (FEMP). M&V Guidelines: Measurement and Verification for Performance-Based Contracts; FEMP: Washington, DC, USA, 2015.
[12] ASHRAE—American Society of Heating. Refrigerating and Air-ConditioningEngineers, Guideline 14 2002, Measurement of Energy and Demand and Savings; ASHARE: Atlanta, GA, USA, 2002.

CHAPTER 3

Whole building energy analysis

3.1 Introduction and organization of the research

In this Thesis, methods described in the previous chapter will be applied for several case studies. The main phases leading to the energy analysis of the complex building system will be described, namely:

- data collection to characterize the building envelope and the technical systems;
- model calibration to ensure the reliability of the results.

The software used for these phases - for all the case studies that will be treated in this Thesis - are, as mentioned in chapter 2, DesignBuilder® and EnergyPlus. In detail, DesignBuilder® is used to create the geometric model and to characterize the thermophysical parameters by setting the data required by its various modules - activity, construction, openings, lights, HVAC system - described in section 2.2. Once the model is developed, commonly it is exported to EnergyPlus for dynamic energy simulations, which allow the knowledge of many data, among which the energy consumption, air flow rates, individual zone temperatures, etc. EnergyPlus implements detailed building physics for air, moisture, and heat transfer including treating radiative and convective heat-transfer; calculates lighting, shading, and visual comfort metrics; supports flexible component-level configuration of HVAC, plant, and refrigeration systems; simulates sub-hourly time steps to handle fast system dynamics and control strategies. Therefore, it allows to simulate any energy systems.

In the following subsections, from 3.1.1 to 3.1.3, the stages of data collection and model calibration will be applied to building with different

intended uses, in detail: industrial, office and historical buildings. These three typologies, together with the residential buildings (which will be considered in the Section 3.3), represent the entire European - in this context Italian - building stock. It is clear that the approach to modeling, calibrating and simulating the building does not change with the intended use of the building itself, however the systems used to ensure microclimatic control, the use of the building by the occupants and in some cases even the thermophysical properties of the building (think of historic buildings) can be very different. With the descriptions provided in the following subsections the idea is to cover most of the existing types of building stock. With these examples, the difficulty of the modeling phase (followed by the simulation phase), which was dealt with in Chapter 2 from a purely theoretical point of view, will be rendered in practical form.
We will be faced with a bi-objective problem (Section 3.2):

- complexity in the search and definition of the parameters that define the behavior of a building which translates into a high computational burden;
- reliability of the results.

As in all the multi-objective problems, the goal is to find the best trade-off between the objective functions. This research will be addressed in Sections 3.3 and 3.4, focusing on the inter-building effect and the development of a tool for building modeling and simulation, respectively. In detail, in Section 3.3, the aim is to understand if and in which cases it is possible to avoid the modeling of the urban context, by reducing the modeling and the simulation times, without compromising the reliability of the results. In section 3.4 instead, a new tool for the building modeling and simulation phase is proposed and validated. It simplifies the phase of defining the parameters that describe the behavior of the building while ensuring accurate results.

3.1.1 Industrial building

The first case study concerns an existing industrial building, built in 2014. Here, the final scope was to evaluate the influences of different retrofit measures in order to minimize the primary energy consumption, global cost and thermal discomfort, but in this phase only the energy modeling of the building will be described [1]. The building, located in Southern Italy, in climate zone D [2], is structurally divided into 2 main areas:

- the office area, which in turn consists of 9 zones,
- the workshop area, for a total of about 1380 m^2.

The geometrical model was realized by using the graphical interface DesignBuilder® (Figure 3.1), so all the information in terms of location, thermal characteristics of the opaque and transparent envelope, the intended use of the zones, operation, and type of system, and all other information required by the software have been defined. As far as localization is concerned, the software presents a database with meteorological data of the typical year for various locations, so these data are automatically loaded. As for the thermo-physical characteristics of the building envelope, these were taken from the construction plans. In particular, as external masonry, there is an insulated self-supporting metal wall made of prefabricated sandwich elements, having a thermal transmittance value (U-value) equal to 0.31 W/m^2K. The transparent building envelope has double glazing (U_g = 2.67 W/m^2K), with aluminum frames with thermal break. The building is located in an industrial area and is isolated, therefore it is not necessary to model the surrounding context.

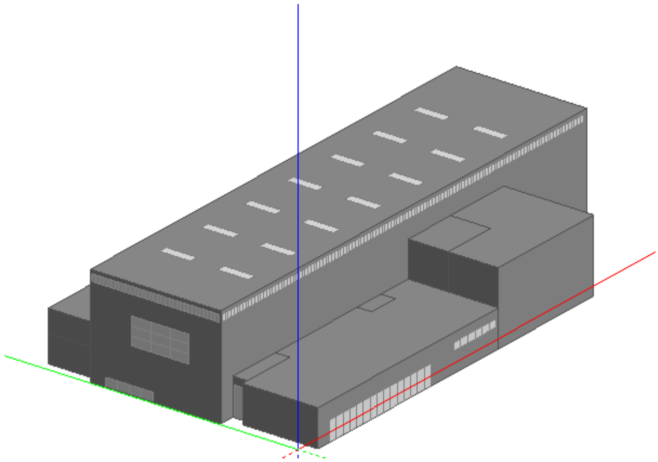

Figure 3.1: Building model through DesignBuilder®

As concern the microclimatic control the building is equipped with an all-air system consisting of:

- Heat Pump: 491 kW, EER 2.88 in cooling mode; 522 kW, COP 3.31 in heating mode. This is a reversible unit to produce chilled/heated water, with an additional exchanger downstream of the compressor to exploit the superheat heat. The heat recovered is, approximately, equal to 20% of the cooling capacity. This function allows the production of hot water to be sent to the post-heating coil in the AHU;
- Two Air Handling Units, one of 8750 m^3/h for the office area and the other of 45000 m^3/h for the workshop zone, each with two fans (supply and extraction) at constant flow rate, heating/cooling coil, post-heating coil and a liquid water humidifier. A heat recovery unit is not present;
- The aeraulic channels are located in the false ceiling. The terminals that serve the office/laboratory area are aluminum vents. In the workshop area, there are aeraulic channels in galvanized sheet.

Furthermore, a centralized control system is installed that allows to manage and monitor the operation of the plant. It allows to act only on two sizes, the temperature (T) and the relative humidity (%), by adjusting the thermostat and humidistat placed in the air return channel.

In the modeling of the system for the microclimatic control, the main defined components and equipment are:

- Air-cooled electric chiller: this simulates the summer operation of the heat pump, characterized by the technical data provided by the HP manufacturer's catalog concerning summer operation;
- Heat pump water heating system: modules of EnergyPlus have been used, by assuming technical data supplied by the HP manufacturer's catalog concerning the winter operation of the system;
- The Air Handling Unit with the two supply and return fans, at a constant flow rate, the heating and cooling coils, the adiabatic humidifier, and the post-heating coil. The airflow rate supplied by the AHU has been provided by the manufacturer's catalog.

Furthermore, it is necessary to define “schedules”, and thus operating programs that allow the reproduction of the actual operation of the system for the heating and cooling availability and set point and AHU availability. At this point, it is necessary to calibrate the numerical model of the building-plant system. In this case, the calibration was carried out by comparing simulated indoor conditions to those provided by a wide microclimatic monitoring. In particular, a comparison was made of the outputs of the energy model - obtained through the EnergyPlus software - with respect to the monitored temperature trends in the individual zones, as acquired through sensors. For the acquisition of the zone temperatures, commercial data loggers were used, whose main characteristics are described in [1]. The data loggers have been installed at the center of each room, at a height equal to 1.5 meters above the floor. It was possible to set the storage interval, the alarm limits, the acquisition mode, and all the necessary programming functions. The following figure

(Figure 3.2) shows a comparison between the data acquired through measurements and those obtained from the simulation, for a single zone of the building.

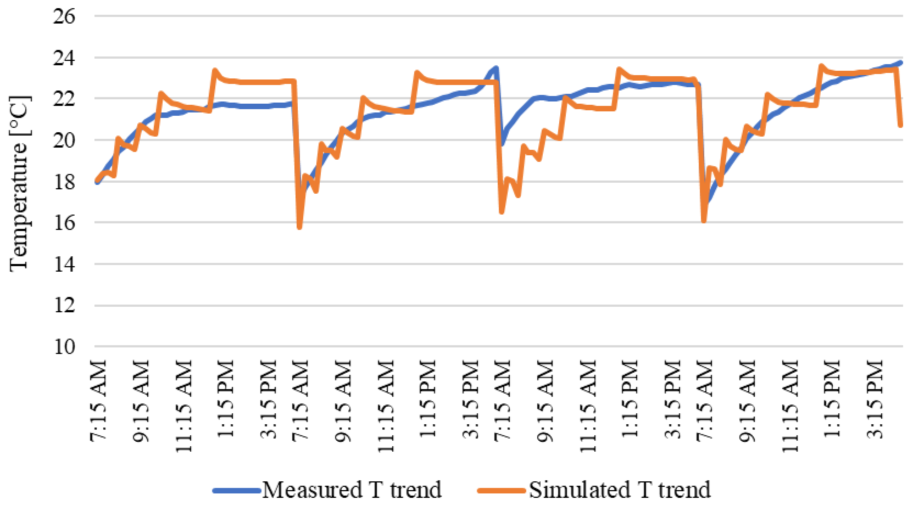

Figure 3.2: Comparison between measured and simulated Temperature trend

Then, the indicator MBE and CV(RMSE) were evaluated for each zone of the building, obtaining the results of Table 3.1.

Table 3.1: Indicators for the calibration of the model

	%MBE	CV(RMSE)
Limit value for M&V Guidelines	±5%	±10%
Limit value for ASHRAE Guideline 14	±5%	±15%
Zone 1	4.1%	5.9%
Zone 2	4.8%	8.3%
Zone 3	4.9%	7.1%
Zone 4	3.9%	7.7%
Zone 5	3.3%	8.4%
Zone 6	-0.8%	7.7%
Zone 7	0%	5.7%

The indicators are fully within the thresholds suggested by authoritative references. Therefore, the model can be considered calibrated, and it can be concluded that it performs very closely to the real behavior of the building. Consequently, it is possible to investigate the simulation outputs that will be considered reliable, through EnergyPlus software.

3.1.2 Office building

The second case study concerns an office building that belongs to the University of Naples Federico II. It was built between 1971 and 1975, and like all buildings built between 1960 and 1980, it has a structural frame in reinforced concrete. It is included in a densely built urban context (Figure 3.3A). It consists of a rectangular block, made up of 9 floors with a total height of 31.5 m, and two lateral blocks made up of only 2 floors (Figure 3.3C).

In this case, the thermophysical characteristics of the building and of the systems installed are obtained from an energy diagnosis conducted on the building. As regards the opaque envelope:

- external vertical walls are made up of prefabricated panels, layers in asbestos cement with the interposition of 6 cm of polystyrene. The U-value is 0.58 W/m²K;
- the horizontal structures (ceiling, floor, roof) are mixed in reinforced concrete and bricks, the reinforced concrete joists are alternated with intermediate lightening elements. The U-value of the roof is 1.7 W/m²K, the U-value of the slab on the ground is 1.25 W/m²K.

As regards the transparent building envelope, there is double glazing with an aluminum frame without thermal break, with a transmittance value U = 3.16 W/m²K. Considering the dense urban context, it is necessary to model the surrounding buildings which produce a shading effect on the building in question, reducing its exposure to solar radiation.

Figure 3.3: Urban context (A), Building under investigation (B), Section of the building investigated (C)

The microclimatic control is obtained by means of a boiler and a chiller combined with fan coils positioned in the zones. The seasonal average performance of the heating system, taking into account the generation system, the installation, the regulation, the distribution, the emission (so the all-plant subsystems) is deduced from the energy diagnosis conducted on the building and is equal to 0.56. The boiler has a nominal thermal capacity of about 737 kW. The chiller has a nominal thermal capacity of about 1090 kW and a COP=3.

In this case, the model is calibrated by comparing the energy consumptions obtained from the energy simulation with those deduced from the natural gas and electricity bills available for the examined building. The comparisons are shown in the Figure 3.4.

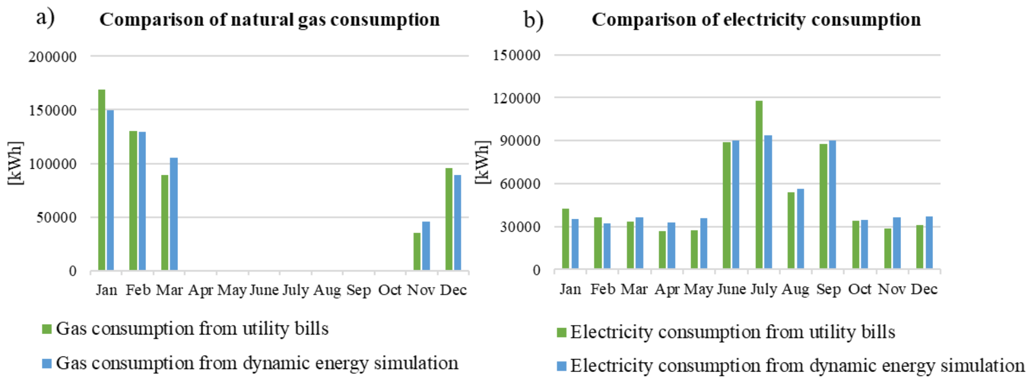

Figure 3.4: Comparison of measured and simulated energy consumption for natural gas (a) and electricity (b)

As in the previous case study, the MBE and the CV(RMSE) indicators are evaluated, and their values are shown in the Table 3.2.

Table 3.2: MBE and CV(RMSE) for the model calibration

	MBE [%]	CV(RMSE) [%]
Limit value for ASHRAE Guideline 14	±5%	**15%**
Natural Gas	-0.15%	18.51%
Electricity	-0.42%	17.01%

For both energy vector and sources (namely, electricity and natural gases), the MBE index falls within the range envisaged by the ASHRAE. Regarding the CV(RMSE) index, we are slightly outside the expected range. As regards the electricity consumption, the available data is a single bill for the entire building. There are no sub-meters for single use of electricity, i.e., there are no data on the socket panel, light panel, panel for each floor. The same occurs for the gas consumption. The available data relates to the delivery point, but the operation – in terms of activation and required temperature in each zone – for each terminal is not known.

There are therefore many degrees of freedom that I cannot manage, so that an indicator value just above the limit set by the protocols is an acceptable condition for the case under analysis.
Therefore, the model is calibrated, and it is possible to conduct an analysis of the energy consumptions under EnergyPlus environment. The availability of models capable to reliably represent the behavior of the building allows for a realistic response when different energy interventions are applied and investigated.

3.1.3 Historical building

The last case study presented concerns the model of a historic building: the fourteenth-century church of Donnaregina [3]. The original church was built in XIV century, and its plant follows the Franciscan rule and presents a single hall covered with trusses, which ends with a cross-vaulted Apse ribbed on a pentagonal plan, preceded by a rectangular module, characterized by high mullioned windows. The Choir, not finding a place behind the Apse or in the Nave, was placed on two rows of octagonal pillars, which support cross vaults. The church, therefore, presents a first tripartite space of double height and a second space of full height, bright and imposing for its Gothic forms. A very rich cycle of frescoes furtherly embellishes the church. Around 1620, the church underwent substantial changes because the construction of a new church, closer to the tastes of the time, was commissioned. Given the impossibility of extending the construction towards the current largo Donnaregina, the Choir of the nuns of the new church almost completely invaded the Apse of the fourteenth-century church, now used as a warehouse. When, in 1861, the convent was suppressed, the fourteenth-century church was acquired by the municipality of Naples and used for various and improper functions that favored the degradation. Coming to recent years, since 1975, the church has been the seat of the School of Specialization in Architectural Heritage and Landscape of the University of Naples, and it still retains this destination today, thanks to an agreement signed between the City of Naples, the University of Naples "Federico II" and the Archbishop's Curia of Naples.

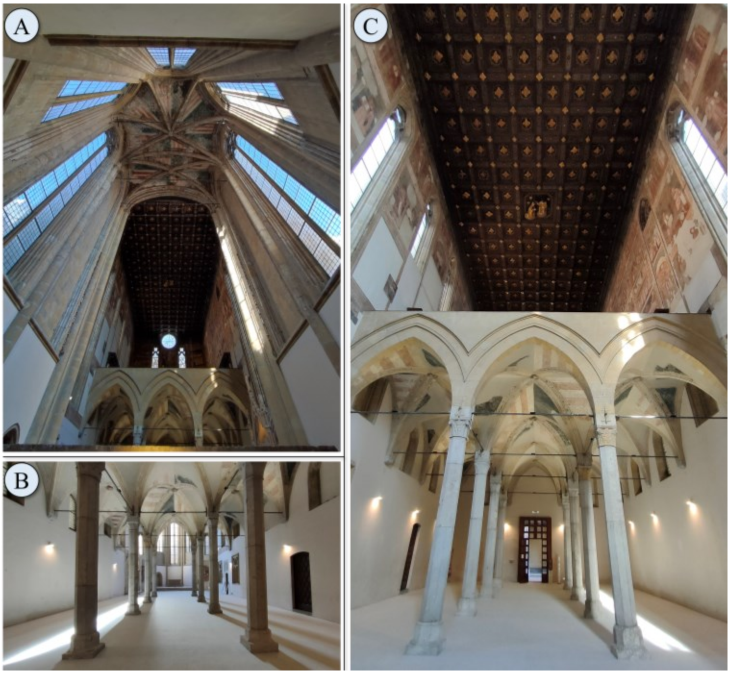

Figure 3.5: The church of of "Santa Maria Donnaregina Vecchia": a) the Apse, b) the Nave, c) the Nave and the Choir

The numerical model for the building energy simulation was developed, also in this case, through DesignBuilder®. The occupancy, as the lighting activation, was scheduled in compliance with the real profile of use of the church which is occasionally used for meetings. Besides the lighting system, any other electric device was considered. Currently, the church is not equipped with cooling, heating, or mechanical ventilation systems. Regarding the thermophysical properties of the envelope, these are typical of a fourteenth-century church: roof slab with wooden trusses above the Nave, roof slab in wrought lapillus above the Apse, and massive tufa walls of 1 m, coated with 3 cm of gypsum plasterboard only on the inside façade. The transparent envelope is characterized by single glasses with a solar transmittance of 0.48, and metal frames.

To calibrate the model, an appropriate monitoring of the indoor climatic conditions was carried out, positioning 9 sensors at different height levels. Figure 3.6. In this case study, 1 sensor was located outside to monitor the outdoor microclimatic conditions. The data collected through this sensor, related to the temperature and the relative humidity, were used to update the weather file of Naples. In this way the building was simulated in the real monitored conditions for the outdoor environment. The main characteristics of the installed sensors are described in [3].

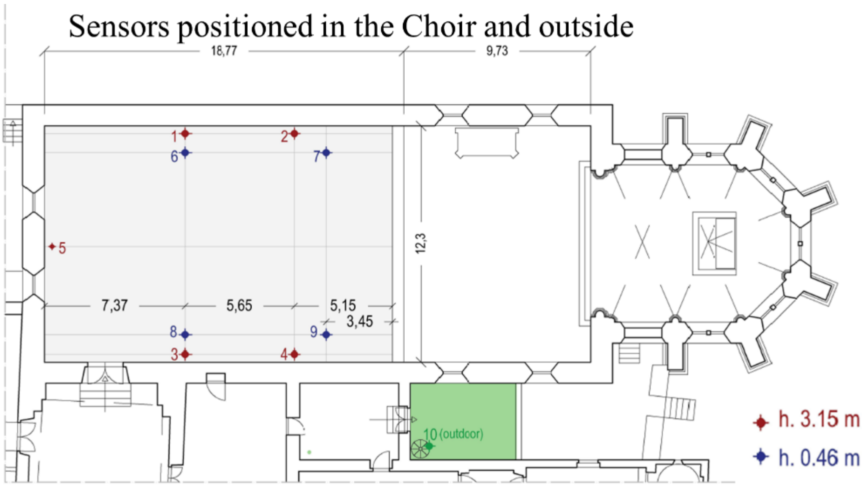

Figure 3.6: The sensor's position in the Choir

The final aim of the study was the modeling and the evaluation of a radiant system for the microclimatic control of the choir environment, and more information is provided in [3]. For this reason, the calibration of the model was conducted by evaluating the MBE for temperature and relative humidity in the choir zone. This is a novelty, and thus the calibration performed not with reference to the energy consumption but on the basis of monitored and simulated microclimatic parameters. The comparison between the measured and simulated temperature and relative humidity in the choir is shown in the following figures (Figure 3.7, Figure 3.8).

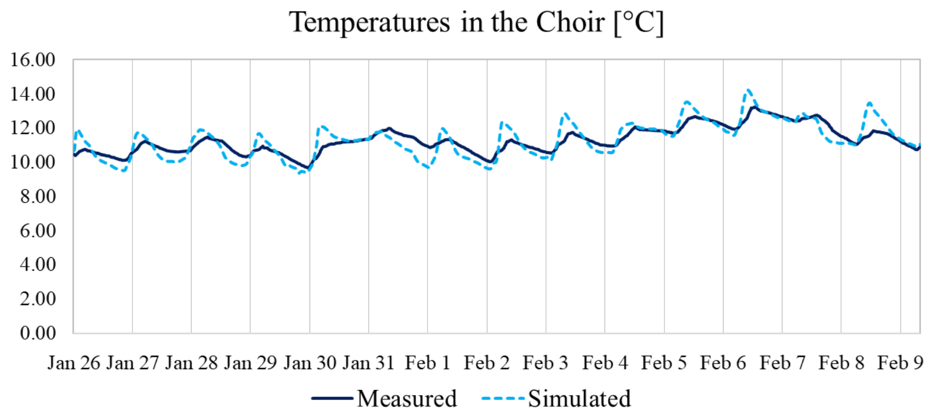

Figure 3.7: Comparison between measured and simulated temperatures

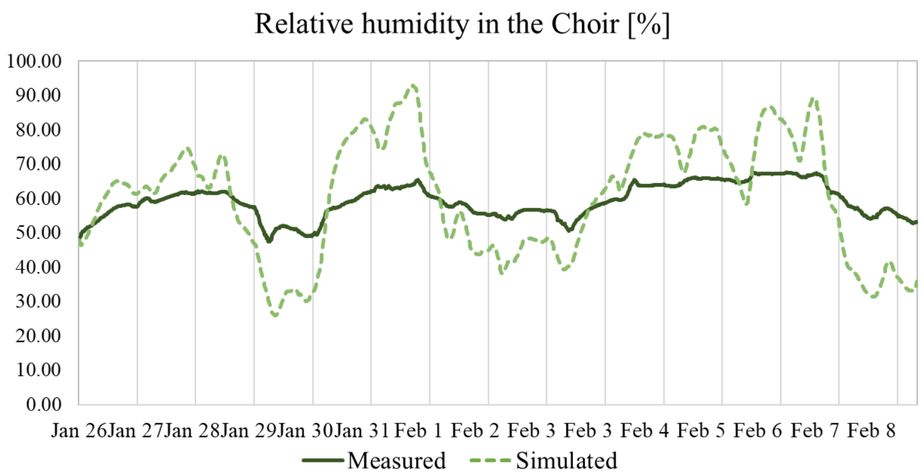

Figure 3.8: Comparison between measured and simulated relative humidity

Furthermore, the following monthly average gaps were evaluated:

- MBE = -0.1% for temperatures;
- MBE = -1.1% for relative humidity.

The MBE values are perfectly in the range suggested by M&V and ASHRAE protocol. Therefore, the model can be considered calibrated and the results of the dynamic simulation, obtained through EnergyPlus, can represent with reliability the real behavior of the building.

3.2 Issues and criticalities

In chapter 2, the need to access very detailed data of all the parameters that influence the behavior of the building has already been highlighted. This is essential to obtain detailed and reliable results of the energy performance of a building through a dynamic thermo-energy simulation.

The case studies just discussed show that the generation of a reliable model requires many inputs, such as data concerning the climatic conditions, the building envelope, the installed energy systems, the occupation, the electrical equipment, and the operation schedules. The access to these information can be obtained through documents (Section 3.1), energy audits (Section 3.1.2), on-site inspections (Section 3.1.3), or a combination of them. The in-depth knowledge of all the factors involved allows a greater detail of the results but this implies a greater computational burden, due both to the finding and definition of the factors themselves and to the conduction of each simulation.

Another important factor is the context in which the building is located. Information about the surrounding environment is needed, as it can affect the thermal load and gains. Therefore, the inter-building effect (IBE) should be considered to obtain reliable models. The modeling of the urban context, albeit simplified compared to the modeling of the building under investigation (as the important thing is to take into account the shading effect produced), requires a time from a design point of view but above all a computational burden (for the simulation program) to simulate the shadow effect. The IBE can cause significant discrepancies in the prediction of both heating/cooling loads [4] and artificial lighting needs [5] between a standalone building model and a detailed model of the same building reliably located inside its external environment. Han et al. [6] sought a systematic approach to quantify the influence of mutual shadows reflection within a network of buildings, showing that the shading effect plays a more significant role in affecting energy consumption respect to the reflection one. The surrounding environment can affect each floor of the building differently, especially in multi-storey [7] edifices. The impact of neighboring buildings can also highly affect the effectiveness of energy retrofit measures [8]. Therefore, in most cases, the IBE needs to be considered to perform reliable energy simulations of buildings in dense urban contexts, aiming at accurate predictions of primary energy consumption and related costs.

At the same time, the installed shading systems and their use patterns should be carefully modeled as well. They must provide sun protection during the summer season but should not hinder solar contribution in the winter season, not reduce natural lighting, and not prevent correct natural ventilation. The high amount of required input data – as well as the need to consider the inter-building effect and the shading systems to accomplish reliable building energy simulations – may generate complex and time-expensive models. This involves a high computational burden for simulation programs, which have to process lots of information with a consequent increase in calculation times. The high complexity in data collection often pushes professionals in the sector to resort to simplified tools based on stationary and or semi-stationary analyzes, compromising the outcomes' accuracy and reliability. There are no validated user-friendly BES tools that ensure accurate predictions of dynamic building energy performance requiring only few numerical inputs.

It is a problem with two-objectives between complexity (and therefore computational burden) and reliability and the goal is to find a compromise. The search for such compromise is discussed in the following paragraphs in which two aspects are addressed:

- Is it fundamental to model the interbuilding effect for reliable building energy simulations? Also evaluating the interaction with shading systems;
- Proposal of a reliable and easy-to-use, flexible tool for building energy modeling and simulation.

3.3 Inter-building effect

To investigate how much the interbuilding effect affects, two typical buildings, located in Naples (South Italy, Mediterranean coastline), in a dense urban context, are investigated [9]. In addition, the impact of different shading types – i.e., shading color, radiative characteristics, and position – and shading operation setpoints are analyzed.
Energy simulations are performed through different modeling approaches: detailed modeling, different shading systems, different shading set-points, no shading, no inter-building effect, and the pair no shading and no inter-building effect (simplest model). Figure 3.9 represents the steps described in the following subsections to evaluate the influence of the IBE effect.

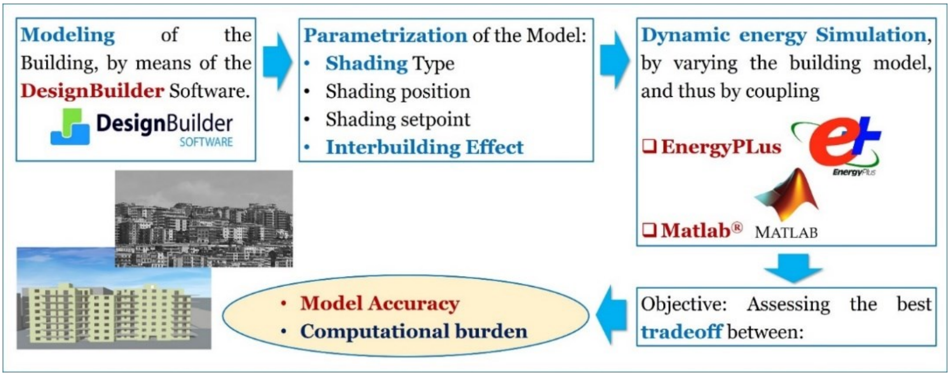

Figure 3.9: Graphical representation of the steps for the evaluation of the influence of the IBE effect

3.3.1 Methods

The energy and geometrical model of the building is realized by following the method described in Chapter 2, and by using DesignBuilder® software. The external environment surrounding the modeled building(s) – including, e.g., other constructions – is modeled by using opaque or semi-opaque blocks that produce shading effects.

To find the best trade-off between accuracy and computational load, the energy performance of the building, with reference to both buildings, was simulated using the different modeling approaches previously mentioned. In addition, different simulation time steps – and thus the number of energy balances per hour performed by the EnergyPlus simulations – are set for each modeling approach. More in detail, the time step is the incremental change in time for which the equations are being solved. In each time step, boundary conditions and dynamic input variables are held constant. At the expense of processing resources, effort and runtime, the solution is typically more accurate the smaller the time step.

The most detailed model contemplates the interbuilding effect and all shading systems, using the highest number of simulations time steps. As a result, it is the most accurate. However, it plainly requires a major complexity in modeling and simulations, as well as a great deal of computational burden, principally because a precise and timely shadow calculation necessitates long simulation times. On the other hand, simplified models aim to reduce such complexity and burden by not considering the IBE and/or shading systems, and by reducing the number of timesteps.

The shading device is modeled by a diffusing shade that may be placed inside or outside the window and has solar control as its basis for operation. If the solar setpoint (in W/m2) entered is exceeded by incident solar radiation on the window, shading is activated.

To carry out a comprehensive comparison of the performance indicators provided by the different approaches, a coupling between EnergyPlus and MATLAB® is developed and exploited. Notably, the EnergyPlus input files are parameterized and a MATLAB® code is written to automatically launch the EnergyPlus simulations related to the different modeling approaches. The parameterized variables are those that identify: the timestep value, the shading type, the shading position, the shading setpoint, and the IBE. The Matlab code allows to associate different values to these variables, and therefore to automatically switch from one modeling approach to another. The recorded simulation outputs are the thermal energy demands for heating and cooling (TED_h, TED_c), the primary energy consumption for heating, cooling, and lighting (PEC_h, PEC_c, PEC_l), as well as the required simulation time, by using, of course, the same personal computer. At this point, some indicators are used for comparing the models to the most detailed one and the savings in terms of computational time are assessed. The indicators used for this comparison are those used in international calibration procedures to evaluate the capability of the model in predicting real building performances. In addition to the indicators shown in Chapter 2, i.e., the MBE and the CV(RMSE), the following two are used:

- the error (ERR) in the monthly and annual energy consumption (3.1), (3.2):

$$ERR_{month}(\%) = \frac{D_{month} - S_{month}}{D_{month}} \tag{3.1}$$

$$ERR_{average\ year}(\%) = \frac{\sum ERR_{month}(\%)}{N_{month}} \tag{3.2}$$

where:

- "D" denotes the performance indicators referring to the most detailed model with the same shading systems, position and operation setpoint of the model under evaluation;
- "S" denotes the performance indicators referring to the simplified model under evaluation;
- N_{month} = 12, months in the years.

In this case, the comparison is made between the more detailed model and the simplified ones. The simplest models will be regarded as acceptable if the evaluated indicators (ERR, MBE, and CV(RMSE), some of these already described in the chapter 2) fall within the eligibility thresholds, which are:

- $ERR_{month} \leq 15\%$;
- $ERR_{averageyear} \leq 10\%$;
- $MBE \leq 5\%$;
- $CV(RMSE) \leq 15\%$.

This means that, with more or less significant savings in time and computational effort, and complexity, the simplified model can replace the most detailed one in the assessment of energy needs.

3.3.2 Building models

The two investigated buildings are typical constructions of the Italian residential stock, built during the sixties and seventies, often by a deep and dense transformation of urban areas and they are characterized by a reinforced concrete structural frame with uninsulated walls. They are included in an urban context (Figure 3.10), densely built as typical of an expansion neighborhood. Hereinafter, the buildings are denoted with the letters "A" and "B".

Figure 3.10: The dense residential districts built in Naples during the sixties and the seventies: from the top to the bottom (A) and vice versa (B).

Building A (see Figure 3.11-A, left side) is entirely occupied by residential dwellings, and it presents the longest facades oriented to the northeast and the southwest, respectively. Building B (see Figure 3.11-B) has the first two floors dedicated to retail sales and offices, while the rest (major part) is occupied by residential dwellings.

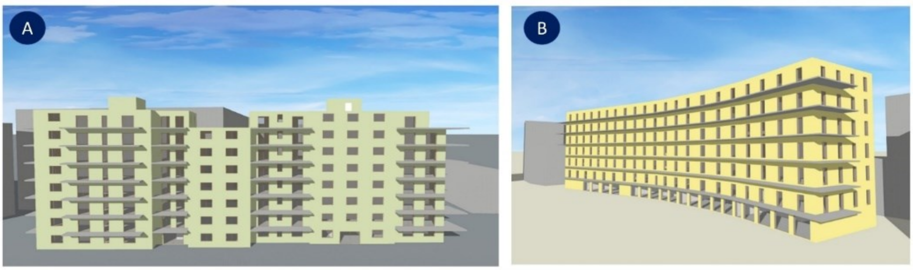

Figure 3.11: Renderings, starting from DesignBuilder® visualisation, of Building A (A) and Building B (B)

The thermophysical properties of both buildings and their main technical characteristics are described in [9]. For each building, several simulations are performed, by investigating the combinations of the following five parameters:

- the first parameter is the number of timesteps per hour in EnergyPlus simulations. Three possible values are here considered, i.e., 2, 4 and 6 timesteps per hour. This input is used as the driving timestep for heat transfer and load calculations;

- the second parameter considers the building in two different configurations: with the inter-building effect, thus the building with its urban context, and the standalone building, and thus without modeling the inter-building effect;
- the third parameter considers the different value of the shading setpoint and thus an activation threshold at 150, 300 or 450 W/m²;
- the fourth parameter takes into account the position of the shading system, which can be internal or external;
- the fifth parameter considers six types of shading systems, with different values of solar transmittance and solar reflectance, described in Table 3.3.

Table 3.3: Shading types

Shading Type	Solar transmittance	Solar reflectance	Description
1	0.1	0.2	Low reflect – Low trans
2	0.4	0.2	Low reflect – Medium trans
3	0.7	0.2	Low reflect – High trans
4	0.1	0.5	Medium reflect – Low trans
5	0.4	0.5	Medium Reflect – Medium trans
6	0.1	0.8	High reflect – Low trans

Globally, there are 222 combinations with reference to each building.

3.3.3 Description of the results

The discrepancies in heating, cooling, and lighting needs, between the simplified models and the detailed one, are assessed, initially, on annual basis, through the evaluation of the ERR, according to equation (3.2).

__Building A__

Table 3.4 and Table 3.5 show the ERR_{year} values, with reference to the thermal energy demand for space conditioning (heating + cooling) –

denoted as TED_{sc} – in the cases of "*internal*" and "*external*" shadings, respectively.

Table 3.4: ERR_{year} related to TED_{sc} for internally positioned shading systems.

Internal shading systems	***ERR_{year}* related to thermal energy demand for space conditioning**								
	Shading 1			**Shading 2**			**Shading 3**		
	150 W/m²	**300 W/m²**	**450 W/m²**	**150 W/m²**	**300 W/m²**	**450 W/m²**	**150 W/m²**	**300 W/m²**	**450 W/m²**
IBE* ts6** (detailed)	-	-	-	-	-	-	-	-	-
IBE ts4	0.1%	0.1%	0.1%	0.1%	0.1%	0.1%	0.1%	0.1%	0.1%
IBE ts2	1.8%	1.8%	1.9%	2.0%	1.9%	2.0%	2.1%	2.1%	2.1%
Isolated* ts6	-16.0%	-16.8%	-17.7%	-16.3%	-17.2%	-18.0%	-16.8%	-17.6%	-18.4%
Isolated ts4	-15.6%	-16.3%	-17.3%	-15.8%	-16.7%	-17.5%	-16.2%	-17%	-17.8%
Isolated ts2	-14.6%	-15.5%	-16.4%	-14.7%	-15.5%	-16.5%	-14.9%	-15.7%	-16.6%
Internal shading systems	**Shading 4**			**Shading 5**			**Shading 6**		
	150 W/m²	**300 W/m²**	**450 W/m²**	**150 W/m²**	**300 W/m²**	**450 W/m²**	**150 W/m²**	**300 W/m²**	**450 W/m²**
IBE ts6 (detailed)	-	-	-	-	-	-	-	-	-
IBE ts4	0.1%	0.1%	0.1%	0.1%	0.1%	0.1%	0.1%	0.1%	0.1%
IBE ts2	2.1%	2.1%	2.1%	2.3%	2.2%	2.2%	2.6%	2.4%	2.3%
Isolated ts6	-9.5%	-11.9%	-14.1%	-9.8%	-12.3%	-14.5%	-2.5%	-6.5%	-10.2%
Isolated ts4	-9.0%	-11.4%	-13.7%	-9.3%	-11.7%	-13.9%	-2.2%	-6.1%	-9.7%
Isolated ts2	-7.7%	-10.2%	-12.6%	-7.7%	-10.4%	-12.7%	-0.3%	-4.5%	-8.3%

* IBE = the interbuilding effect is modeled; Isolated = the building is modeled as standalone

**ts6 = 6 timesteps per hour; ts4 = 4 timesteps per hour; ts2 = 2 timesteps per hour

Based on these first evaluated indicators, two cases are chosen, the "best" and the "worst", for performing a deepening and thus an analysis on a monthly and daily basis. The choice is reduced to cases where the building is modeled as "standalone", obviously, because the aim is to verify whether the simplified models, which do not consider IBE, can replace the most detailed one with good reliability. The worst and best cases analyzed are, respectively:

- Shading type 3 (solar transmittance =0.7, solar reflectance =0.2), in the internal position with a shading setpoint =450 W/m² and a timestep value =6, (reported in Table 3.4, Isolated ts6) for which ERR = -18.4%;
- Shading type 4 (solar transmittance =0.1, solar reflectance =0.5) in the external position with a shading setpoint =150W/m² and a timestep value =4, (reported in Table 3.5, Isolated ts4), with an ERR = -0.1%.

For both cases, it has been provided a comparison with the most detailed model, which has the same shading system, position and operating setpoint of the model under evaluation.

Table 3.5: ERR_{year} related to TED_{sc} for externally positioned shading systems.

External shading systems	***ERR_{year}* related to thermal energy demand for space conditioning**								
	Shading 1			**Shading 2**			**Shading 3**		
	150 W/m²	**300 W/m²**	**450 W/m²**	**150 W/m²**	**300 W/m²**	**450 W/m²**	**150 W/m²**	**300 W/m²**	**450 W/m²**
IBE*ts6** (detailed)	-	-	-	-	-	-	-	-	-
IBE ts4	0.1%	0.1%	0.1%	0.1%	0.1%	0.1%	0.1%	0.1%	0.1%
IBE ts2	2.5%	2.4%	2.3%	2.4%	2.3%	2.2%	2.2%	2.2%	2.1%
Isolated* ts6	-1.5%	-5.5%	-9.3%	-8.3%	-11.1%	-13.4%	-15.4%	-16.5%	-17.4%
Isolated ts4	-1.2%	-5.0%	-8.8%	-7.8%	-10.5%	-12.8%	-14.8%	-15.9%	-16.7%
Isolated ts2	0.8%	-3.5%	-7.4%	-6.2%	-9.3%	-11.5%	-13.5%	-14.7%	-15.5%
External shading systems	**Shading 4**			**Shading 5**			**Shading 6**		
	150 W/m²	**300 W/m²**	**450 W/m²**	**150 W/m²**	**300 W/m²**	**450 W/m²**	**150 W/m²**	**300 W/m²**	**450 W/m²**
IBE ts6 (detailed)	-	-	-	-	-	-	-	-	-
IBE ts4	0.1%	0.05%	0.1%	0.1%	0.1%	0.1%	0.05%	0.1%	0.1%
IBE ts2	2.5%	2.4%	2.3%	2.4%	2.3%	2.2%	2.6%	2.4%	2.3%
Isolated ts6	-0.3%	-4.6%	-8.7%	-7.1%	-10.4%	-12.9%	1.1%	-3.5%	-7.9%
Isolated ts4	-0.1%	-4.1%	-8.1%	-6.7%	-9.8%	-12.3%	1.3%	-3.1%	-7.4%
Isolated ts2	2.0%	-2.5%	-6.8%	-5.0%	-8.4%	-11.0%	3.5%	-1.3%	-6.0%

* IBE = the interbuilding effect is modeled; Isolated = the building is modeled as standalone

**ts6 = 6 timesteps per hour; ts4 = 4 timesteps per hour; ts2 = 2 timesteps per hour

Figure 3.12 reports the daily trends in thermal energy demand, for heating and cooling, for the detailed and simplified model, in the worst case, that is shading type 3, internal position and shading setpoint = 450 W/m² with a timestep value of 6.

It shows that the simplified model provides lower thermal energy demand for heating and a higher one for cooling. This phenomenon is clearly connected to the failure to consider the interbuilding effect in the simplified model. The lack of surrounding buildings, and the shadow effect produced by them, means that the building is more exposed to sunlight. This is a positive phenomenon in winter, which causes a reduction in energy demand, but negative in summer because of increasing solar gains.

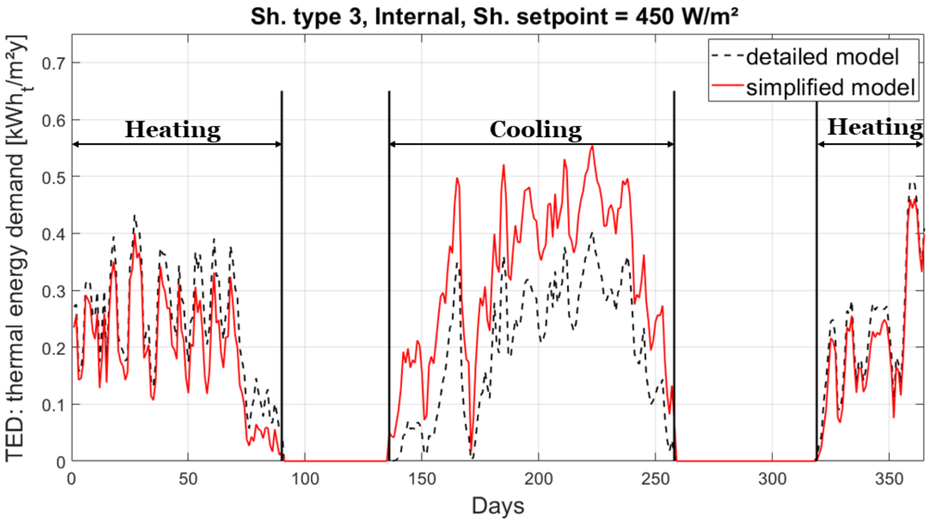

Figure 3.12: Thermal energy demand trend during the year (Shading type 3 in internal position, activation 450 W/m²)

In order to identify a compromise between model accuracy and computational burden, the following figures outline the simulation times.

In Figure 3.13, each point identifies a different combination of the above-described parameters (timestep, shading setpoint, construction with and without IBE), having fixed shading type and its position (i.e., shading type 3 and internal position).

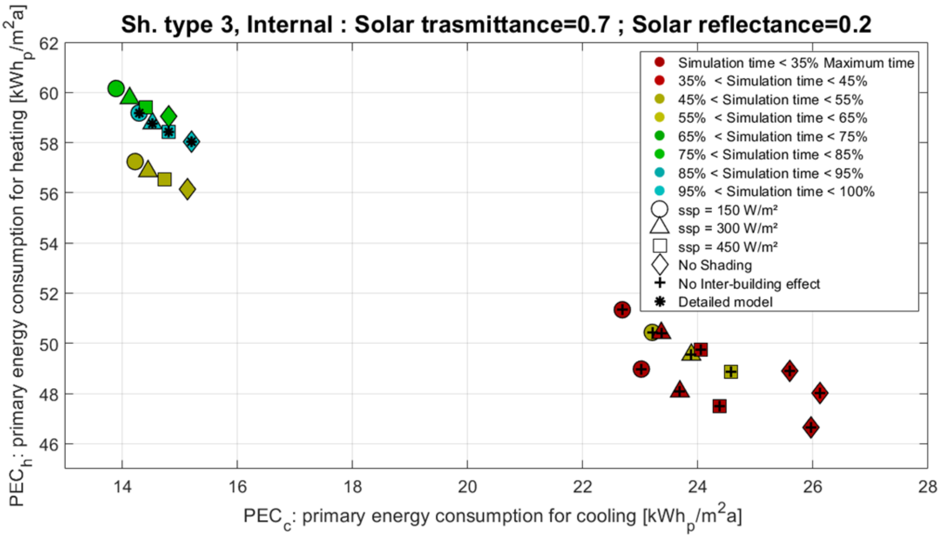

Figure 3.13: PEC heating vs PEC cooling for the different modeling approaches: Simulations times are outlined with reference to the most detailed model (maximum time) (Shading Type 3, Internal)

For each of these points, the simulation time is depicted in reference to the maximum one, related to the most detailed model. It's clear that the absence of the urban context determines a drastic reduction of such times, and thus of the required computational burden. However, to better understand this aspect, Figure 3.14 reports the difference in terms of primary energy consumption (PEC) for heating, cooling, and lighting, compared to the detailed model versus the simulation time. The simulation time is related to the characteristics of the computer, it is used an AMD Ryzen © 5 3600 @ 3.6 GHz processor.

The models not considering the IBE provide reductions of computational times between 50-70%, while the discrepancy in PEC prediction is less than 7%. The discrepancies are a measure of the error in annual primary energy consumption ERR_{year}.

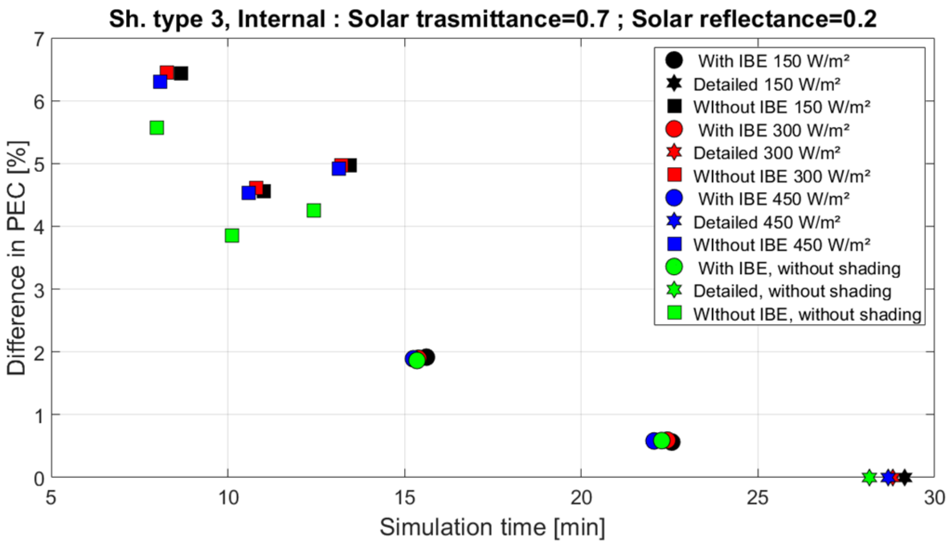

Figure 3.14: Differences primary energy consumption compared to the simulation time (Shading Type 3, Internal)

The use of simplified model (building standalone, timestep value = 6, with shading type 3, internal position and shading setpoint = 450 W/m²) compared to the detailed model (i.e., interbuilding effect, timestep value = 6 and the same shading type, position and operation setpoint of the simplified) leads to a 54.2% reduction in simulation time. The comparison between the detailed model and the simplified one, on monthly basis, is carried out both in terms of thermal energy demand and primary energy consumption, as shown in Table 3.6.

Table 3.6: Comparison between the detailed model and the simplified one for internal shading type 3 and shading set-point 450W/m²

	MBE (%)	CV(RMSE) (%)	TIME
TED	-18.6%	50%	-54.2%
PEC	5%	21.4%	

Despite the evident high reduction in terms of simulation times, from Table 3.6 it is clear that the use of the simplified model determines significant errors as concerns the TED, MBE=-18.4% and CV(RMSE)=50%. These are values very far from the acceptable ranges previously reported, MBE ≤ 5%, CV (RMSE) ≤ 15%. As concerns PEC predictions, from Table 3.6 it is observed a value of MBE at the limit of acceptable ones, MBE = 5% and a value of CV (RMSE) outside the allowed range. The use of this simplified model leads to an excessive loss of information, especially in reference to TED. This had already been highlighted on an annual basis, ERR_{year}=-18.4% from Table 3.4.

The same analysis for the best case is shown below. In the simplified model, building A is modeled as standalone, timestep value is 4, shading type is the number 4 of Table 3.3 (solar transmittance =0.1, solar reflectance =0.5), it is positioned externally and the shading setpoint is 150 W/m². The most detailed model simulates the same building, A, with IBE, a timestep value of 6 and the same shading systems, position and operation setpoint of the simplified model. Figure 3.15 reports the daily trends in thermal energy demand, for heating and cooling, for the detailed and simplified model, in the best case.

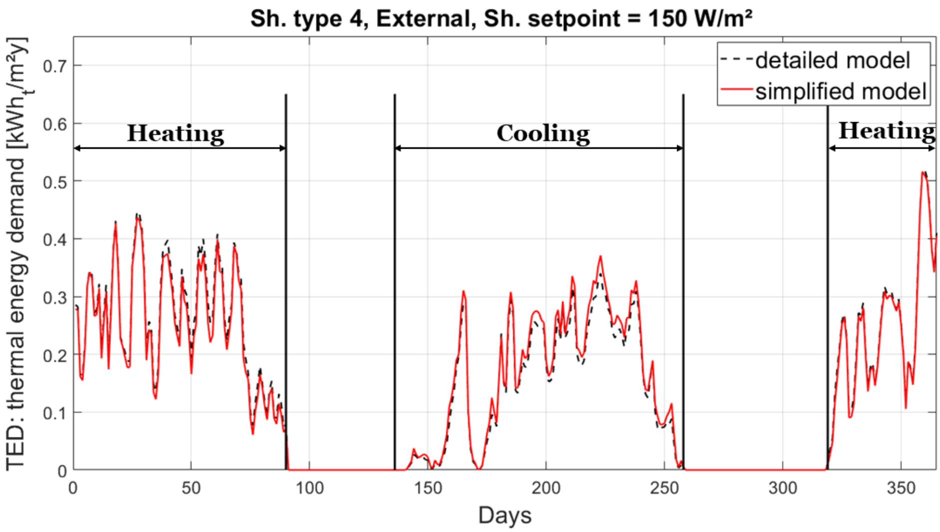

Figure 3.15: Thermal energy demand trend during the year (Shading Type 4 in external position, activation 150 W/m²)

The trend is the same as in the previous case, Figure 3.12, i.e., the simplified model provides lower thermal energy demand for heating and a higher one for cooling, but the deviation is less than in the previous case. In order to identify a compromise between model accuracy and computational burden, Figure 3.16 outlines the simulation times.

From this figure it is observed that the points representing the building modeled as standalone and those that represent it with the IBE, are much closer than in the previous case (Figure 3.13). This denotes a smaller deviation in terms of PEC_h and PEC_c between the simplified and the most detailed model.

At the same time, it is noted a variation of the simulation time, with the simplified models requiring a minor simulation time than the most detailed one. Furthermore, from Figure 3.16 it is observed that, with increasing the value of shading setpoint, the distance between the points, which represent the building with and without IBE, is greater.

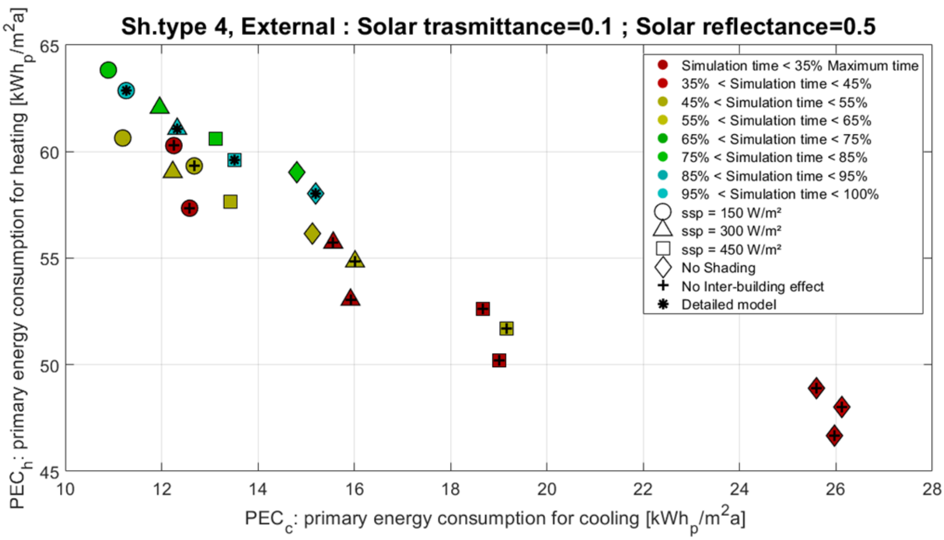

Figure 3.16: PEC heating vs PEC cooling for the different modeling approaches: Simulations times are outlined with reference to the most detailed model (maximum time) (Shading Type 4, External)

The Table 3.7 shows the evaluated indicators. The comparison between the detailed model and the simplified one, on a monthly basis, is carried out both in terms of thermal energy demand and primary energy consumption.

Table 3.7: Comparison between the detailed model and the simplified one for external shading type 4 and shading set-point 150W/m²

	MBE (%)	CV(RMSE) (%)	TIME
TED	-0.06%	7.3%	-61.1%
PEC	6.%	6.8%	

The use of simplified model (i.e., building standalone, timestep value = 4, with shading type 4, externally positioned and shading setpoint = 150 W/m²) compared to the detailed model (i.e., with the interbuilding effect, timestep value = 6 and the same shading type, position and operation setpoint of the simplified), leads to a 61.1% of saved computational time. The evaluated indicators, as concerns the TED, are MBE = -0.06% and CV(RMSE) = 7.3%. As concerns PEC predictions, MBE = 6% and CV(RMSE) = 6.84%. These values fall within the acceptable ranges MBE ≤ 5%, CV (RMSE) ≤ 15%, with the exception of MBE as regards the PEC. From the indicators shown, it can be observed the use of the simplified model can represent a good compromise, it would lead to limited deviations and a high reduction of the computational burden, in particular a simulation time of 61.1% less.

Building B

The analysis just described for the residential building has been repeated on the second examined building and is shown below. The ERR_{year} values with reference to the thermal energy demand for space conditioning (heating + cooling) – denoted as TED_{sc} – for the internal and external shadings, are evaluated and shown in the following tables.

From a first analysis of the data, it is observed that the deviations, in terms of TED, of each simplified model compared to the most detailed one, are low, much lower compared to the Building A. This trend is confirmed by the investigations carried out on a daily and a monthly basis shown below. The cases analyzed are the same as in the previous case (Building A), and thus:

- Shading Type 3 (solar transmittance =0.7, solar reflectance =0.2) in the internal position with a shading setpoint=450 W/m² and a timestep value =6, (reported in Table 3.8, Isolated ts6) for which ERR = -5.9%;

Table 3.8: ERR_{year} related to TED_{SC} for internally positioned shading systems

Internal shading systems	ERR_{year} related to thermal energy demand for space conditioning								
	Shading 1			Shading 2			Shading 3		
	150 W/m²	300 W/m²	450 W/m²	150 W/m²	300 W/m²	450 W/m²	150 W/m²	300 W/m²	450 W/m²
IBE* ts6** (detailed)	-	-	-	-	-	-	-	-	-
IBE ts4	0.3%	0.3%	0.3%	0.3%	0.3%	0.3%	0.4%	0.3%	0.3%
IBE ts2	0.5%	0.5%	0.4%	0.5%	0.4%	0.3%	0.4%	0.4%	0.3%
Isolated* ts6	-6.4%	-6.1%	-6.1%	-5.3%	-5.6%	-5.9%	-4.9%	-5.6%	-5.9%
Isolated ts4	-6.1%	-5.8%	-5.8%	-4.9%	-5.2%	-5.5%	-4.6%	-5.2%	-5.4%
Isolated ts2	-6.3%	-6.1%	-6.1%	-5.3%	-5.7%	-6.1%	-5.0%	-5.7%	-6.0%
Internal shading systems	**Shading 4**			**Shading 5**			**Shading 6**		
	150 W/m²	**300 W/m²**	**450 W/m²**	**150 W/m²**	**300 W/m²**	**450 W/m²**	**150 W/m²**	**300 W/m²**	**450 W/m²**
IBE ts6 (detailed)	-	-	-	-	-	-	-	-	-
IBE ts4	0.2%	0.2%	0.3%	0.3%	0.3%	0.3%	0.3%	0.3%	0.2%
IBE ts2	0.5%	0.5%	0.3%	0.5%	0.4%	0.4%	0.6%	0.4%	0.3%
Isolated ts6	-3.7%	-4.7%	-5.3%	-2.5%	-4.1%	-5.0%	-0.7%	-3.0%	-4.2%
Isolated ts4	-3.5%	-4.5%	-5.0%	-2.2%	-3.7%	-4.6%	-0.5%	-2.8%	-3.8%
Isolated ts2	-3.4%	-4.6%	-5.3%	-2.3%	-4.1%	-5.1%	-0.3%	-2.9%	-4.2%

* IBE = the interbuilding effect is modeled; Isolated = the building is modeled as standalone

**ts6 = 6 timesteps per hour; ts4 = 4 timesteps per hour; ts2 = 2 timesteps per hour

- Shading Type 4 (solar transmittance =0.1, solar reflectance =0.5) in the external position with a shading setpoint=150W/m² and a timestep value = 4, (reported in Table 3.9 Isolated ts4) for which the ERR = 0.9%.

Table 3.9: ERR_{year} related to TED_{SC} for externally positioned shading systems

External shading systems	ERR_{year} related to thermal energy demand for space conditioning								
	Shading 1			Shading 2			Shading 3		
	150 W/m²	300 W/m²	450 W/m²	150 W/m²	300 W/m²	450 W/m²	150 W/m²	300 W/m²	450 W/m²
IBE* ts6** (detailed)	-	-	-	-	-	-	-	-	-
IBE ts4	0.1%	0.1%	0.3%	0.2%	0.2%	0.3%	0.4%	0.3%	0.4%
IBE ts2	0.6%	0.5%	0.4%	0.5%	0.5%	0.4%	0.5%	0.5%	0.4%
Isolated* ts6	-0.1%	-2.6%	-4.0%	-2.0%	-3.8%	-4.8%	-4.5%	-5.4%	-5.7%
Isolated ts4	0.1%	-2.3%	-3.6%	-1.7%	-3.4%	-4.4%	-4.1%	-4.9%	-5.2%
Isolated ts2	0.4%	-2.4%	-3.9%	-1.7%	-3.7%	-4.8%	-4.5%	-5.4%	-5.8%
External shading systems	**Shading 4**			**Shading 5**			**Shading 6**		
	150 W/m²	**300 W/m²**	**450 W/m²**	**150 W/m²**	**300 W/m²**	**450 W/m²**	**150 W/m²**	**300 W/m²**	**450 W/m²**
IBE ts6 (detailed)	-	-	-	-	-	-	-	-	-
IBE ts4	0.3%	0.2%	0.3%	0.3%	0.3%	0.3%	0.2%	0.3%	0.3%
IBE ts2	0.7%	0.4%	0.4%	0.5%	0.5%	0.4%	0.7%	0.5%	0.4%
Isolated ts6	0.6%	-2.3%	-3.8%	-1.2%	-3.5%	-4.7%	1.4%	-1.9%	-3.6%
Isolated ts4	0.9%	-1.9%	-3.4%	-0.9%	-3.1%	-4.2%	1.7%	-1.5%	-3.2%
Isolated ts2	1.2%	-2.0%	-3.6%	-0.9%	-3.3%	-4.6%	2.0%	-1.5%	-3.4%

* IBE = the interbuilding effect is modeled; Isolated = the building is modeled as standalone

**ts6 = 6 timesteps per hour; ts4 = 4 timesteps per hour; ts2 = 2 timesteps per hour

The general results are in line with those obtained for the previous investigated building. From Figure 3.17, which shows the comparison of the thermal energy requirement between the detailed model and the simplified one, it is observed that the simplified model has a lower thermal energy requirement for heating and a higher one for cooling.

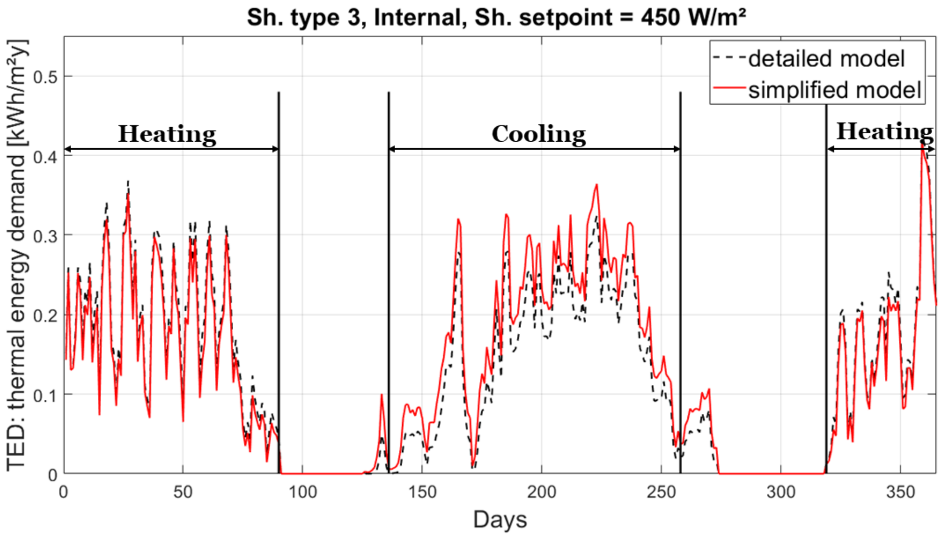

Figure 3.17: Thermal energy demand trend during the year (Shading type 3 in internal position, activation 450 W/m²)

The reason is once again, due to the failure to consider the interbuilding effect in the simplified model. The building is more exposed to sunlight because there aren't any nearby buildings to cast shadows on it. This phenomenon is beneficial in the winter because it lowers energy consumption, but it is detrimental in the summer because of rising solar gains. In order to identify a compromise between model accuracy and computational burden, the following figures (Figure 3.18,Figure 3.19) outline the simulation times. From Figure 3.18 it is deduced that the lack of the urban backdrop results in a significant decrease in such times and, thus, in the required computing load.

Conversely, from Figure 3.19 it is observed that while the difference in PEC prediction is less than 6.5%, the models that do not consider the IBE offer a reduction of the calculation times between 37.5 and 60%.

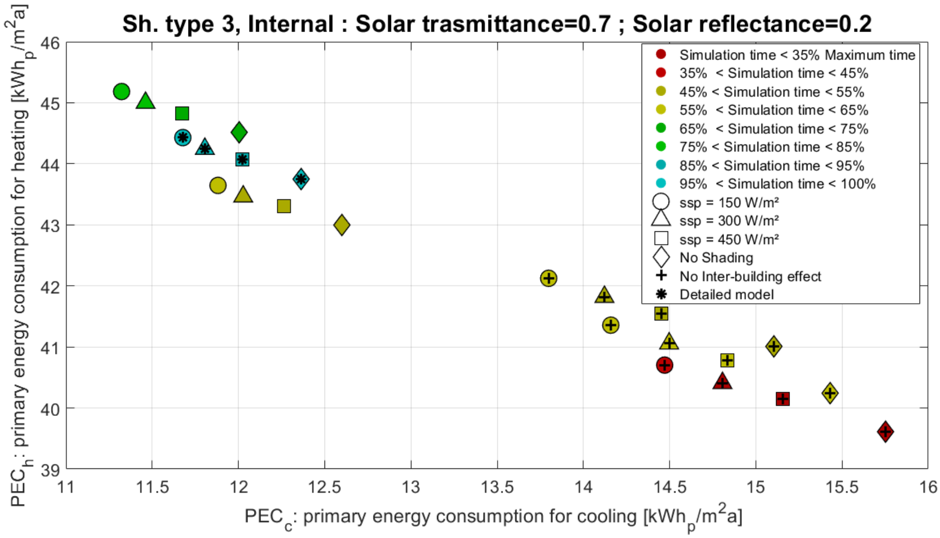

Figure 3.18: PEC heating and PEC cooling for different modeling approaches and simulation time (Shading type 3 in internal position)

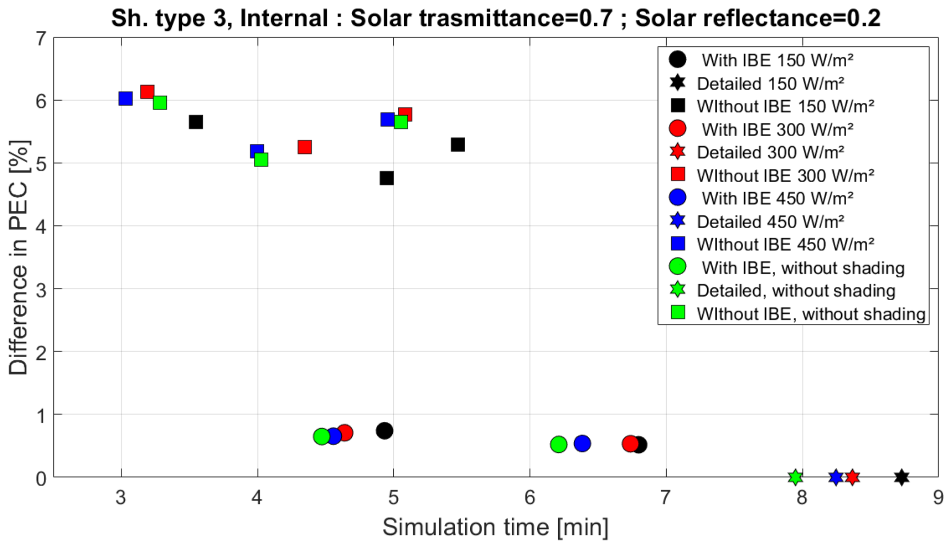

Figure 3.19: Differences in primary energy consumption compared to the simulation time (Shading Type 3 in internal position)

The use of the simplified model (i.e., building standalone, timestep value = 6, with shading type 3, internal position and shading setpoint = 450 W / m²) compared to the detailed model (i.e., with interbuilding effect, timestep value = 6 and the same shading type, position and operation setpoint of the simplified), determines a 40.3% reduction in simulation time (Table 3.10). Also in this case, the comparison between the detailed model and the simplified one, on a monthly basis, is carried out both in terms of thermal energy demand and primary energy consumption.

Table 3.10: Comparison between the detailed model and the simplified one for internal shading type 3 and shading set-point 450 W/m²

	MBE (%)	CV(RMSE) (%)	TIME
TED	-5.8%	18.3%	-40.3%
PEC	5.7.%	10.9%	

The use of the simplified model determines significant errors as concerns the TED, MBE=-5.8% and CV(RMSE)=18.3%. These values are slightly outside the acceptable ranges previously reported, MBE ≤ 5%, CV (RMSE) ≤ 15%. Moreover, for what concerns the PEC predictions, from Table 3.10 it is observed a value of MBE slightly outside the allowed range MBE=5.7%, and a value of CV (RMSE) acceptable, CV(RMSE)=10.9%. The use of this simplified model leads to a slight loss of information.

The same analysis for the other case - and thus the external shading type 4 (solar transmittance =0.1, solar reflectance =0.5), activation with solar radiation of 150 W/m² is shown below. In the simplified model, building B is modeled as standalone. The most detailed model, also in this case, simulates the same building, with IBE, a timestep value of 6 and the same shading systems, position, and operation setpoint of the simplified model. Figure 3.20 reports the daily trends in thermal energy demand, for the space heating and cooling, with reference to the detailed and simplified model.

An almost total coincidence and perfect overlapping of the two trends is observed. There are very few points where the typical phenomenon of neglecting the IBE can be observed (i.e., a lower thermal energy demand for heating and a higher need of cooling), but these gaps are really imperceptible.

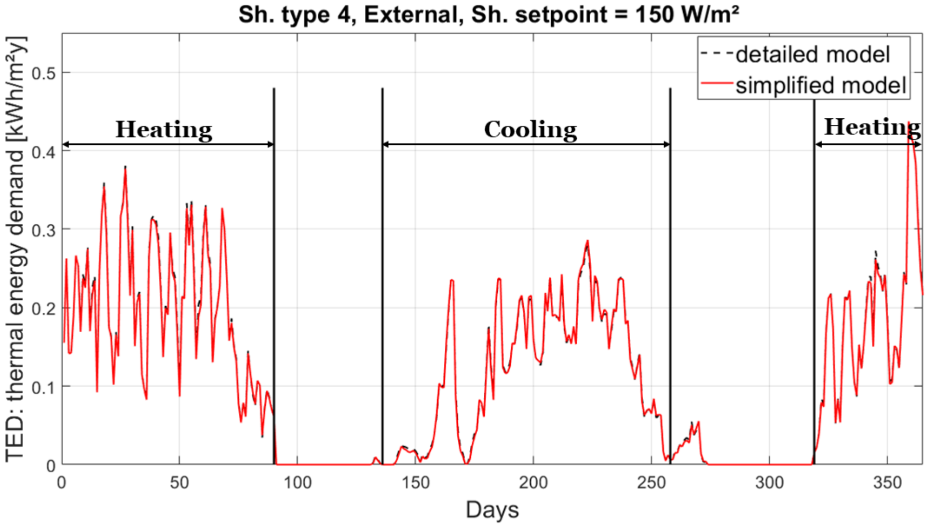

Figure 3.20: Thermal energy demand trend during the year (Shading type 4 in external position, activation 150 W/m²)

To consider the computational burden Figure 3.21 outlines the simulation times. Here, it can be observed that the points related to the building modeled as standalone and those representing it with the IBE, are much closer than in the previous case (Figure 3.18). This denotes a smaller deviation in terms of PEC_h and PEC_c between the simplified and the most detailed model. At the same time, it is noted a variation of the simulation time, with the simplified models requiring a minor simulation time than the most detailed one. Furthermore, from Figure 3.21, it can be observed that, with the increase of the shading setpoint value, the distance between the points, which represent the building with and without IBE, increases. This denotes an increasing deviation in terms of PEC_h and PEC_c between the simplified and the most detailed model.

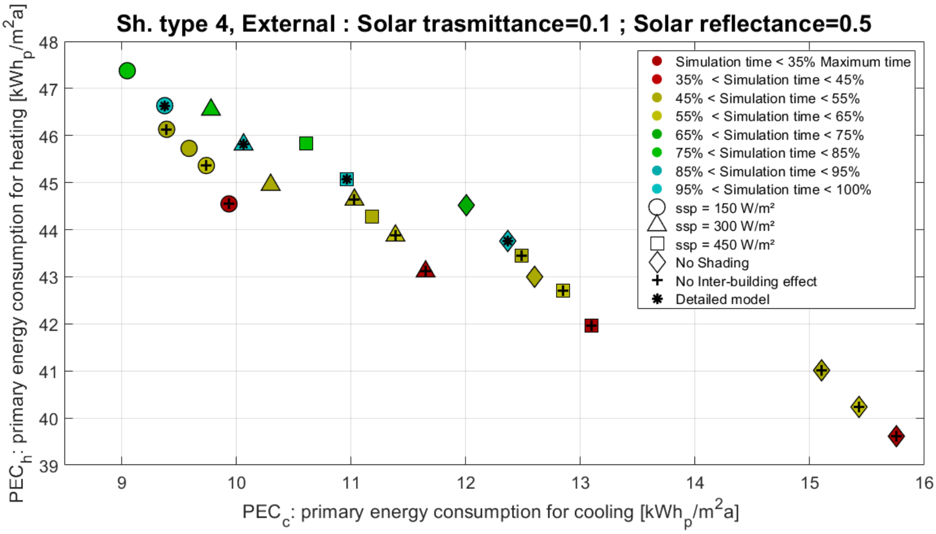

Figure 3.21: PEC heating and PEC cooling for the different modeling approaches and simulation time

Table 3.11 shows the evaluated indicators with reference to both thermal energy demand and primary energy consumption.

Table 3.11: Comparison between the detailed model and the simplified one for external shading type 4 and shading set-point 150W/m²

	MBE (%)	CV(RMSE) (%)	TIME
TED	0.87%	1.6%	-45.8%
PEC	1.3.%	2.9%	

Some comments follow also in this case; it can be seen that the use of the simplified model (building standalone, timestep value = 4, with shading type 4, externally positioned and shading setpoint = 150 W/m²) compared to the detailed model (i.e., inclusive of interbuilding effect, timestep value = 6 and the same shading type, position and operation setpoint of the simplified), implies a reduction of computational time of about 45.8%. The indicators evaluated, by the comparison between the most detailed and the simplified model, as regards the TED, are MBE=0.87% and CV(RMSE)=1.6%. As concerns PEC predictions, the MBE and

CV(RMSE) are 1.6% and 1.9%, respectively. Finally, all values perfectly fall within the acceptable ranges MBE ≤ 5%, CV (RMSE) ≤ 15%. From the evaluated indicators, it is deduced that the use of the simplified model represents a good compromise between accuracy and computational burden.

3.3.4 Discussion

The achieved findings showed that IBE can highly influence building energy needs, but, at the same time, there are cases where this effect is minimal and the use of simplified models can provide reliable predictions with simulation time reductions.

In particular, it is observed that IBE has a greater impact on the first case study (Building A) because it is surrounded by other buildings on all four sides, and thus the urban context is denser. Conversely, the second case study (Building B) has one of the longest sides fully exposed, and thus the IBE is less influential. This phenomenon is evident both from an analysis on an annual and monthly basis. For building A, ERR_{year} reaches values of -18.4% while for building B the maximum value is -6.3%.

For both buildings, two configurations were analyzed on a monthly basis:

1. building modeled as standalone, timestep 6, shading type 3, internal position with shading set-point of 450 W/m²;
2. building modeled as standalone, timestep 4, shading type 4, external position with shading setpoint of 150 W/m².

The results showed that the first configuration causes high errors and so it is unacceptable as a simplification of the more detailed model (IBE is modeled, timestep 6, the same shading systems, position and operation setpoint of the simplified model). As been previously mentioned, it is also evident on a monthly basis that IBE has a greater impact on building A.

For instant- in the case of Shading Type 4 (Table 3.3), external position and shading set-point 150 W/m² - the simulation quality indicators are:

- Building A: MBE = 6% and CV (RMSE) = 6.8%;
- Building B: the MBE =1.3 CV (RMSE) =2.9%.

However, it is possible to make a comparison in which the type of shading is the only parameter that varies. For example, choosing the case in which the building is modeled as standalone, timestep = 4, the shading is positioned externally, and the shading setpoint is equal to 150 and considering shading types 3 and 4 from the comparison with the most detailed models is obtained:

- for building A: ERR_{year} value for Shading Types 3 and 4 are -14.8% and -0.1%, respectively (see Table 3.5);
- for building B: ERR_{year} value for Shading Types 3 and 4 are -4.1 and 0.9%, respectively (see Table 3.9).

This implies that the intrinsic properties of the shading system have an effect. More in detail, the shadings differ for the position but also for what concerns the radiative characteristics:

- Shading Types 3: solar transmittance = 0.7, solar reflectance = 0.2;
- Shading Types 4: solar transmittance = 0.1, solar reflectance = 0.5;

Therefore, in a building whose shading system has a low solar transmittance value and a medium solar reflectance, it is acceptable to consider a simplified model in the assessment of energy needs.

Furthermore, the study reveals that as the setpoint shading value increases, using the standalone building model, the error committed in assessing the building's energy needs increases. This phenomenon is more relevant when the shading system is positioned externally (as shown in Figure 3.16 and Figure 3.21). On the other hand, if attention is paid to comparison of the cases in which the IBE is modeled, and the simulation timestep is the only parameter that changes, it is observed:

- for Building A, the ERR_{year} values which oscillate between 0.1% and -2.5%;
- for Building B, the ERR_{year} values which oscillate between 0.1% and 0.7%.

It is evident that these errors are low, but the savings are quite significant in terms of simulation times:

- for the Building A, the savings range between 22.1% and 47%, while when the building is modeled as standalone it ranges between 52.6% and 72.4%;
- for Building B, the savings range between 19% and 45.2%, while when the building is modeled as standalone it ranges between 35.6% and 63.4%.

However, the study confirms that when the timestep decreases, there is less accuracy in the assessment of the building's energy needs. Usually, the lack of accuracy is limited and often acceptable.

3.3.5 Conclusions about the inter-building effect impacts

The study aims at understanding whether it is essential to model the inter-building effect for reliable energy simulations. In this vein, two real buildings located in Naples (South Italy, Mediterranean coastline) have been investigated. The energy performance of the buildings is simulated via different modeling approaches: different shading systems, different shading set-points, no shading, no inter-building effect (IBE) and the pair no shading and no inter-building effect (simplest model).

For each approach different simulation timesteps have been considered. The coupling between EnergyPlus and MATLAB® is implemented to compare the predictions of thermal and primary energy demands of the

simplified approaches versus to the most detailed one (IBE, shading systems, highest number of timesteps).
The main findings show that the IBE can highly affect building energy needs, but, at the same time, there are cases in which this effect is minimal and the use of simplified models can provide reliable predictions – mean bias error lower than 1.5% – with reductions of simulations times of 46% (building B, Shading type 4, external shading position, shading set-point 150W/m²).
Notably, the IBE has a higher impact on the first case study (Building A) because it is surrounded by other buildings on all four sides, and thus the external urban context is denser. Conversely, the second case study (Building B) has one of the longest sides completely exposed, and thus the IBE is less influential. This phenomenon is evident both from an analysis on an annual and monthly basis. It is important that the model gives reliable results at an annual level since the building's energy performance generally refers to the annual span. Furthermore, a reliable prediction of the model on an annual basis can allow a robust assessment of energy performance and also of operating costs.
In addition, other key outcomes unveil that the intrinsic properties of the shading type influence the possibility of utilizing a simplified model without IBE: its use is acceptable if the solar transmittance is low. Also, the shading set-point is an influential parameter: as it increases, information lost in the transition from the most detailed model to the simplified one also increases.
Finally, the study offers deeps insights into the possible approaches for accurate building modeling answering the question: Is it fundamental to model the interbuilding effect for reliable building energy simulations? In this regard, the answer based on the performed investigation is that it depends, so that not a unique way can be chosen, definitively.

In detail, the configuration of the building and the external context are two fundamental aspects for the realization of a model. They should be analyzed before the modeling phase to evaluate whether it is actually essential to model the IBE. In this regard, modeling of the interbuilding effect (IBE) is not fundamental when:

- the building is not completely surrounded by other buildings, as is the case of Building B;
- the building has externally positioned shielding systems characterized by low solar transmittance values and medium/high values for solar reflectance;
- the solar setpoint value at which the screens are activated is low.

In these cases, the use of a simplified model determines acceptable discrepancies in the assessment of the building's energy needs. Using lighter models, requiring a lower computational power and effort, could be a huge benefit, especially in the energy optimization phases.
Indeed, the use of a simplified, accurate model with compatible calculation times, can speed up the study, can allow to investigate more solutions and allows to obtain the right combination in less time, with improved computational effort.

3.4 Conceptualization, validation and development of EMAR

In this paragraph, a novel accurate but user-friendly tool for building modeling and energy simulation is proposed. The tool is denoted as EMAR, because it is based on the advanced coupling between **E**nergyplus and **MA**tlab® addressing **R**esidential buildings, which are a major part of the existing stocks. Figure 3.22 represents the steps described in the following subsections.

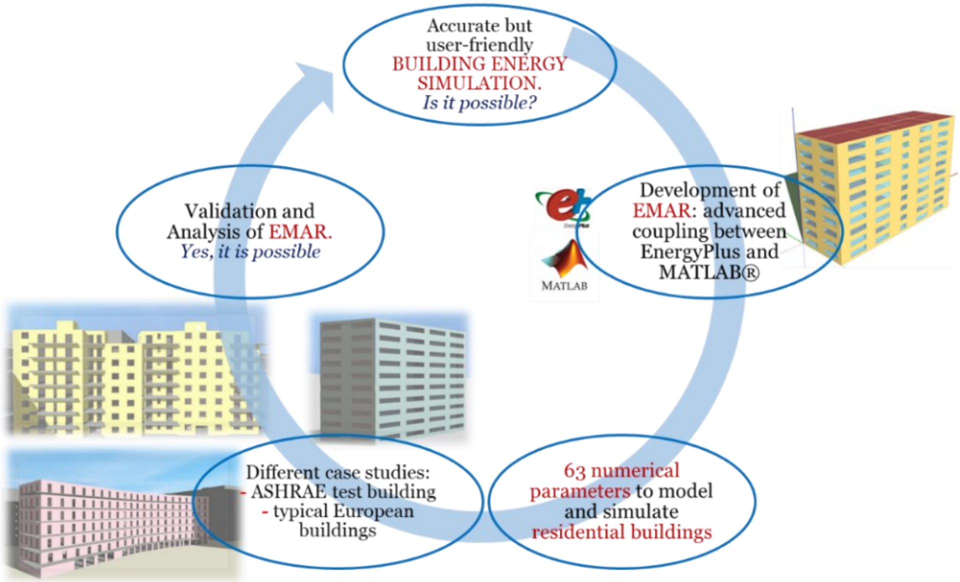

Figure 3.22: Graphical representation of the steps for the development of EMAR

3.4.1 Building energy simulation: Background

Several software and engines are available, and the best choice depends on many factors such as the aim (*e.g.,* accurate prediction or energy labeling), the clients' needs, the designer skills. For instance, Poel *et al.* [10] proposed a comprehensive overview of the most used tools to assess the energy performance of residential buildings. Globally, the approaches can be classified in white-box, grey-box and black-box models [11],[12]. The white-box models are totally based on a theoretical structure developed through physical laws [13],[14]. The grey-box models couple a theoretical structure with measured or simulated data, ensuring higher adherence to reality [15],[16]. The black-box models provide hidden functions that correlate the outputs to the inputs (building characteristics), and are generally totally data-driven, based on the processing of historical data without the detailed knowledge of on-site physical information [11]. They usually apply meta-modeling, developing surrogate models through statistical regression, support vector machine (SVM), artificial neural networks (ANNs) or further machine learning techniques [17]. Definitely, the most consistent choice is using suitable BES tools that perform reliable dynamic simulations [18], *e.g.,* EnergyPlus, TRNSYS, ESP-r, IDA ICE, which provide accurate predictions of energy needs for the investigated scenarios after the proper development of calibrated building models. These tools are widely employed by the scientific community given their high capability and reliability [19]. They are white-box models based on robust and complex theoretical structures of physical laws, but they are often used as a sort of black-box models since the user is rarely able to handle such theoretical structures. Nevertheless, as outlined in [11], their high accuracy derives from high complexity in their use and low running speed, which do not allow their wide diffusion in the professionals' community. This issue is amplified when BEO is applied because optimization algorithms need to be applied to explore large solutions domains, thereby increasing the computational burden. That is why building professionals usually prefer other tools based on white box models, which apply simplified assumptions, such as semi-steady-state conditions, resistance-capacitance (RC) equivalent networks, degree day method, temperature frequency method, residential load factor method [11]. These latter ensure user-friendliness and high running speed at the cost of lower accuracy [11]. Therefore, as mentioned, they are often unreliable because they cannot properly simulate the dynamics in weather conditions and building performance as concerns envelope, energy systems, use and operation, such as schedules of occupation or HVAC (heating, ventilating and air conditioning) setpoints.

Finally, there is an open issue that should be faced:

- the community of building professionals has few user-friendly but reliable options for the prediction of building energy performance.

As highlighted in [11], this is a critical issue because building energy simulation is fundamental for different crucial aims and functions, such as: *i)* optimization of building energy design/retrofit, *ii)* demand side management, *iii)* energy labeling, *iv)* energy mapping of geographical areas, *v)* establishing benchmarks for multi-scale building communities. Accordingly, the attention of building scientists, policymakers and all involved stakeholders is increasingly focused on such an issue, struggling for the development of new BES tools that can have a wide diffusion among practitioners [20]. In this vein, Ascione *et al.* [21] proposed a user-friendly tool denoted as EMA by coupling EnergyPlus and MATLAB® to predict different indicators related to building energy, environmental and economic performance. However, such tool was usable only for simplified office buildings, and was not subjected to a robust validation. The inter-building effect (abbreviated "IBE"), that is a further aspect of building models' simplification has been addressed in the previous paragraph [9], investigating whether IBE is fundamental or not for reliable simulations. The outcomes showed that the IBE can be neglected with good reliability in some cases, *e.g.,* when there is an intensive use of shading systems, but the study did not answer the approached issue because a complex BPS tool – *i.e.,* EnergyPlus – was used. Thus, the IBE can be often neglected with acceptable approximation in building modeling, but which BES tool can be user-friendly and reliable? Cucca and Ianakiev [22] combined DesignBuilder® (and thus EnergyPlus) with Modelica-Dymola to achieve a simpler and clearer representation of energy systems and associated control schemes, but building modeling still featured high complexity considering the computational burden for co-simulation too. In this regard, building information modeling (BIM) software can help the users in combining different tools for a comprehensive and interactive design process, including BES tools to predict building energy performance at different design stages [23],[24]. However, the issue is still open because a smart and flexible tool is required, able to perform accurate energy simulations extrapolating the required inputs data from the building model under development.

3.4.2 Contribution of the study

Further similar papers may be cited but the scientific literature shows a crucial knowledge gap, *i.e.,* to the authors' knowledge, there are no validated user-friendly BES tools that ensure accurate predictions of dynamic building energy performance requiring only few numerical inputs. Such a tool would provide worthy contributions to the body of knowledge to promote the transition to a low energy and low carbon building stock, fundamental in the path of sustainable development. Indeed, it would ensure:

- user-friendly, fast but reliable predictions of building energy performance and energy labeling;
- easy/flexible integration in optimization and BIM frameworks to address building energy design/retrofit, thereby supporting the diffusion of robust building energy optimization in the community of professionals;
- easy/flexible integration in frameworks for the large-scale analysis of building energy performance, thereby supporting the energy transition of whole neighborhoods, districts and stocks, as well as the optimization of public energy policies for the building sector.

In this regard, the study proposed in this section of the Thesis aims at filling such a knowledge gap by proposing a reliable but user-friendly and flexible tool for building energy modeling and simulation, which can provide the mentioned novel contributions. The tool is denoted as EMAR because it is based on the advanced coupling between EnergyPlus [25] and MAtlab® [26] addressing Residential building. It requires only (a maximum of) 63 numerical inputs, and offers several possible outputs concerning energy (environmental) and economic performance. It derives from a deep enhancement of EMA [21], by increasing the level of detail in building modeling, addressing also residential buildings, and performing a robust validation against detailed EnergyPlus models of an ASHRAE test building and of two typical European buildings. As discussed, EMAR can be a precious tool for building stakeholders to perform user-friendly but accurate energy simulations, thereby supporting computer-aided design and optimization with a view to urban sustainable growth.

3.4.3 Material and methods: EMAR

This sub-section proposes EMAR, which is a novel, user-friendly building energy simulation (BES) tool, based on the advanced coupling between Energyplus and MAtlab®, to predict the energy performance of Residential buildings, which are a major part of existing stocks, worldwide. The following steps will be described in detail below:

- Framework;
- Inputs;
- Outputs;
- Novelties compared to EMA [21].

Let's start with the description.

Framework

As shown in the framework of Figure 3.23, EMAR works under MATLAB® environment and needs only numerical inputs to generate simplified building models and perform accurate energy simulations. No drawings, no schemes of energy systems, no deep modeling expertise are required, but only few numbers. The available outputs are numerous referring to energy, environmental, economic performance as well as thermal comfort.

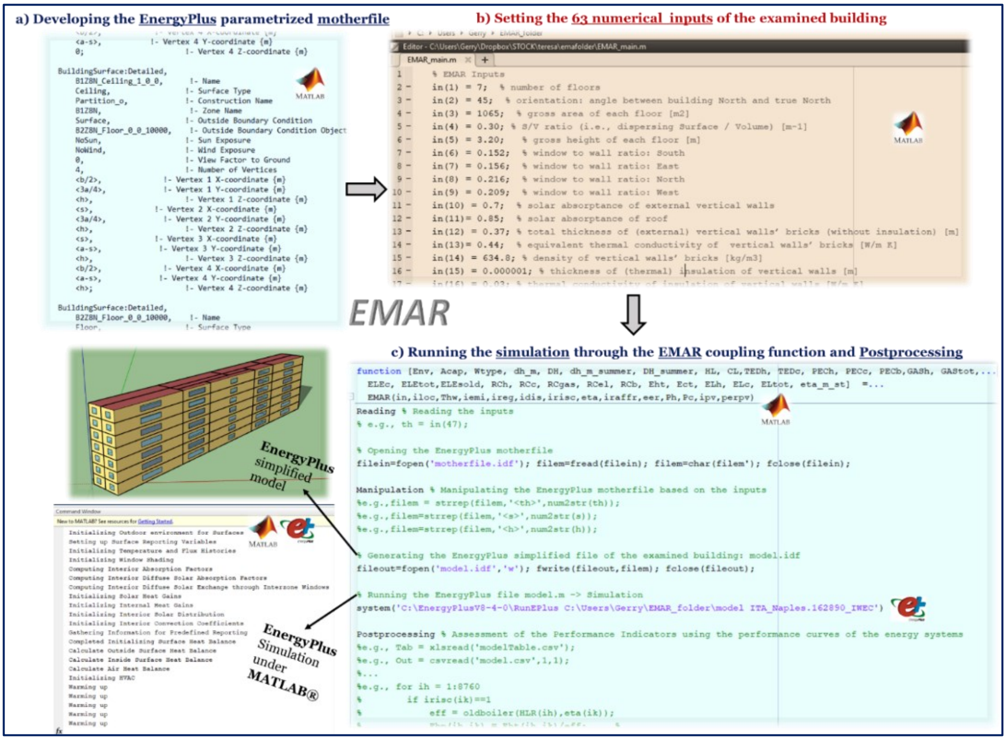

Figure 3.23: EMAR framework

EnergyPlus is used as simulation engine because of its high capability and reliability that make it the most used BES engine for building energy optimization [27]. Notably, EnergyPlus needs text-based inputs, the so-called *.idf* files, and provides *.csv* (comma separated variables) outputs. However, when it is used stand-alone, EnergyPlus features high modeling complexity and needs deep simulation expertise, especially as concerns building geometry and energy systems. Therefore, EMAR uses MATLAB® to simplify building modeling and simulation as well as for post-processing, offering a simple user-interface that requires only 63 numerical inputs.

The framework is based on an EnergyPlus parametrized mother-file *.idf* (text-based, see Figure 3.23a), where the building characteristics related to geometry, envelope and systems are parametrized. This means that parameters are present instead of typical EnergyPlus input data. Each parameter is enclosed between the symbols “<” and “>”, as shown for example in Figure 3.23a.

An EMAR simulation related to a specific building comprises the following steps, performed under MATLAB® environment:

step 1) the user sets: *i)* the 63 EMAR inputs (Figure 3.23b); *ii)* the weather data file to be employed, which can be downloaded from EnergyPlus website [28]; *iii)* the required outputs, *i.e.,* performance indicators, to be assessed;

step 2) MATLAB® runs an EnergyPlus simulation via a coupling function denoted as EMAR (Figure 3.23c) and collects the simulation output data (*.csv*), which refer to a typical climatic year;

step 3) a post-process MATLAB® code simulates the performance of the energy systems, and provides the required outputs.

In particular, when the user sets the inputs (**step 1**), EMAR generates a specific *.idf* file for the investigated building from the mother-file, properly replacing the mentioned parameters (“<>”). The model presents a simplified geometry (Figure 3.24a), as in [21], [29], because a regular rectangular plan is assumed with equal-height floors, setting a thermal zoning (Figure 3.24b) typical of the investigated use destination. Two dwellings per floor are considered, each dwelling subdivided in two night-zones and two day-zones, according to standard architectural designs. The two dwellings of each floor are separated by a landing, *i.e.,* a circulation zone. In addition, the windows’ positions are fixed, but the “window to wall ratio” (%) can vary for each exposure. Six windows are assumed for each dwelling and one for each landing, having half area compared to the other windows of the same façade, with a symmetrical layout (Figure 3.24a). The vertical centre of the windows is at half height of the floor. The windows' height is equal to 1.5 m, if sufficient to ensure the window to wall ratio set by the user, or 2.4 m otherwise, while the width is computed from height and window to wall ratio [21],[29]. The mentioned simplifications about the building geometry facilitate the parameterization process, and these are suitable for most buildings, given the high percentage of rectangular shapes [29].

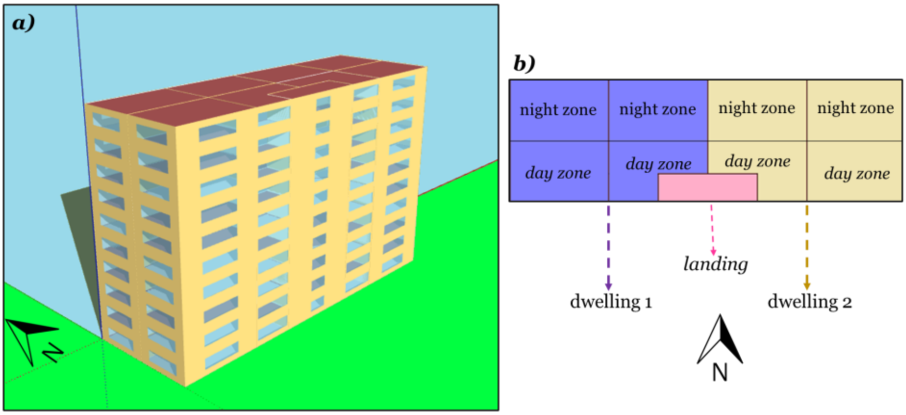

*Figure 3.24: **a)** 3D view of a building model developed through EMAR; **b)** plan view and thermal zones*

Then, **step 2** is performed. EnergyPlus simulation's output data consist of the hourly values for each dwelling of:

- thermal energy demands for space heating and space cooling;
- electricity demands for direct electric uses, *i.e.,* electrical equipment and artificial lighting;
- thermal comfort indicators;
- produced energy by photovoltaics, if present.

Finally, in **step 3**, the post-process MATLAB® code handles such data and applies the performance curves of the energy systems, which can be also set by the user. These curves provide the efficiency of each system as a function of nominal value at rated conditions, hourly part load ratio, temperatures of heat transfer fluid and outdoor environment (only for some systems such as air-source chillers and heat pumps). A database developed in MATLAB® enables to associate each technology chosen by the user with a proper performance curve. Using such curves, primary energy conversion factors and specific energy costs, the hourly values of thermal energy demand are converted into primary energy consumption and related costs. The on-site electricity conversion by possible photovoltaic systems is taken into account through hourly energy balances. Surplus energy can be stored and then used, sold to the grid or wasted. Finally, the required outputs are assessed both at dwelling and building levels, concerning energy, environmental, economic performance, thermal comfort as well as the geometry and thermal characteristics of the building envelope.

Inputs

The 63 EMAR numerical inputs (denoted with “i”) are shown in Table 3.12, where they are classified in four groups, related to geometry, envelope, HVAC and photovoltaics, respectively.

Notably, no inputs related to building operation are present because only residential cases are addressed. Therefore, the values and schedules of building-plants use, occupation, operation of electric equipment and artificial lighting are set according to typical residential buildings from previous studies [9], [30],[31],[32] and can be modified depending on the examined case study. Domestic hot water consumption is considered fixed, equal to 25 kWh_p/m^2a, as typical of Italian dwellings [33], since it is not affected by the complex dynamics of the building envelope/systems. In any case, this value can be modified according to the case study. So this does not prejudice the general code’s reliability. It is noticed that the framework can be easily enhanced to consider different use destinations.

Table 3.12: EMAR inputs

EMAR inputs	
<u>Geometry</u> i_1) number of floors i_2) orientation: angle between building north and true north i_3) gross area of each floor [m^2] i_4) S/V ratio (*i.e.,* dispersing surface / volume) [m^{-1}] i_5) gross height of each floor [m] i_6) window to wall ratio: south i_7) window to wall ratio: east i_8) window to wall ratio: north i_9) window to wall ratio: west <u>Envelope</u> i_{10}) solar absorptance of walls i_{11}) solar absorptance of roof i_{12}) thickness of walls' bricks (without insulation) [m] i_{13}) equivalent thermal conductivity of walls' bricks [W/m K] i_{14}) equivalent density of walls' bricks [kg/m^3] i_{15}) thickness of (thermal) insulation of walls [m] i_{16}) thermal conductivity of insulation of walls [W/m K] i_{17}) equivalent density of insulation of walls [kg/m^3] i_{18}) position of insulation of walls i_{19}) thickness of roof block (without insulation) [m] i_{20}) equivalent thermal conductivity of roof block [W/m K] i_{21}) equivalent density of roof block [kg/m^3] i_{22}) thickness of (thermal) insulation of roof [m] i_{23}) thermal conductivity of insulation of roof [W/m K] i_{24}) equivalent density of insulation of roof [kg/m^3] i_{25}) position of insulation of roof i_{26}) thickness of ground-floor block (without insulation) [m] i_{27}) equivalent thermal conductivity of ground-floor block [W/m K] i_{28}) equivalent density of ground-floor block [kg/m^3] i_{29}) thickness of (thermal) insulation of ground-floor [m] i_{30}) thermal conductivity of insulation of ground-floor [W/m K] i_{31}) equivalent density of insulation of ground-floor [kg/m^3] i_{32}) position of insulation of ground-floor i_{33}) fraction of dwellings with single-glazed, aluminum framed windows i_{34}) fraction of dwellings with single-glazed, wood framed windows	i_{35}) fraction of dwellings with double-glazed, aluminum framed windows i_{36}) fraction of dwellings with double-glazed, wood framed windows i_{37}) shading systems' type: south i_{38}) shading systems' type: east i_{39}) shading systems' type: north i_{40}) shading systems' type: west i_{41}) shading systems' position: south i_{42}) shading systems' position: east i_{43}) shading systems' position: north i_{44}) shading systems' position: west i_{45}) shading systems' radiation setpoint: south [W/m^2] i_{46}) shading systems' radiation setpoint: east [W/m^2] i_{47}) shading systems' radiation setpoint: north [W/m^2] i_{48}) shading systems' radiation setpoint: west [W/m^2] i_{49}) equivalent thickness of horizontal partitions [m] <u>Heating, Ventilating and Air Conditioning (per dwelling)</u> i_{50}) heating setpoint temperature [°C] [vector]* i_{51}) cooling setpoint temperature [°C] [vector]* i_{52}) efficiency of heating distribution-emission-regulation system [vector]* i_{53}) supply water temperature of heating terminals [vector]* i_{54}) type of heating generation system [vector]* i_{55}) efficiency of heating generation system [vector]* i_{56}) type of cooling generation system [vector]* i_{57}) energy efficiency ratio of cooling generation system [vector]* i_{58}) natural ventilation setpoint temperature [vector]* i_{59}) natural ventilation ACH [h^{-1}] [vector]* <u>PhotoVoltaics</u> i_{60}) type of PV panels i_{61}) percentage of roof covered by PV panels i_{62}) azimuth of PV panels i_{63}) tilt of PV panels

*the vectors include one value per dwelling

Most inputs have simple explanation and thus the attention is focused on the inputs that need further clarifications:

- the opaque components of the external building envelope (usually multi-layer) are modeled with equivalent mono-layer ones – with the same thickness t [m] (i_{12}, i_{19}, i_{26}) – that ensure the same values of thermal conductance K [W/m^{2}K] (and thus of thermal transmittance U [W/m^{2}K]) and areal heat capacity C_a [J/m^{2}K], because such physical quantities define the thermal performance of the building envelope, as concerns the resistance to heat transfer and the thermal inertia, respectively. In this regard, in order to reduce EMAR inputs simplifying its implementation, the specific heat c [J/kg K] of each opaque material is set equal to 1000 J/kg K – noting that most materials used in building applications have c around such a value –, while an equivalent density ρ_{eq} [kg/m^3] must be properly set to ensure the same C_a of the actual components;
- the equivalent thermal conductivity λ_{eq} [W/m K] of external walls, roof and ground-floor (i_{13}, i_{20}, i_{27}) must be set to ensure the same K [W/m^{2}K] of the actual multi-layer components, not including the possible thermal insulation layers, *i.e.,* $\lambda_{eq} = K \cdot t$. The insulation layers are excluded from λ_{eq} assessment because they are considered separately to appreciate the different performance due to the insulation position (i_{18}, i_{25}, i_{32}), which can be internal, external, or in-cavity. Indeed, this position affects the thermal inertia of the building envelope (the profiles of walls' temperature change), and thus it highly impacts envelope energy performance in transient conditions;
- the equivalent density ρ_{eq} [kg/m^3] of external walls, roof and ground-floor (i_{14}, i_{21}, i_{28}) and related insulation layers (i_{17}, i_{24}, i_{31}) must be set to

ensure the same C_a of the actual components, *i.e.,* $\rho_{eq} = \frac{C_a}{t \cdot c}$ where c = 1000 J/kg K;

- the equivalent thickness of horizontal partitions t_{ho} [m] (i_{49}) is used to model the internal thermal inertia, since such partitions usually provide a predominant share of building internal mass. Also in this case, an equivalent mono layer is assumed, with density ρ_{ho} = 1000 kg/m^3 and specific heat c_{ho} = 1000 J/kg K. t_{ho} must be set to ensure the same C_a of the actual components, *i.e.,* $t_{ho} = \frac{C_a}{\rho_{ho} \cdot c_{ho}}$;
- as concerns the transparent envelope, the dwellings can be provided with different windows' types. Thus, different windows' options can be defined as shown in Table 3.12, and the user sets the fractions (*i.e.,* probabilities) of dwellings associated with each option. Clearly, also other options – not reported in Table 3.12 that refers to the examined case studies – can be considered. Infiltration is modeled as a function of the windows' type. Accordingly, the ACH (air changes per hour) value due to infiltration is set equal to 0.7 h^{-1} for old windows with low airtightness, and to 0.3 h^{-1} for new windows with high airtightness. Such values can be modified and customized for each dwelling according to windows' type and opening, linked to the occupant behavior.
- the shading systems are differentiated as a function of the exposure, which clearly affects their use. They are characterized by type, position and radiation setpoint. Different types can be selected, such as: *1)* no shading systems; *2)* low reflective – low transparent blinds (solar reflectance SR = 0.2, solar transmittance ST = 0.1); *3)* low reflective – medium transparent blinds (SR = 0.2, ST = 0.4); *4)* low reflective – high transparent blinds (SR = 0.2, ST = 0.7); *e)* medium reflective – low transparent blinds (SR = 0.5, ST = 0.1); *5)* medium reflective – medium transparent blinds (SR = 0.5, ST = 0.4); *6)* high reflective – low

transparent blinds (SR = 0.8, ST = 0.1); *7)* blinds with inclined slats, *e.g.,* (see Figure 3.25 and some case studies in Section 3.4.4) with an inclination of 45°, thermal conductivity of 0.9 W/m K, solar reflectance for both front and back side equal to 0.5, solar transmittance equal to 0; etc.. The position can be internal or external, while the activation setpoint is intended as the value of incident solar radiation on the windows that triggers the shading use. It is generally included between 150 to 450 W/m² [9] depending on the occupants' behavior;

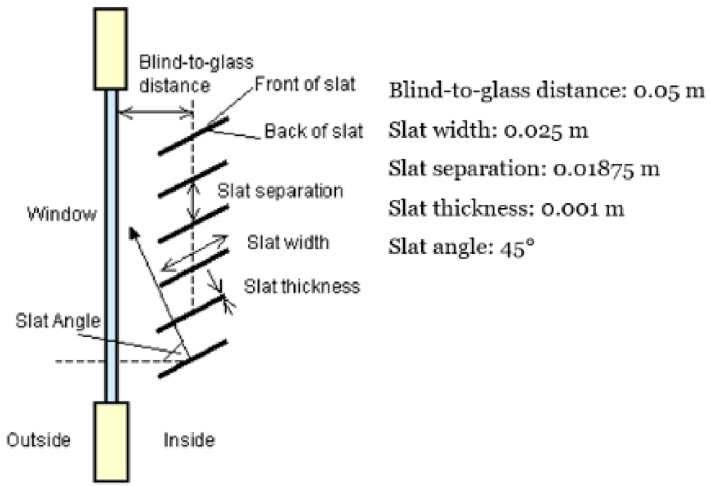

Figure 3.25: Shading system 7: blinds with inclined (45°) slats

- the heating, ventilating and air conditioning (HVAC) systems and operation can be differentiated for each dwelling. Therefore, each HVAC input is defined through a vector that collects the value for each dwelling. The EMAR database of performance curves enables to select different heating systems, *e.g.,* old (inefficient) gas boilers, condensing gas boiler, air-source heat pumps, ground-source heat pumps, and cooling systems, *e.g.,* old (inefficient) and new (efficient) electric air-source chillers, electric water-source chillers. Also reversible heat pumps and centralized HVAC plants can be simulated. In addition, the user can provide itself the performance curves of the considered energy systems;

- also natural ventilation can be considered. It is modeled by setting the natural ventilation setpoint temperature and ACH for each dwelling by means of two vectors of inputs, *i.e.,* i_{58} and i_{59}, respectively. The setpoint provides the temperature above which ventilation is activated. The ACH represents the air changes per hour due to ventilation, which should be carefully set by the user according to windows' size and opening, linked to the occupant behavior, deeply affecting the ventilation pattern;
- only photovoltaic panels are considered as renewable energy source systems because they are by far the most used and cost-effective one at the building level [29]. They are considered installed on the building roof to comply with architectural integration, and they can be defined in typology, size and panels' layout.

Outputs

EMAR can provide numerous outputs as concerns energy and economic performance, as well as thermal comfort, such as:

- discomfort hours and percentage of discomfort hours on occupied hours as concerns both the whole year and the cooling season to enable the investigation of summer overheating. Discomfort hours can be assessed according to the zone thermal comfort ASHRAE 55-2010 adaptive model [34] – 80% acceptability status or 90% acceptability status – or to the zone thermal comfort CEN 15251-2007 adaptive model [35] – category I (90% acceptability status), category II (80% acceptability status) or category III (65% acceptability status);
- heating and cooling loads, which can support the design of the HVAC systems;

- thermal energy demand and primary energy consumption for space heating and cooling;
- total primary energy consumption for all energy uses;
- fuel consumption;
- electricity consumed, self-used and supplied to the urban grid in presence of photovoltaics;
- running costs for space heating, cooling as well as for all uses.

These outputs are assessed for each dwelling – differentiated for exposure and floor number – and the arithmetic means provide the values related to the whole building, since the dwellings have the same extension, *i.e.,* useful and net area, which corresponds to the conditioned area (A_c).

In addition, EMAR provides precious indications about geometry and thermal characteristics of the building envelope, *i.e.*,:

- the area of all opaque and transparent components;
- the gross, net and conditioned volumes;
- the global heat transfer coefficient of the envelope;
- the thermal capacity of the envelope and of the whole building (considering internal partitions too).

Finally, also a 3d CAD model of the building is generated (see previous Figure 3.24).

<u>*Novelties compared to EMA [21]*</u>

As aforementioned, EMAR derives from a deep enhancement of EMA [21], and provides the following main novelties:

- the tool is enhanced to be applied to residential buildings, using a more complex and realistic internal subdivision into thermal zones;
- the level of detail in building modeling is increased, especially as concerns:

- the geometry, since the input variable aspect ratio is replaced with the S/V ratio providing a simplified building model more consistent with the actual building;
- the multi-layer components of the building envelope, which are modeled through the use of equivalent mono-layer ones;
- the windows, since different dwellings can be modeled with different windows, as often occurs in the reality;
- the HVAC systems, which are differentiated for each dwelling (each input is a vector), as often occurs in reality. In addition, further inputs are used to enhance the modeling reliability, *i.e.,* the efficiency of heating distribution-emission-regulation systems, the supply water temperature of heating terminals and the ventilation patterns;

- the possible outputs, which are provided both at dwelling and building levels, and increased in number including, *e.g.,* different thermal comfort models [34],[35];
- a robust validation is performed against detailed EnergyPlus models of an ASHRAE test building and of two typical European buildings, as shown in the following lines.

3.4.4 Case studies for EMAR validation

Three buildings are investigated in order to test, validate and analyze EMAR:

- an ASHRAE test building [30],[31];
- two typical buildings of the European building stock, which have been already investigated by the authors in previous studies for different aims [9],[32].

The outputs of EMAR are compared against the outcomes of detailed building models developed under EnergyPlus environment, which have been calibrated and validated against real data in the mentioned previous studies.

ASHRAE test building

The ASHRAE test building belongs to the 90.1 prototype building models developed by Pacific Northwest National Laboratory (PNNL) for the U.S. Department of Energy (DOE) [30],[31].

The prototypes models have been developed to quantify energy savings from newly published editions of ASHRAE Standard 90.1. The detailed building descriptions and EnergyPlus models can be found in [30],[31]. The examined building hosts only dwellings, it is located in Denver (U.S.A, "BSk" semi-arid climate according to the Köppen–Geiger classification [30]) and characterized by ten floors. The inter-floor height is 3.05 m, each floor has a gross area of 783.6 m^2 with eight dwellings of 88.2 m^2 each, and a connection corridor of 77.7 m^2. The building has a regular shape and a rectangular plant, the total area is 7836.5 m^2 and the conditioned one is 7059.9 m^2. The overall height of the building is 30.5 m, the length 46.3 m and the width 16.9 m, so that a gross volume of about 23884 m^3 is calculated. The longest façades have north and south exposures. The building is shown in Figure 3.26 and characterized in Table 3.13.

The main characteristics of the building thermal envelope are listed below:

- the walls have thermal transmittance (U value) of 0.312 W/m^2K, and consist of an external layer of 2.5 cm of external plaster, 1.6 cm of gypsum board, a block with thermal resistance of 2.8 m^2K/W, an inside layer of 1.6 cm of gypsum board;
- the roof slab has U value of 0.18 W/m^2K and is characterized by a block with thermal resistance of 5.3 m^2K/W and very thin external and internal coatings;

- the ground-floor has U value of 2.14 W/m^{2}K and has a concrete slab of 20 cm and a carpet coating on the inner side;
- the inner floors have two different lavers, *i.e.,* a concrete floor of 10 cm and a carpet coating;
- the windows are double glazed with U value of 2.25 W/m^{2}K;
- there are no shading systems.

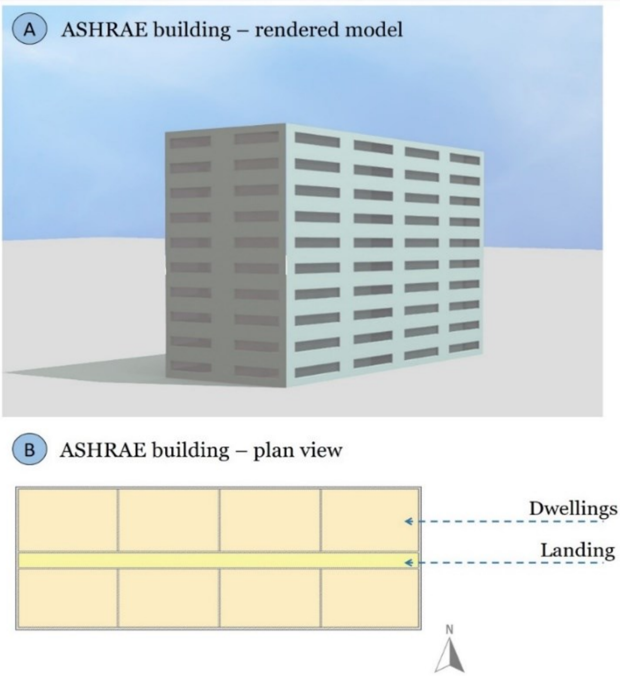

*Figure 3.26: ASHRAE test building: **a)** 3D view; **b)** plan view and thermal zones*

The heating and cooling services are provided by air circuits, with dedicated heating and cooling water, fueled by DX (direct expansion) heating and cooling coils, with COP – coefficient of performance, winter operation – and EER – energy efficiency ratio, summer operation – at rated conditions equal to 4.3 and 4.2, respectively. Thus, there is central air system terminal and a regulation thermostat for each dwelling.

Table 3.13: Characterization of the ASHRAE test building

ENVELOPE - WINDOW TO WALL RATIO					
	Total	South	East	North	West
Gross wall area [m^2]	3855	1412	516	1412	516
Window opening area [m^2]	1150	424	153	424	153
Gross window-wall ratio	29.8%	30.0%	29.7%	30.0%	29.7%
INTERNAL GAINS					
Lighting system [W/m^2]	9.36	Light control is based on scheduled periods			
Electric equipment [W/m^2]	6.67	Occupancy [m^2/person]		35.3	
BOUNDARY CONDITIONS					
Weather data	DENVER INTL AP CO USA TMY3 WMO#=725650				
Number of conditioned zones	80	Heating setpoint [°C]			21.7
Number of unconditioned zones	90	Cooling setpoint [°C]			24.4
Natural ventilation is calculated based on the window opening area of 0.1181 m^2. It is activated from 6:00 a.m. to 10:00 p.m. and when these conditions occur:		a) the indoor temperature is higher than 18.89 °C b) the indoor temperature is lower than 25.56°C c) the outdoor temperature is higher than 15.56 °C d) the outdoor temperature is lower than 26.67 °C e) the wind speed is lower than 40 m/s f) the difference between indoor and outdoor temperature is higher than -100 °C			
HEATING AND COOLING SYSTEMS					
Water to air heat pump COP [-] (heating mode)	4.30	Water to air heat pump EER [-] (cooling mode)			4.20

Typical European building 1

The typical European building 1 has been already investigated by the authors in [32] for what concerns the effects of the occupant behavior on energy performance. The building hosts only dwellings, it is located in Naples (Italy, Mediterranean “Csa” climate according to the Köppen–Geiger classification [36]) and it consists of two adjacent construction blocks, with an overall surface of 4985 m^2, a total height of 25.6 m. Length and width are 62.0 m and 10.5 m, respectively. The building, provided with two staircases, has six dwellings for each floor, with globally eight stories, including the ground-floor. Thus, the number of dwellings is 48. The conditioned floor area, excluding the staircases and the two entries, is 3877 m^2. The building is typical – for what concerns construction technology (reinforced concrete with a structural frame of pillars and beams) and heating systems – of the European building stock built in

during 60ies-70ies, when most existing European buildings were constructed, due to the urban growth and development.
The building is shown in Figure 3.27 and characterized in Table 3.14.

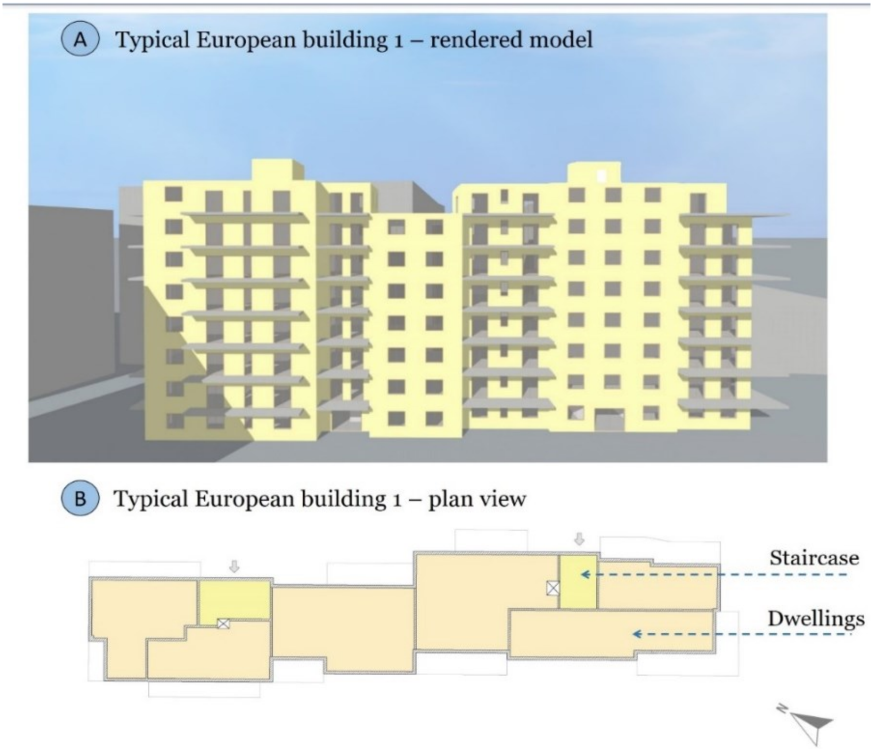

Figure 3.27: Typical European building 1: a) 3D view; b) plan view and thermal zones

The main characteristics of the envelope are listed below:

- the walls have U value of 1.01 W/m^{2}K, and consists of two layers of blocks – 12 cm the outer one, made of hollow blocks, 8 cm the inner layer, made of lapillus bricks – separated by an air cavity (12 cm), with cement plaster outside (3 cm) and lime plaster inside (2 cm);
- the roof slab has a U value of 1.01 W/m^{2}K, with structural layer in reinforced concrete (beams, joists of 20 cm with interposed clay brick, and superior slab of 6 cm). At the bottom, the structure is plastered, at

the top there is a further layer of lightweight concrete of 15 cm to give the right slope for the rainwater canalization, and waterproof layer;

- the ground floor has U value of 1.35 W/m^2K, and the structure is similar to the roof with the exception of the slope layer. There is a thin light concrete slab as base of the ceramic pavement;
- the inner floors have mixed joists and hollow blocks structure, plastered at the bottom, with reinforced concrete slab, lightweight concrete slab and pavement at the top;
- the inner walls are made with lapillus blocks, typical of the region, plastered on both sides;
- the windows are single-glazed and wooden framed, with U value of 4.9 W/m^2K. Averagely, one dwelling per floor has more recent windows (after refurbishment), double-glazed, wooden framed with U value of 2.8 W/m^2K;
- the shading systems are external blinds with inclined slats (see Figure 3.25). The shading is on when the direct solar radiation on window is > 150 W/m^2. Each slat has a slope of 45° and a conductivity of 0.9 W/m K. The slat solar reflectance, both for the front and back side, is 0.5.

As concerns the heating system, there is a centralized natural gas boiler, not-condensing, with a thermal efficiency of 0.80 and thermal capacity of about 460 kW (slightly oversized, as typical for old buildings). The hot water is supplied to all dwellings through not-insulated vertical pipes, crossing the perimeter walls, and the in-room heat terminals are hot water radiators with thermostatic valves. The efficiency of heating distribution-emission-regulation system is 0.86, therefore the overall heating system efficiency is 0.69. Dwellings are equipped with DX cooling systems with EER equal to 3.0.

Table 3.14: Characterization of the typical European building 1

ENVELOPE - WINDOW TO WALL RATIO					
	Total	South	East	North	West
Gross wall area [m^2]	4514	480	1756	509	1769
Above ground wall area [m²]	3920	419	1527	438	1537
Window opening area [m^2]	743	51	323	40	330
Gross window-wall ratio	19.0%	12.26%	21.1%	9.1%	21.5%
INTERNAL GAINS					
Lighting system [W/m^2 - 100 lux]	2	Light control according to the daylight illuminance (dimming)			
Electric equipment [W/m^2]	4	Occupancy [person/m²]		0.04	
BOUNDARY CONDITIONS					
Weather data	NAPLES – ITA IWEC Data WMO #=162890				
Number of conditioned zones	48	Heating setpoint [°C]			20
Number of unconditioned zones	20	Cooling setpoint [°C]			26
Natural ventilation (time-dependent, till a maximum of 4 h^{-1}) is activated when both summer conditions occur:		a) the zone air temperature is higher than 27 °C b) the outdoor temperature is at least 2°C lower than indoor one			
HEATING AND COOLING SYSTEMS					
Efficiency of heating distribution-emission-regulation system [-]	0.86				
Efficiency of heating generation system [-]	0.80	Nominal heating capacity			463 kW_t
Packaged terminal air conditioner EER [-]	3.00	Nominal cooling capacity (assumed)			180 kW_t

Typical European building 2

The typical European building 2 has been already investigated by the authors in [9] as concerns the impact of inter-building effect and shading systems on energy needs. The building is shown in Figure 3.28, characterized in Table 3.15.

The building is located in Naples, in the same neighborhood of the previous case study, and hosts different use destinations.

Length and width are 80 m and 14 m, respectively. The longest facades are oriented to north-west and south-east, respectively. The total building area is 7456 m² and the conditioned area is 6707.5 m². The building is made up of seven floors and the inter-floor height is 3.2 m. The first one hosts retails, the second one hosts offices and the other floors have a residential use. Dwellings have different net area and can accommodate about from two to six people. The access to the dwellings is guaranteed by three stairwells. This case study is investigated to test EMAR on buildings that are partially (in this case for most part) residential hosting also other use destinations. Since EMAR is conceived for residential buildings, only the outcomes related to the dwellings – *i.e.,* floors 3-7 – are examined. The building has the same building envelope and energy systems of the typical European building 1, being representative the European building stock built in during 60-70ies.

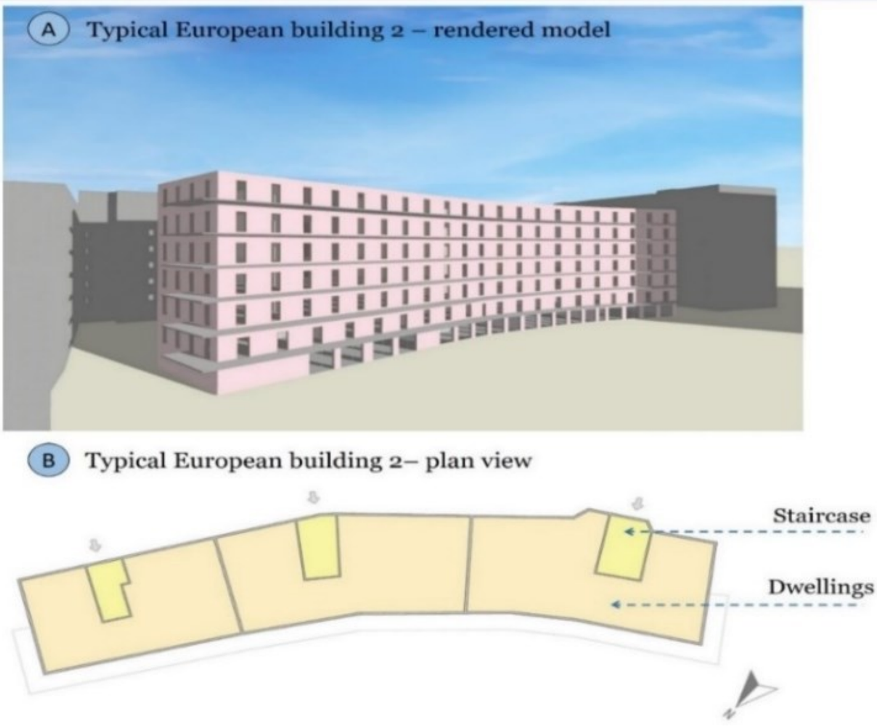

Figure 3.28: Typical European building 2: a) 3D view; b) plan view and thermal zones

Table 3.15: Characterization of the typical European building 2

ENVELOPE - WINDOW TO WALL RATIO					
	Total	South	East	North	West
Gross wall area [m^2]	4186	844	1025	782	1534
Window opening area [m^2]	778	128	160	169	321
Gross window-wall ratio	18.6%	15.2%	15.6%	21.6%	20.9%

INTERNAL GAINS			
Lighting system dwellings [W/m^2 - 100 lux]	5	Light control according to the daylight illuminance (dimming)	
Lighting system retail zones [W/m^2 - 100 lux]	6	Light control according to the daylight illuminance (dimming)	
Lighting system office zones [W/m^2 - 100 lux]	6	Light control according to the daylight illuminance (dimming)	
Electric equipment residential zones [W/m^2]	4		
Electric equipment retail zones [W/m^2]	7.5		
Electric equipment office zones [W/m^2]	2.5		
BOUNDARY CONDITIONS			
Weather data	NAPLES – ITA IWEC Data WMO #=162890		
Number of conditioned zones	28	Heating setpoint [°C]	20
Number of unconditioned zones	20	Cooling setpoint [°C]	26
Natural ventilation (time-dependent, till a maximum of 4 h^{-1}) is activated when both summer conditions occur:	a) the zone air temperature is higher than 27 °C b) the outdoor temperature is at least 2°C lower than indoor one		
HEATING AND COOLING SYSTEMS			
Efficiency of heating distribution-emission-regulation system [-]	0.86		
Efficiency of heating generation system [-]	0.80	Nominal heating capacity	300 kW_t
Packaged terminal air conditioner EER [-]	3.00	Nominal cooling capacity (assumed)	180 kW_t

3.4.5 Results: Validation and analysis of EMAR

This section of the Thesis shows the validation of EMAR as well as a detailed analysis of performance and outcomes of such a tool, addressing the aforementioned three case studies. The detailed EnergyPlus models of the three buildings have been developed, calibrated and validated in previous works [9], [30],[31],[32]. On the other hand, as concerns EMAR simulations, the used numerical inputs are reported in Table 3.16.

Table 3.16: EMAR inputs for the case studies (no photovoltaics → the inputs i_{60}, i_{61}, i_{62} and i_{63} are not used)

EMAR inputs	ASHRAE test building	typical European building 1	typical European building 2
i_1) number of floors	10	8	7
i_2) orientation: angle building north - true north	90°	0°	45°
i_3) gross area of each floor	784 m^2	600 m^2	1065 m^2
i_4) S/V ratio	0.23 m^{-1}	0.32 m^{-1}	0.30 m^{-1}
i_5) gross height of each floor	3.05 m	3.2 m	3.2 m
i_6) window to wall ratio: south	30.0%	12.2%	15.2%
i_7) window to wall ratio: east	29.7%	21.1%	15.6%
i_8) window to wall ratio: north	30.0%	9.1%	21.6%
i_9) window to wall ratio: west	29.7%	21.5%	20.9%
i_{10}) solar absorptance of walls	0.70	0.70	0.70
i_{11}) solar absorptance of roof	0.70	0.85	0.85
i_{12}) thickness of walls' bricks	0.072 m	0.37 m	0.37 m
i_{13}) equivalent thermal conductivity of walls' bricks	0.024 W/m K	0.44 W/m K	0.44 W/m K
i_{14}) equivalent density of walls' bricks	1388 kg/m^3	634.8 kg/m^3	634.8 kg/m^3
i_{15}) thickness of insulation of walls	absent	absent	absent
i_{16}) thermal conductivity of insulation of walls	-	-	-
i_{17}) equivalent density of insulation of walls	-	-	-
i_{18}) position of insulation of walls	-	-	-
i_{19}) thickness of roof block	0.026 m	0.44 m	0.44 m
i_{20}) equivalent thermal conductivity of roof block	0.005 W/m K	0.514 W/m K	0.514 W/m K
i_{21}) equivalent density of roof block	1328 kg/m^3	1212 kg/m^3	1212 kg/m^3
i_{22}) thickness of insulation of roof	absent	absent	absent
i_{23}) thermal conductivity of insulation of roof	-	-	-
i_{24}) equivalent density of insulation of roof	-	-	-
i_{25}) position of insulation of roof	-	-	-
i_{26}) thickness of ground-floor	0.20 m	0.35 m	0.35 m
i_{27}) equivalent thermal conductivity of ground-floor	0.67 W/m K	0.603 W/m K	0.603 W/m K
i_{28}) equivalent density of ground-floor	2322 kg/m^3	1112 kg/m^3	1112 kg/m^3
i_{29}) thickness of insulation of ground-floor	absent	absent	absent
i_{30}) thermal conductivity of insulation of ground-floor	-	-	-
i_{31}) equivalent density of insulation of ground-floor	-	-	-
i_{32}) position of insulation of ground-floor	-	-	-
i_{33}) dwellings with single-glazed, aluminum windows	0%	0%	0%
i_{34}) dwellings with single-glazed, wood windows	0%	83 %	50 %
i_{35}) dwellings with double-glazed, aluminum windows	100%	0%	0%
i_{36}) dwellings with double-glazed, wood windows	0%	17 %	50 %
i_{37}) shading systems' type: south	absent	7: inclined (45°) slats	7: inclined (45°) slats
i_{38}) shading systems' type: east	absent	7: inclined (45°) slats	7: inclined (45°) slats
i_{39}) shading systems' type: north	absent	7: inclined (45°) slats	7: inclined (45°) slats
i_{40}) shading systems' type: west	absent	7: inclined (45°) slats	7: inclined (45°) slats
i_{41}) shading systems' position: south	-	exterior	exterior
i_{42}) shading systems' position: east	-	exterior	exterior
i_{43}) shading systems' position: north	-	exterior	exterior
i_{44}) shading systems' position: west	-	exterior	exterior
i_{45}) shading systems' radiation setpoint: south	-	150 W/m^2	150 W/m^2
i_{46}) shading systems' radiation setpoint: east	-	150 W/m^2	150 W/m^2
i_{47}) shading systems' radiation setpoint: north	-	150 W/m^2	150 W/m^2
i_{48}) shading systems' radiation setpoint: west	-	150 W/m^2	150 W/m^2
i_{49}) equivalent thickness of horizontal partitions	0.10 m	0.35 m	0.35 m
i_{50}) heating setpoint temperature*	21.7 °C	20 °C	20 °C
i_{51}) cooling setpoint temperature*	24.4 °C	26 °C	26 °C
i_{52}) efficiency of distribution-emission-regulation*	-	0.86	0.86
i_{53}) supply water temperature of heating terminals*	50 °C	70 °C	70 °C

i_{54}) type of heating generation system*	water to air heat pump	gas boiler	gas boiler
i_{55}) efficiency of heating generation system*	COP = 4.30	η = 0.80	η = 0.80
i_{56}) type of cooling generation system (chiller)*	water to air heat pump	electric air-source	electric air-source
i_{57}) energy efficiency ratio of cooling system*	4.20	3.00	3.00
i_{58}) ventilation setpoint temperature*	27 °C	27 °C	27 °C
i_{59}) ventilation ACH*	4 h^{-1}	4 h^{-1}	4 h^{-1}

*all dwellings have the same input, therefore a unique value is reported instead of a vector

The following steps will be described in detail below:

- Validation;
- Analysis of EMAR outputs;
- Example of photovoltaics' simulation.

Validation

The comparison between the outputs of the detailed EnergyPlus models and EMAR simulations is shown in Table 3.17 for validation purposes. The considered performance indicators refer to space conditioning demands, since these represent the most complex outputs to be assessed through building performance simulations tools, being highly affected by the dynamic behavior of building envelope and energy systems, as well as by the variable (during the year) boundary conditions linked to climatic conditions, building use and occupant behavior. Thus, Table 3.17 reports:

- TED_h: thermal energy demand for space heating [kWh_t/m^2a];
- TED_c: thermal energy demand for space cooling [kWh_t/m^2a];
- TED_{sc}: thermal energy demand for space conditioning = TED_h + TED_c [kWh_t/m^2a];
- PEC_h: primary energy consumption for space heating [kWh_p/m^2a];
- PEC_c: primary energy consumption for space cooling [kWh_p/m^2a];
- PEC_{sc}: primary energy consumption for space conditioning = PEC_h + PEC_c [kWh_p/m^2a];

Table 3.17: Validation results: Detailed EnergyPlus models vs EMAR simulations

		A_c [m^2]	TED_h	TED_c [kWh_t/m^2a]	TED_s	PEC_h	PEC_c [kWh_p/m^2a]	PEC_{sc}
ASHRAE test building	detailed EnergyPlus	7060	12.8	34.5	47.3	21.9	20.6	42.5
	EMAR	7266	12.6	34.6	47.2	21.9	20.9	42.9
	Discrepancy	*2.8%*	*-1.6%*	*0.3%*	*-0.2%*	*0%*	*1.4%*	*0.9%*
typical European Building 1	detailed EnergyPlus	3877	35.3	18.3	53.6	63.1	11.6	74.7
	EMAR	4119	35.4	17.2	52.6	63.6	10.9	74.5
	Discrepancy	*5.9%*	*0.3%*	*-6.4%*	*-1.9%*	*0.8%*	*-6.4%*	*-0.3%*
typical European Building 2	detailed EnergyPlus	4873	24.4	17.1	41.5	40.8	10.8	51.6
	EMAR	4661	23.2	18.0	41.2	39.0	11.9	50.9
	Discrepancy	*-4.6%*	*-5.2%*	*5.0%*	*-0.7%*	*-4.6%*	*9.2%*	*-1.4%*

As concerns PEC, the primary energy conversion factor is set equal to 1.05 for natural gas and 1.95 for electricity [37]. In addition, even the building conditioned area (A_c) is shown given that, clearly, EMAR provides different values because it automatically generates simplified building geometries. As aforementioned, for the typical European building 2 the outputs refer to the dwellings, *i.e.,* floors 3-7.

The validation results are very satisfactory. Concerning the energy performance indicators, as regards the ASHRAE building, the discrepancy between EMAR and EnergyPlus is always very low, under 2%. For the typical European buildings, discrepancies are slightly higher – around 5% as mean values – and the highest value of 9.2% (PEC_c for typical European building 2) is widely acceptable given the drastic simplification introduced by EMAR as concerns building modeling and simulation.

The results can be partly justified by the geometrical differences between the buildings under investigation. The ASHRAE building has a regular shape and the same plan subdivision for each floor, thus the simplified building model generated by EMAR has a major geometry correspondence with the original building, with a discrepancy in A_c lower than 3%. The typical European building 1 has a rectangular shape but the last floor has a different area than the other ones. The EMAR building has all floors with the same area and geometry, causing a discrepancy in A_c around 6%. The typical European building 2 has an irregular plan with a curved front. In this case, the EMAR building has an equivalent rectangular plant, resulting in A_c discrepancy around -5%. Thus, for the last two case studies, the higher discrepancies in TED and PEC are motivated by the higher level of geometry simplification. Finally, EMAR shows good reliability and accuracy ensuring at the same time a user-friendly implementation. Notably, since the discrepancies are always lower than 10%, EMAR can be considered validated because the threshold of ±10% – assessed on yearly basis – is typically used at international level to assess the calibration/validation of building energy models [9], [38],[39].

Analysis of EMAR outputs

With the aim of conducting a comprehensive analysis of EMAR, the outputs achieved at dwellings' level are reported in Table 3.18, Table 3.19, and Table 3.20 for the three investigated buildings, respectively. As concerns the typical European building 2, the results related to the first two floors are not shown because there are not dwellings but retails and offices, while EMAR focuses on residential case studies. The analysis is not limited to TED and PEC, but – in order to show EMAR potentials – it addresses also the assessment of:

- heating (HL) and cooling loads (CL), which can support the design of the HVAC systems;
- discomfort hours (DH) for both the whole year and the cooling season (linked to summer overheating), which are assessed based on the

ASHRAE 55-2010 adaptive model [28] with 80% acceptability, which is the most used worldwide for residential buildings. Even the DH percentages with respect to the occupied hours are reported to provide a clearer snapshot of thermal discomfort/comfort.

The outcomes allow to assess the differences among dwellings as a function of floor, exposure, and windows' type. For instance, dwellings at the ground floor have the lowest values of cooling demands because they can exploit the inertia of the whole building envelope and are subjected to a lower solar load, while dwellings at the top floor have the highest values given the major solar load. In addition, these latter – even if they feature double glazed windows for the typical European building 2 (Table 3.20) – have higher values of space heating demands because they are characterized by larger dispersing surfaces (roof surface). Clearly, as concerns the two typical European buildings, dwellings with double-glazed windows have lower values of heating demands, because such windows increase the envelope thermal resistance even if they imply a slight reduction of the solar heat gain coefficient. On the other hand, they increase the overheating risk, thereby exerting a lower influence on cooling demands, since there are contrasting effects. Fixing the windows type (see Floors 4, 6 and 7 of Table 3.20) dwellings with south exposure – compared to the north one – tend to have (slightly) lower heating demands and higher cooling demands because of the different solar gains/loads.

Table 3.18: EMAR outputs at dwellings' level for the ASHRAE test building

		Thermal Comfort: Discomfort Hours (DH) and their percentage with respect to the occupied hours [%]**		Heating (HL) and Cooling (CL) Loads [W/m^2]		Thermal Energy Demand (TED) [kWh$_t$/m^{2}a]		Primary Energy Consumption (PEC) [kWh$_p$/m^{2}a]		
		year DH [h]	%	HL	CL	TED$_h$*	TED$_c$*	PEC$_h$*	PEC$_c$*	PEC$_{tot}$*
Dwelling Floor 1	North	11.5	0.3%	17.4	15.1	16.6	18.4	27.4	11.6	131.1
Dwelling Floor 1	South	10.5	0.3%	15.9	18.2	14.2	18.5	23.8	11.8	127.6
Dwelling Floor 2	North	148.8	3.5%	16.3	19.8	11.8	32.3	20.7	19.4	132.1
Dwelling Floor 2	South	129.5	3.0%	16.2	24.6	11.8	31.0	20.7	19.2	131.9
Dwelling Floor 3	North	209.8	4.9%	16.4	21.1	10.9	36.9	19.5	21.8	133.3
Dwelling Floor 3	South	193.0	4.5%	16.3	26.0	10.9	35.4	19.4	21.6	133.1
Dwelling Floor 4	North	229.5	5.4%	16.5	21.4	10.6	38.1	19.1	22.5	133.6
Dwelling Floor 4	South	212.8	5.0%	16.4	26.2	10.7	36.6	19.0	22.3	133.3
Dwelling Floor 5	North	233.3	5.5%	16.6	21.4	10.6	38.4	19.0	22.6	133.6
Dwelling Floor 5	South	217.0	5.1%	16.4	26.3	10.6	36.9	19.0	22.4	133.4
Dwelling Floor 6	North	233.3	5.5%	16.6	21.4	10.7	38.3	19.2	22.6	133.7
Dwelling Floor 6	South	217.5	5.1%	16.5	26.2	10.8	36.8	19.2	22.3	133.5
Dwelling Floor 7	North	230.5	5.4%	16.7	21.4	10.9	38.1	19.6	22.4	134.0
Dwelling Floor 7	South	213.0	5.0%	16.6	26.2	11.0	36.5	19.6	22.2	133.7
Dwelling Floor 8	North	207.5	4.9%	17.2	21.5	12.2	37.7	20.9	22.3	135.2
Dwelling Floor 8	South	225.8	5.3%	16.9	26.8	11.5	35.3	20.4	21.3	133.7
Dwelling Floor 9	North	222.0	5.2%	17.9	21.8	13.1	37.3	22.9	22.1	137.0
Dwelling Floor 9	South	205.5	4.8%	17.7	26.8	13.3	35.9	23.0	21.8	136.9
Dwelling Floor 10	North	223.0	5.3%	21.9	24.6	19.3	37.4	32.4	22.5	146.9
Dwelling Floor 10	South	207.0	4.9%	21.9	30.0	19.5	36.3	32.6	22.6	147.2

* subscripts: h = heating; c = cooling; tot = all uses

** summer overheating never occurs

Table 3.19: EMAR outputs at dwellings' level for the typical European building 1

	Thermal Comfort: Discomfort Hours (DH) and their percentage with respect to the occupied hours [%]				Heating (HL) and Cooling (CL) Loads [W/m²]		Thermal Energy Demand (TED) [kWh$_t$/m²a]		Primary Energy Consumption (PEC) [kWh$_p$/m²a]		
	year DH [h]	%	summer DH [h]	%	HL	CL	TED$_h$*	TED$_c$*	PEC$_h$*	PEC$_c$*	PEC$_{tot}$*
Dwelling North Floor 1	988.8	24.1%	404.8	12.0%	88.2	19.5	45.6	3.1	79.4	2.3	173.7
Dwelling South Floor 1	991.0	24.2%	415.0	12.3%	81.3	18.8	41.3	3.1	73.2	2.2	167.5
Dwelling North Floor 2	879.0	21.4%	424.8	12.6%	76.8	32.5	34.1	14.3	61.9	9.2	163.2
Dwelling South Floor 2	908.5	22.2%	450.3	13.3%	77.6	33.2	34.5	14.6	62.6	9.3	163.9
Dwelling North Floor 3**	689.3	16.8%	356.5	10.6%	52.8	35.4	20.3	17.0	39.3	10.9	142.2
Dwelling South Floor 3	867.0	21.1%	431.0	12.8%	76.8	36.1	33.3	18.6	60.6	11.8	164.4
Dwelling North Floor 4**	709.5	17.3%	379.3	11.2%	53.1	36.4	20.5	17.9	39.5	11.3	142.9
Dwelling South Floor 4	867.0	21.1%	437.5	13.0%	76.9	36.5	33.3	19.4	60.5	12.2	164.8
Dwelling North Floor 5	881.3	21.5%	444.3	13.2%	77.4	36.4	33.6	19.4	61.1	12.2	165.3
Dwelling South Floor 5	865.5	21.1%	436.8	12.9%	76.8	36.7	33.3	19.4	60.6	12.2	164.9
Dwelling North Floor 6	909.3	22.2%	456.0	13.5%	78.8	36.0	34.9	19.1	63.1	12.0	167.1
Dwelling South Floor 6	899.3	21.9%	454.8	13.5%	78.1	36.5	34.3	19.4	62.1	12.2	166.4
Dwelling North Floor 7	987.5	24.1%	499.5	14.8%	81.2	37.3	37.2	19.8	66.6	12.4	171.1
Dwelling South Floor 7	964.5	23.5%	492.8	14.6%	80.6	37.6	36.4	20.1	65.4	12.6	170.1
Dwelling North Floor 8	1301.8	31.8%	686.3	20.3%	93.0	49.6	47.5	24.7	81.8	15.8	189.6
Dwelling South Floor 8	1282.8	31.3%	674.5	20.0%	92.4	49.9	46.8	25.0	80.7	15.9	188.7

* subscripts: h = heating; c = cooling; tot = all uses

** dwellings with double glazed windows; the other ones have single-glazed windows

Table 3.20: *EMAR outputs at dwellings' level for the typical European building 2*

	Thermal Comfort: Discomfort Hours (DH) and their percentage with respect to the occupied hours [%]				Heating (HL) and Cooling (CL) Loads [W/m^2]		Thermal Energy Demand (TED) [kWh$_t$/m^{2}a]		Primary Energy Consumption (PEC) [kWh$_p$/m^{2}a]		
	year DH [h]	%	summer DH [h]	%	HL	CL	TED$_h$*	TED$_c$*	PEC$_h$*	PEC$_c$*	PEC$_{tot}$*
Dwelling North Floor 3	735.5	17.9%	348.3	10.3%	69.7	37.3	28.4	15.8	47.6	10.5	150.2
Dwelling South Floor 3**	567.3	13.8%	278.5	8.3%	46.9	38.6	16.3	14.8	27.7	10.1	129.8
Dwelling North Floor 4	703.3	17.2%	339.5	10.1%	68.2	39.1	27.3	17.2	45.9	11.3	149.2
Dwelling South Floor 4	698	17.0%	338.5	10.0%	67.8	38.9	27.2	17.3	45.7	11.3	149.0
Dwelling North Floor 5**	646.3	15.8%	382.8	11.4%	46.2	42.8	15.6	16.9	26.6	11.3	129.9
Dwelling South Floor 5	711.8	17.4%	350.3	10.4%	67.9	39.1	27.3	17.7	45.9	11.5	149.4
Dwelling North Floor 6**	708.3	17.3%	401.5	11.9%	49.0	42.2	17.6	17.6	29.8	11.6	133.5
Dwelling South Floor 6**	706.	17.2%	414.3	12.3%	48.3	42.3	17.0	17.8	28.8	11.7	132.5
Dwelling North Floor 7**	1153	28.1%	662.8	19.7%	66.3	55.9	27.8	22.4	46.2	15.0	153.3
Dwelling South Floor 7**	1149.3	28.0%	659.8	19.6%	65.9	55.9	27.7	22.4	46.1	15.0	153.1

* subscripts: h = heating; c = cooling; tot = all uses

** dwellings with double glazed windows; the other ones have single-glazed windows

Definitely, EMAR can provide precious information to investigate energy demand and thermal comfort as well as to design the HVAC systems – thanks to the assessment of heating and cooling loads – for each dwelling.

Finally, EMAR provides outputs about the thermal characteristics of the building envelope, such as the global heat transfer coefficient (H) and the thermal capacity (C) of the external envelope and of the whole building (considering internal partitions too), as reported in Table 3.21. Clearly, these outputs refer to the simplified building models developed by EMAR. Therefore, there is not a perfect matching with the actual building data, but they provide a reliable snapshot of envelope thermal performance.

Table 3.21: EMAR outputs related to the thermal characteristics of the building envelope

	ASHRAE test building	typical European building 1	typical European building 2
H [kW/K]	5.43	8.23	10.26
$C_{external}$ [MJ/K]	670	1180	1740
C_{total} [MJ/K]	1370	2520	3820

Example of photovoltaics' simulation

The case studies do not feature the presence of photovoltaics (PV). Thus, in order to show how PV systems can be simulated through EMAR, an example is provided referring to the typical European building 2, since this latter is the most complex building investigated. The implementation of PV systems is simulated performing both energy and cost-optimal analyses to outline the capabilities of EMAR. Systems of different type and size are investigated:

- cells in poly- and mono-crystalline silicon, with investment costs equal to 1500 €/kW_{peak} and 1700 €/kW_{peak}, respectively, taken from a market research;
- PV panels are installed on the building roof to ensure architectural integration. The roof area covered by panels varies in the range 0 – 100% with a step of 10%.

Thus, 21 possible PV configurations are examined. In all cases, the panels' location is optimized setting the tilt angle equal to 30° and the azimuth angle to 0° (orientation to south) to maximize the annual electric conversion for the considered location – Naples, latitude 40° 51' 22 N, longitude 14° 14' 47 E. For each combination, EMAR enables to predict total primary energy consumption and global cost of the building facility as shown in Figure 3.29 and Figure 3.30. In addition, even the discounted payback period is provided – Figure 3.31 – for a more comprehensive economic analysis. Primary energy consumption includes all energy uses taken from EnergyPlus simulations. Global costs are assessed over a calculation period (τ) of 20 years to match a conservative PV lifespan. They include the investment cost for PV and the running cots over τ, which are actualized considering a discount factor of 3% [40]. In order to simulate the PV implementation, EMAR performs hourly balances between produced and required electrical energy. The PV hourly electrical conversion is achieved from EnergyPlus simulations. Surplus electricity is sold to the grid. According to the Italian context, the specific cost of electricity is set equal to 0.22 *€/kWh*$_{el}$ (today, this value seems low, but it was the most reliable one according to Eurostat at 2020-2021, when the study has been developed) the remuneration for the electricity sold to the grid to 0.07 *€/kWh*$_{el}$ (around 1/3 of the purchase cost [41]), the natural gas cost (for running cost assessment) to 0.90 *€/m*^{3} (also this value strongly increased in the second half 2022).

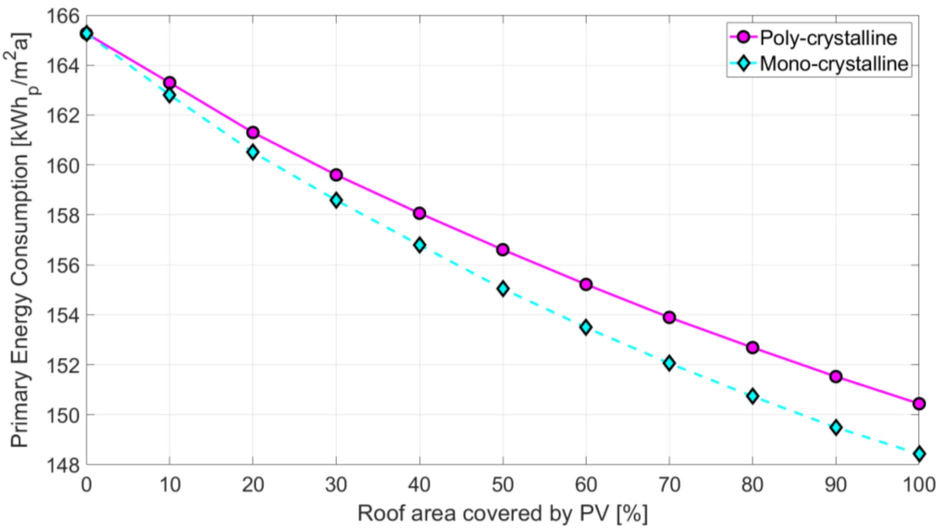

Figure 3.29: Energy analysis of PhotoVoltaics: total primary energy consumption vs PV size

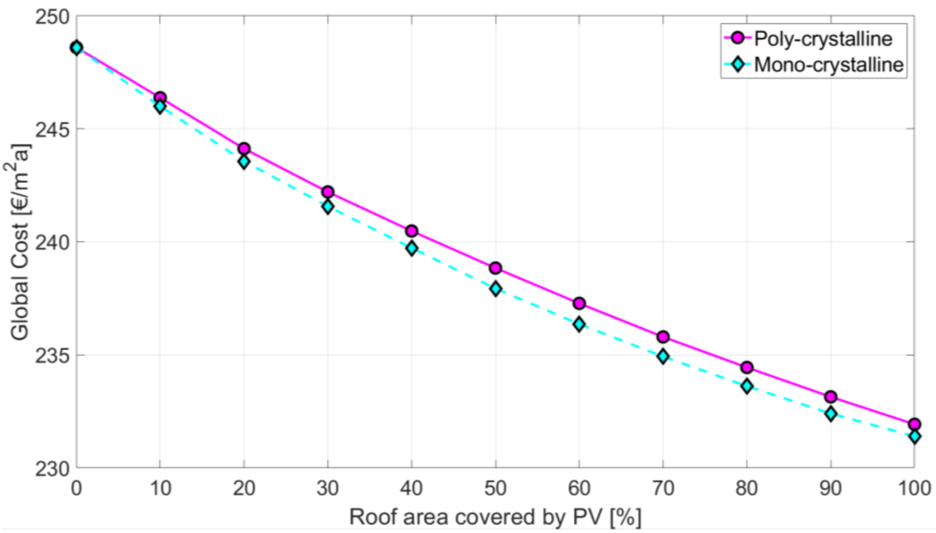

Figure 3.30: Cost analysis of PhotoVoltaics: global cost vs PV size

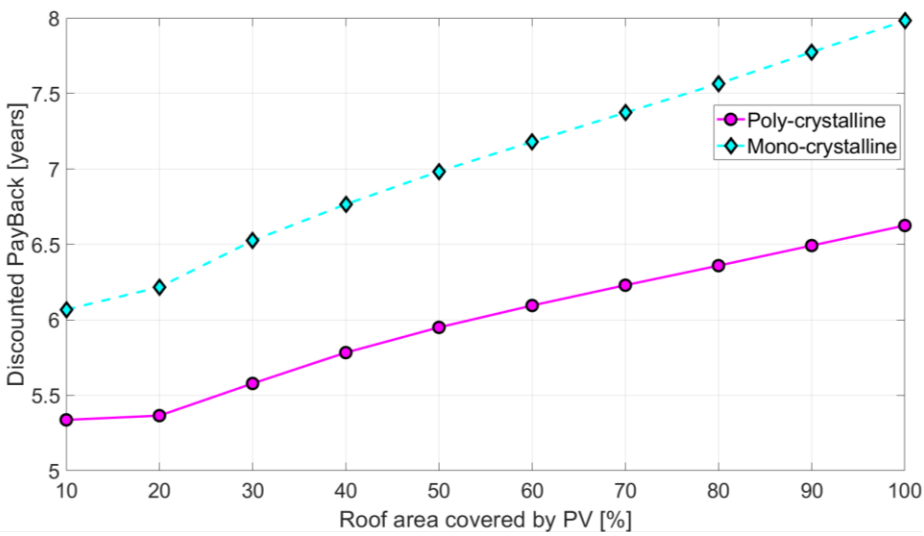

Figure 3.31: Cost analysis of PhotoVoltaics: discounted payback time vs PV size

The outcomes show that the maximum size of photovoltaic – *i.e.,* a full-roof PV system – is the optimal solution from both energy and economic perspectives, even if the payback time is the highest one, given the higher investment cost, but acceptable (lower than 10 years). In this regard, such systems usually receive public financial grants that increase their cost-effectiveness. Clearly, EMAR can consider such grants in the cost analysis. This result is motivated by the cost reduction – due to technology development and macro-scale economic – that PV systems have experienced in the last years. That is why they are by far the most effective renewable energy system at the building level. The investigation shows a simple example of how EMAR can be used to optimize building energy performance performing a cost-optimal analysis as well. Therefore, it can be a precious tool for building professionals and public stakeholders to promote a more energy-efficient and cost-effective building stock.

3.4.6 Conclusions about the development and testing of EMAR

Are few numerical inputs sufficient for accurate energy simulations of residential buildings?

This study answers “*Yes*” by proposing EMAR, an accurate but user-friendly tool for energy modeling and simulations of residential buildings. EMAR is based on the coupling between EnergyPlus and MATLAB® and it is a deep upgrade of a previous version – EMA – conceived for office buildings. It works under MATLAB® environment and needs only 63 numerical inputs to carry out modeling and simulations. No drawings, no schemes of energy systems, no deep modeling expertise are required but only few numbers. EMAR is validated against detailed EnergyPlus models of an ASHRAE test building and of two typical European buildings. The discrepancies are lower than 10% as concerns thermal energy demand and primary energy consumption for space conditioning, and in most cases are lower than 5%. The lowest discrepancies – always lower than 3% – are achieved for the ASHRAE test building because this latter is isolated (no external shading elements, such as other constructions) and has a regular rectangular shape. Thus, the simplified building model generated by EMAR has a higher geometry correspondence with the original building. Nonetheless, EMAR shows good reliability for irregular buildings too, as the other two case studies, whose original models take into account the external environment and shading elements (urban context) too. On the other hand, EMAR introduces a drastic reduction of modeling and computational burden, so that it can be easily used by building professionals. In addition, EMAR can provide outputs at dwellings' level, thereby enabling deep investigations of energy demands, thermal comfort and heating/cooling loads for different stakeholders. Accordingly, the public actors can achieve precious guidelines to drive energy audit, design and retrofit of entire building stocks, while the private actors, *i.e.,* the building tenants, can obtain detailed information about energy performance and labeling of their houses, as well as for HVAC systems' design. Moreover, indicators related to the building thermal envelope – *e.g.,* global heat transfer coefficient and capacity – are assessed providing a comprehensive outline of the building system's energy performance. Therefore, EMAR can be a precious tool to perform user-friendly but accurate building energy modeling and simulations, which are fundamental for a wide diffusion of methodologies and procedures addressing the energy transition of the building stock towards nearly-zero energy buildings. For instance, EMAR can be integrated in tools and frameworks for: a) building energy audit and labeling, design of HVAC systems; b) building information modeling (BIM); c) building energy optimization for the design of new buildings or the retrofit of existing ones; d) large-scale analysis of buildings stock to address public energy policies. Future studies will aim at the development of free graphical interfaces (without the use of MATLAB®) as well as to the integration of EMAR in some of the aforementioned frameworks.

CHAPTER 3 - Nomenlcature

Acronyms		
ACH	Air changes per hour	
AHU	Air Handing Unit	
ANN	Artificial neural network	
ASHRAE	American Society of Heating, Refrigerating and Air-Conditioning Engineers	
BES	Building energy simulation	
BEM	Building Energy Modeling	
BIM	Building information modeling	
BPS	Building performance simulation	
CL	Cooling load	
CV(RMSE)	Coeff of variation of Root Mean Square Error	
DH	Discomfort hours	
EMAR	EnergyPlus + MAtlab® for Residential	
ERR_{month}	Error in the monthly consumption	
ERR_{year}	Error in the annual consumption	
HL	Heating load	
HP	Heat Pump	
HVAC	Heating, ventilating and air conditioning	
IBE	Inter-building effect	
MBE	Mean Bias Error	
PEC	Primary Energy Consumption	
PNNL	Pacific Northwest National Laboratory	
PV	photovoltaic	
RC	Resistance-capacitance	
SHGC	Solar heat gain coefficient	
SVM	Support vector machine	
TED	Thermal Energy Demand	
Symbols		
A_c	Conditioned area	m^2
ACH	Air changes per hour	h^{-1}
C	Thermal capacity	

c_p	specific heat	J/kg K
COP	Coefficient of Performance	Wh_t/Wh_e
EER	Energy Efficiency Ratio	Wh_t/Wh_e
H	Global heat surface coefficient	
K	thermal conductance	W/m^2 K
SR	Solar reflectance	
ST	Solar transmittance	
U-value	Thermal transmittance	W/m^2K
U_g	Thermal transmittance of window's glass	W/m^2K
ρ	density	kg/m^3
<u>Subscripts</u>		
el	referred to electrical energy	
c	referred to space cooling	
h	referred to space heating	
l	referred to artificial lighting	
p	referred to primary energy	
sc	space conditioning	
t	referred to thermal energy	

CHAPTER 3 - References

[1] Ascione, F., Bianco, N., Iovane, T., Mauro, G. M., Napolitano, D. F., Ruggiano, A., & Viscido, L. (2020). A real industrial building: Modeling, calibration and Pareto optimization of energy retrofit. *Journal of Building Engineering*, *29*, 101186.

[2] D.P.R. (Decree of the President of the Republic) 26 agosto 1993. n. 412 (in Italian).

[3] Ascione, F., De Rossi, F., Iovane, T., Picone, R., Mastellone, M., & Mauro, G. M. (2022, July). Improving indoor conditions in an Italian historical Church: the case study of Donnaregina Vecchia. In *2022 7th International Conference on Smart and Sustainable Technologies (SpliTech)* (pp. 1-6). IEEE.

[4] Li, D. H., & Wong, S. L. (2007). Daylighting and energy implications due to shading effects from nearby buildings. *Applied Energy*, *84*(12), 1199-1209.

[5] Strømann-Andersen, J., & Sattrup, P. A. (2011). The urban canyon and building energy use: Urban density versus daylight and passive solar gains. *Energy and Buildings*, *43*(8)

[6] Pisello, A. L., Xu, X., Taylor, J. E., & Cotana, F. (2012). Network of buildings' impact on indoor thermal performance. *Smart and Sustainable Built Environment*.

[7] Pisello, A. L., Taylor, J. E., Xu, X., & Cotana, F. (2012). Inter-building effect: Simulating the impact of a network of buildings on the accuracy of building energy performance predictions. *Building and environment*, *58*, 37-45.

[8] Capeluto, I. G. (2003). The influence of the urban environment on the availability of daylighting in office buildings in Israel. *Building and Environment*, *38*(5), 745-752.

[9] Ascione, F., Bianco, N., Iovane, T., Mastellone, M., & Mauro, G. M. (2020). Is it fundamental to model the inter-building effect for reliable building energy simulations? Interaction with shading systems. Building and Environment, 183, 107161.

[10] Poel, B., van Cruchten, G., & Balaras, C. A. (2007). Energy performance assessment of existing dwellings. Energy and Buildings, 39(4), 393-403.

[11] Wei, Y., Zhang, X., Shi, Y., Xia, L., Pan, S., Wu, J., ... & Zhao, X. (2018). A review of data-driven approaches for prediction and classification of building energy consumption. Renewable and Sustainable Energy Reviews, 82, 1027-1047.

[12] Langevin, J., Reyna, J. L., Ebrahimigharehbaghi, S., Sandberg, N., Fennell, P., Nägeli, C., ... & Webster, J. (2020). Developing a common approach for classifying building stock energy models. Renewable and Sustainable Energy Reviews, 133, 110276.

[13] Martínez, S., Eguía, P., Granada, E., Moazami, A., & Hamdy, M. (2020). A performance comparison of Multi-Objective Optimization-based approaches for calibrating white-box Building Energy Models. Energy and Buildings, 216, 109942.
[14] Drgoňa, J., Picard, D., & Helsen, L. (2020). Cloud-based implementation of white-box model predictive control for a GEOTABS office building: A field test demonstration. Journal of Process Control, 88, 63-77.
[15] De Coninck, R., Magnusson, F., Åkesson, J., & Helsen, L. (2016). Toolbox for development and validation of grey-box building models for forecasting and control. Journal of Building Performance Simulation, 9(3), 288-303.
[16] Arroyo, J., Spiessens, F., & Helsen, L. (2020). Identification of multi-zone grey-box building models for use in model predictive control. Journal of Building Performance Simulation, 13(4), 472-486.
[17] Bracht, M. K., Melo, A. P., & Lamberts, R. (2021). A metamodel for building information modeling-building energy modeling integration in early design stage. Automation in Construction, 121, 103422.
[18] Lee, S. H., Hong, T., Piette, M. A., & Taylor-Lange, S. C. (2015). Energy retrofit analysis toolkits for commercial buildings: A review. Energy, 89, 1087-1100.
[19] Hamdy, M., & Sirén, K. (2016). A multi-aid optimization scheme for large-scale investigation of cost-optimality and energy performance of buildings. Journal of Building Performance Simulation, 9(4), 411-430.
[20] Mathew, P. A., Dunn, L. N., Sohn, M. D., Mercado, A., Custudio, C., & Walter, T. (2015). Big-data for building energy performance: Lessons from assembling a very large national database of building energy use. Applied Energy, 140, 85-93.
[21] Ascione, F., Bianco, N., De Stasio, C., Mauro, G. M., & Vanoli, G. P. (2017). EMA: A user-friendly tool for reliable simulations of building energy performance in dynamic conditions by coupling EnergyPlus and MATLAB®. In ECOS 2017–The 30th International Conference on Efficiency, Cost, Optimization, Simulation and Environmental Impact of Energy Systems, San Diego [California, USA) 2-6 July 2017.
[22] Cucca, G., & Ianakiev, A. (2020). Assessment and optimisation of energy consumption in building communities using an innovative co-simulation tool. Journal of Building Engineering, 32, 101681.
[23] Andriamamonjy, A., Saelens, D., & Klein, R. (2019). A combined scientometric and conventional literature review to grasp the entire BIM knowledge and its integration with energy simulation. Journal of Building Engineering, 22, 513-527.

[24] Pezeshki, Z., Soleimani, A., & Darabi, A. (2019). Application of BEM and using BIM database for BEM: A review. Journal of Building Engineering, 23, 1-17.
[25] US Department of Energy. Energy Efficiency and Renewable Energy Office, Building Technology Program, EnergyPlus (version 8.4). Available online at: https://energyplus.net/. Accessed in September 2022.
[26] MathWorks, MATLAB – MATrixLABoratory (version 2015). https://it.mathworks.com/products/matlab.html. Accessed in September 2022.
[27] Nguyen, A. T., Reiter, S., & Rigo, P. (2014). A review on simulation-based optimization methods applied to building performance analysis. Applied Energy, 113, 1043-1058.
[28] Available online at: https://energyplus.net/weather. Accessed in September 2022.
[29] Mauro, G. M., Hamdy, M., Vanoli, G. P., Bianco, N., & Hensen, J. L. (2015). A new methodology for investigating the cost-optimality of energy retrofitting a building category. Energy and Buildings, 107, 456-478.
[30] Goel, S., Athalye, R. A., Wang, W., Zhang, J., Rosenberg, M. I., Xie, Y., ... & Mendon, V. V. (2014). Enhancements to ASHRAE standard 90.1 prototype building models (No. PNNL-23269). Pacific Northwest National Lab.(PNNL), Richland, WA (United States).
[31] Goel, S., Rosenberg, M. I., & Eley, C. (2017). ANSI/ASHRAE/IES Standard 90.1-2016 Performance Rating Method Reference Manual (No. PNNL-26917). Pacific Northwest National Lab.(PNNL), Richland, WA (United States).
[32] Ascione, F., Bianco, N., De Masi, R. F., Mastellone, M., Mauro, G. M., & Vanoli, G. P. (2020). The role of the occupant behavior in affecting the feasibility of energy refurbishment of residential buildings: typical effective retrofits compromised by typical wrong habits. Energy and Buildings, 110217.
[33] Oberegger, U. F., Pernetti, R., & Lollini, R. (2020). Bottom-up building stock retrofit based on levelized cost of ved energy. Energy and Buildings, 210, 109757.
[34] Standard, A. S. H. R. A. E. (2010). Standard 55-2010, Thermal environmental conditions for human occupancy. American Society of Heating, Refrigerating and Air Conditioning Engineers.
[35] CEN, (2007). 15251-2007. Criteria for the indoor environment including thermal indoor air quality, light and noise. Brussels: European Committee for Standardization.
[36] Kottek, M., Grieser, J., Beck, C., Rudolf, B., & Rubel, F. (2006). World map of the Köppen-Geiger climate classification updated. Meteorologische Zeitschrift, 15(3), 259-263.

[37] D.M. (Interministerial Decree) 26 giugno 2015. Available online at: http://www.sviluppoeconomico.gov.it/index.php/it/normativa/decreti-interministeriali/2032966-decreto-interministeriale-26-giugno-2015-applicazione-delle-metodologie-di-calcolo-delle-prestazioni-energetiche-e-definizione-delle-prescrizioni-e-dei-requisiti-minimi-degli-edifici#page_top. Accessed in September 2022.
[38] Webster, L., Bradford, J., Sartor, D., Shonder, J., Atkin, E., Dunnivant, S., ... & Schiller, S. (2015). M&V Guidelines: Measurement and Verification for Performance-Based Contracts. Version 4.0, Technical Report.
[39] Ascione, F., Bianco, N., De Masi, R. F., de' Rossi, F., & Vanoli, G. P. (2015). Energy retrofit of an educational building in the ancient center of Benevento. Feasibility study of energy savings and respect of the historical value. Energy and Buildings, 95, 172-183.
[40] European Parliament and the Council Directive 2018/844/EU of 30 May 2018 amending Directive 2010/31/EU on the energy performance of buildings and Directive 2012/27/EU on energy efficiency. Available online at: https://eur-lex.europa.eu/legal-content/EN/TXT/PDF/?uri=CELEX:32018L0844&from=EN. Accessed in September 2022.
[41] Ascione, F., Bianco, N., Mauro, G. M., & Napolitano, D. F. (2019). Retrofit of villas on Mediterranean coastlines: Pareto optimization with a view to energy-efficiency and cost-effectiveness. Applied Energy, 254, 113705.

CHAPTER 4

Technologies for the energy refurbishment of the existing buildings: Double skin façade and responsive elements

4.1 Introduction about building envelopes and energy efficiency

A sustainable future must necessarily pass through the energy efficiency of the built environment, which features ancient buildings, above all inefficient from both energy and well-being points of view, as previously discussed in Chapter 1. To achieve a sustainable and almost completely decarbonized system by 2050, the average annual renewal rate of the built environment must increase. By 2021, this rate is still too low, estimated at around 1%/a.

Energy renewal can be achieved through interventions that involve the three levers of energy efficiency, and thus the building envelope, the active energy systems and the exploitation of renewable energy sources. This Thesis focuses the attention on the building envelope, since it is the primary subsystem through which energy losses occur between inside and outside environments. The interventions on the envelope component have a longer duration than interventions on the systems. Furthermore, the interventions on the building envelope allow to stabilize the indoor conditions by also acting on the use of air conditioning systems. Finally, the energy efficiency interventions on the envelope can be associated or play a role themselves to adapt and improve the seismic behavior of the building by increasing its structural safety.

4.2 Building envelope: a transition from passive to active component

The component most investigated for the energy efficiency was and still is the opaque and transparent envelopes, to reduce the heat transfer through it, while still ensuring comfort for the occupants. The greatest interest in this component is attributable to its nature as a dividing element between the internal and external environment. In the first environment, adequate conditions are required to ensure the comfort of the occupants, the second is represented by the climatic conditions' characteristic of each area and period of the year.

The performance of the envelope must ensure the thermal and hygrometric comfort in the indoor spaces as well as the limitation of energy consumption and wastes, by satisfying environmental and technological requirements. Due to this crucial role, in recent years, with an increasing awareness in the last two decades, various researchers have investigated different energy efficiency measures for the exterior envelope. In particular, the transparent surface of the envelope, often strongly characterizing buildings' architectural features, is a critical element for both thermal comfort (*e.g.,* often penalized by unsatisfactory conditions of surface radiant temperatures) and energy balances (because of high energy losses and gains).

In recent years, there has been a transformation of the envelope concept through the implementation of responsive building components. From the dissipative culture, the step forward for the building envelope smart design is to conceive technologies capable of exploiting, adaptively, the natural resources to convert energy and protect the indoor environment. In the scientific research and under the technological and architectural experimentations, the building envelope is evolving from a protective barrier-element to a complex filter system, capable of optimizing the interactions between outside and inside environments. Thus, it is necessary to conceive the envelope as a dynamic boundary surface, able to vary its performance as the external environmental conditions change and contemporarily able to accommodate various types of plant engineering devices and equipment. Intelligent, adaptive and interactive architectural envelopes are thus designed and built to adapt, just like a real living component, to the variable conditions of the surrounding environment.

In this context, the following topics will be addressed in this Thesis:

- a review and a discussion of the most recent and cutting-edge researchers in matter of double-skin and responsive façades for the building retrofit;
- the application of passive and active technologies based on the double skin façades (DSF) for the energy retrofit of existing buildings with the analysis of the obtainable advantages.

4.3 The evolution of building energy retrofit via double-skin and responsive façade: a review

In this section it is proposed a review concerning:

- double-skin façades (DSF), as a solution for exploiting both passively and actively the solar radiation;
- responsive building components, which have adaptive thermophysical properties and behavior in order to optimize the interaction with the surrounding environment.

Firstly, DSF systems are investigated as promising passive building technology, also with the integration with building-integrated photovoltaic (BIPV) windows. These PV windows can replace the windows of the outer layer of the DSF, resulting in an amount of energy produced from renewable sources. A DSF surrounds the entire building, by having a protective function and aiming to enclose the existing construction in a new environment (the interspace that is created) that has more favorable thermo-hygrometric conditions (*e.g.,* temperature) compared to the outside environment. The cavity, that is created between internal and external environment, has to beneficially exploit natural ventilation, solar radiation, and thermal insulation. Clearly, suitable management is needed, during the whole year, so as fully take advantage of the potential benefits and avoid criticalities (for instance, indoor overheating during the warmer periods). Transparent photovoltaics (PV) and DSFs can be even combined by achieving multiple goals, *i.e.,* energy needs' reduction, improved thermal behavior because of the shading effects from cells (if opaque) and on-site generation of clean electricity.

Furthermore, a review of the retrofit solution that implements the transformation of the building envelope from passive to active components is proposed. The objective is identifying potentialities, recurrent benefits as well as barriers and criticalities that characterize the most innovative and cutting-edge technologies for building retrofit using double-skin and responsive façades. In particular, the main value of the proposed research lies in outlining the high potentials and energy benefits associated with the investigated solutions, which represent a pivotal way to face the renovation of the whole construction sector. Accordingly, a comprehensive snapshot of the evolution of such technologies is provided with original insights into current and future trends of building envelope energy retrofit with a view to low- (or zero-) energy buildings. Implementing eco-sustainable solutions is a way to regenerate the building stock making it technological, innovative and ecological, going in the direction of the energy transition towards electricity from renewables.

In the next sections, according to the layout proposed in the Figure 4.1, a deep and critical review of recent studies is proposed. This is the necessary state of art to consider for novel development of responsive elements.

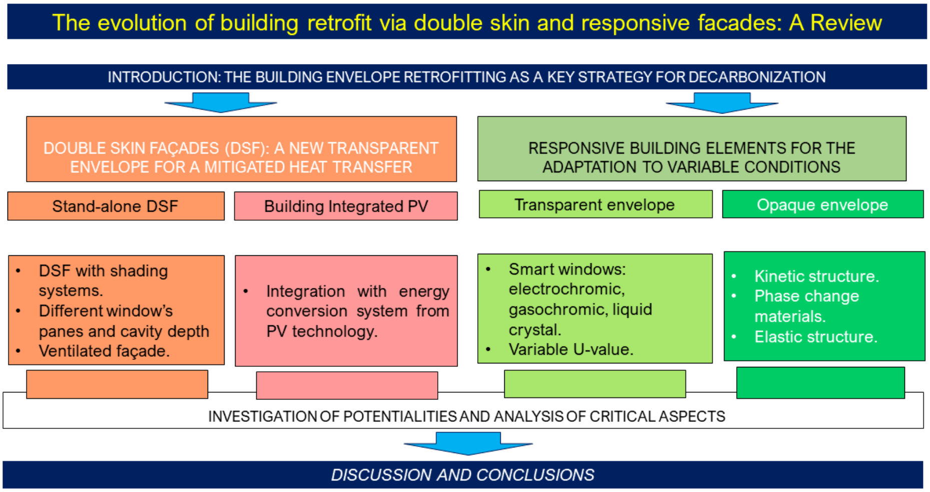

Figure 4.1: Organization of the reviewed studies

4.3.1 Double-skin façades for the building envelope retrofitting

In the last decade there has been an increasing use of double skin façade systems (DSFs). There are several definitions of these systems. In [1], the following definition is given: "A glazed double-skin façade is a hybrid system made of an external glazed skin and the actual building façade, which constitutes the inner skin. The two layers are separated by an air cavity which has fixed or controllable inlets and outlets and may or may not incorporate fixed or controllable shading devices". The cavity size can vary from 0.20 m to 2 m [1]. Really, according to the authors of this paper, a Double Skin Facade is an architectural transparent element of the building envelope. Conversely, in the case of reference to ventilated opaque building components, the definition of "vented wall" would be used. It should be noted that, besides a general phenomenon of ventilation in a cavity, the two systems are completely different, starting from the main aim (the exploitation of solar radiation during the heating season in the first case, the removal of solar heat gains by means of the stack effect in the cavity in the second one), the thermodynamics, costs and so on. From now, we will focus merely on the DSFs.

Double-skin façades can provide several energy benefits, through the creation of a thermal buffer zones, the possibility to preheat the air entering the building for the ventilation. Secondly, by completely enveloping the building, these systems play a protective role from external agents and moreover can accommodate photovoltaic modules [2],[3].

Double-skin façades as a new transparent envelope to mitigate heat transfer

A double skin façade, thanks to the cavity created with its installation, ensures that the internal environment is no longer subject to direct heat exchange with the external one. This determines a less heat loss in the winter periods. At the same time, however, overheating could occur in the summer period with negative consequences for cooling energy demand [4],[5]. Indeed, without a suitable and sufficient ventilation, the greenhouse effects can provide a temperature increase in the cavity, causing a heat transfer in the occupied spaces.

The DSFs result an effective and viable option thanks to the large number of achievable solutions, deriving from the combination of different ventilation strategies, different characteristics of the glasses and shading devices, different configurations of the cavity and its thickness [6], as confirmed by several studies. Accordingly, Pomponi *et al*. [1] investigated a large number of DSF systems in temperate climates. Globally, this system allowed to achieve a reduction in energy consumption of 90% and

30% for heating and cooling, respectively. As regards the cooling loads, energy savings have increased with the integration of shading systems. For example, Baldinelli [7] investigated a double-skin façade in which the external glazing is constituted by a stratified glass matched with movable shading system. The stratified glass consisted of two layers float glass separated by a plastic film, and the shading device is made of anodized aluminum. The examined building was an office located in central Italy and the double-skin façade (here re-proposed in Figure 4.2) is realized only on one side of the building, i.e., south side. The movable shading devices, operated by a hydraulic jack, can assume a horizontal configuration (Figure 4.2a) or a configuration with a high angle of inclination (Figure 4.2b). The first one is adopted in winter season thus allowing the passage of solar radiation. Moreover, thanks to the reflections on the shading surface, an indirect contribution is obtained. During the winter, the temperature in the cavity exceeds that of the outside air, and this implies a positive effect, reducing the heat losses through the outer walls. Furthermore, the buoyancy-induced flow in the cavity preheats the ventilation air.

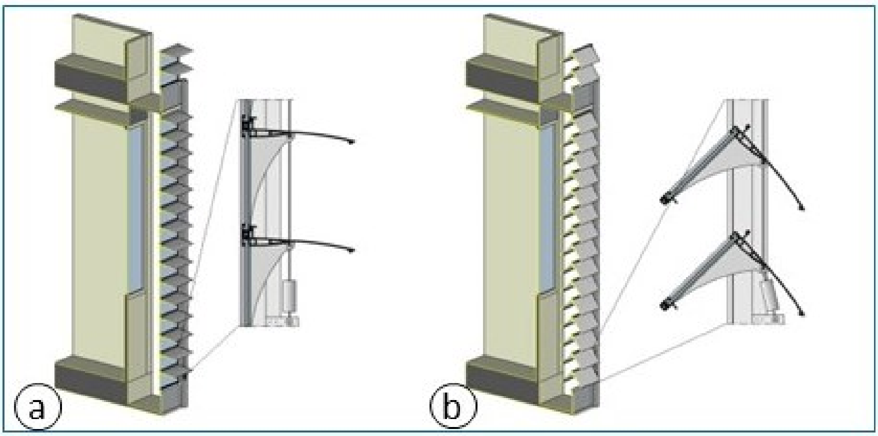

Figure 4.2: Winter (a) and summer configuration (b) (source: Baldinelli [7])

The second configuration, high angle of inclination (*i.e.,* sub-vertical position of slats), is adopted in summer season to stop the solar radiation. In this season, due to the high temperatures that are reached in the cavity, an unpleasant overheating effect is generated. To reduce (and even nullify) this effect, an open configuration is adopted (i.e., the external layer is open). This study highlighted an improvement in the energy performance of the building in comparison with traditional components.

Ghaffarianhoseini *et al. [8]* proposed a complete investigation of the technical characteristics of double-skin façades, the current designs and the advantages obtained from their installation (Figure 4.3).

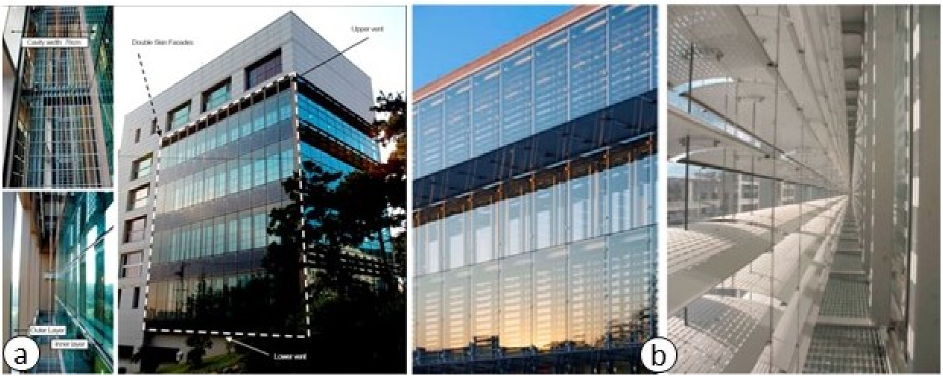

Figure 4.3: Example of DSF: Application on a multi-story building in Korea(a) (source: Ghaffarianhoseini et al. [8]); Cambridge public library, USA (b) (source: Ghaffarianhoseini et al. [8])

The study was conducted on the basis of data collection related to the response of these elements to changes in the characteristics of air gaps, the type of glass used and the heat transfer capability. The manuscript is quite useful to understand the working physical principles, and thus the thermal implications of heat transfer effects.

Chan *et al.* [9] investigated the energy performance of different configurations of a double-skin façade, with an air cavity depth of 1 m. In particular, the analyzed configurations are given from the coupling of two information: glass type (transparent, absorptive or reflective) and number

of glass layers (one or two). The different configurations have been applied to both internal and external position. The efficiency of the system was assessed by applying it to an office building in Hong Kong.
With both internal and external single glasses, the cooling load decreased in the range of 1.5% to 21.2%. A similar result in energy saving, was obtained for the case with double internal and single external glasses, with a maximum saving of 22.1%, achieved with reflective glass in both positions. In the case of single internal and double external glazing, the savings ranged from 0.3% to 26.3%. Finally, with double glazing for both positions, the maximum energy reduction of 26.6% was obtained with a double absorptive glass in internal position and a double reflective glass in the external position. Considering the high cost of double glass, the increase in energy savings, only 0.3% compared to the previous case, did not make it an affordable choice. Furthermore, the study highlighted a long payback period, of about 81 years. In this regard, the opportunity of incentives for DSF to improve building energy performance can be food for thought, as better specified in the following sections.
The overheating effect, in the air cavity, in cooling season had already been highlighted in [7] and it was solved by adopting an open configuration, to allow air to escape from the cavity. In [10], the coupling of the thermal mass technique and air channel of a DSF is proposed to counteract the increase of the air temperature inside the cavity. The system was compared to traditional DSFs, achieving savings of between 21% and 26% between 41% and 59% of cooling and heating loads, respectively.
Joe et al. [11] examined the impact of a DSF system on a multi-story building located in Korea, analyzing 34 different data for the glazing type and different cavity depths ranging from 8 to 148 cm. The DSF system was installed on the south façade, and it presented air intakes both

horizontally and vertically. As regards the glazing type for the internal and external layer of the DSF, the optimal solution was achieved with a single clear external glass and a double low-e selective internal glass.
Furthermore, by reducing the cavity thickness (from 780 mm to 430 mm) the total energy request was reduced by 5.62% compared to the energy demands of the base configuration.
In many studies, the thickness of the cavity represents a decision variable in identifying the configuration that involves the highest energy savings, for each specific boundary condition. For example, Alberto et al. [12] treated a study in the climatic conditions of southern Europe, obtaining a greater energy benefit with a cavity of 100 cm. In detail, the increase in the depth of the cavity to a value equal to 4 times compared to the initial one (initial value of 25 cm) allowed a 9.5% decrease in energy consumption. Other significant sensitivity parameters are the orientation and the association with an outdoor air curtain.
The DSF has a typically glass outer layer (which can then be single or double). A very interesting study is proposed by Scorpio et al [13], that evaluated the use of different plastic materials for the transparent component, in particular plastic fabric, ETFE and white ETFE. Other variables in the study were the depth of cavity, which could take two values, 0.05m and 0.10m, and the transparency of the materials. The materials selected for this analysis guarantee good durability, resistance and quality and for this reason the choice of using them as the outer layer of the DSF is justified. In addition, it deals with cheaper and lighter materials than commonly used glass layers. The analysis was carried out in a sample room in two months: January for heating period and July for cooling period. The results highlighted that the addition of a DSF on the south wall generally determines an increase of the heating energy demand, and thus of related CO_2-eq emissions, because of the lower

solar gains. A different performance was achieved in July, with a reduction of cooling energy of between 34.9 % and 45.1%. A study on the visual comfort, in January, has instead highlighted that with the use of these materials the Useful Daylight Illuminance "overlit" (which is defined by the authors as the UDI when the illuminance from daylight is too high and therefore causes a visual discomfort) is reduced, while the "useful" UDI (defined by the authors as the UDI when the illuminance from daylight provides adequate light) is increased. The same behavior was verified in July.

Blanco *et al*. [14] considered the typology of double-skin façades made with perforated sheet, and thus systems composed of a perforated metal sheet at the outer side, an air channel and an inner glass. The materials used for the metal sheets were anodized aluminum and galvanized steel. The study combined numerical modeling (DesignBuilder® and EnergyPlus), suitably validated against experimental data and other simulation models, also by taking into account deep boundary conditions achieved with specific algorithms implemented by means of MATLAB®, for instance concerning the wind penetration in the perforated coating. Several parameters were evaluated, and thus the influence of colors of sheet (black and white), perforation rate (from 0 to 70%), depth of the air gap (0.05 m and 0.30 m), the aforementioned penetration of wind and the location (in Spain), while further orientations beyond the south-exposure will be studied successively, in further developments. The energy performance of the proposed system was analyzed in different climatic conditions: cold/wet climates and hot/dry climates. The optimal solution, and therefore the greatest energy saving was achieved for the hottest area, with a saving of about 45% (with a percentage of the perforated sheet area equal to p=25%). For the colder areas the maximum energy saving was of about 20%, reached with p=40%. The target was a method for the optimization of this technological building component.

Yoon et al. [15] applied a DSF system, with an external low emissivity double glazing, as retrofit technology to a multi-story building. The building, dedicated to residential spaces, is made up of 25 story and it is located in Seoul, South Korea. The thermal buffer, provided by the DSF, made it possible to obtain a saving of 30% on heating energy request, with reference to the 21st floor.

Figure 4.4: Before and after the installation of a DSF (source: Yoon et al. [15])

It should be noted that, at the 25th floor, the wind speed is approximately 2.3 times that of the lowest floors, while the air temperature differs by about 0.4°C (annual average) between the first floor and the upper one. One of the main findings of the study is that a DFS may be very useful in heating-dominated climates for the energy retrofit of old buildings by replacing balconies (see Figure 4.4), significantly reducing the thermal energy needs because of the lower losses achieved thanks to the buffer.

Definitely, besides the opportunity of lower thermal losses, due to the creation of a second envelope, which allows an intermediate environment at a mitigated temperature (the so-called "thermal buffer"), the necessity of transparency but also of shading in presence of solar radiation has led to DSFs evolution and thus their integration with transparent PV. This is discussed below, in the next sub-sections.

Double-skin façades and Building-integrated photovoltaics: clean electricity, solar protection and multi-functional elements

Often, double-skin façades exploit the integration with photovoltaic (PV) energy conversion systems, being installed on building exposures characterized by high incident solar radiation. In this regard, Peng *et al.* [16] showed the development of a type of ventilated façade (building-integrated photovoltaics) with a double envelope (*i.e.,* a DSF). The façade consists of a photovoltaic module in transparent amorphous silicon, with an efficiency of 6.6%, an air duct of 0.4 mm in depth, and an internal window. The DSF, equipped of upper and lower openings for allowing a proper ventilation of the gap as in [11], is positioned to the south. The air flow that is generated, in addition to ensuring ventilation, counteracts the increasing of PV module temperature.

The system described was tested through experiments conducted in Hong Kong in the first two months of the year. The system was tested in different operating modes, ventilated, non-ventilated, internal windows open or closed, in order to then compare the results obtained. A first result confirmed that the air flow in the duct is able to remove heat, in fact the temperature measured in the upper opening is higher than that measured at the lower level of about 2.2-2.3°C. The simulations conducted with a non-ventilated mode and internal windows open showed that the system, on sunny days, is able to guarantee an indoor comfort temperature, which is not the case on cloudy and cold days. The temperature of the PV module naturally turned out lower on average in the case of ventilated facade, of about 3°C. As regards the SHGC (solar heat gain coefficient) the ventilated PV-DSF, with an average value of 0.1, was the best solution. As regards the heat losses the unventilated PV-DSF obtained the best performance with an average U value of 3.4 W/m²K (the ventilated PV-DSF presented a U value of 4.6 W/m²K). The optimal choice therefore depends on which is the decision-making factor between SHGC and U value, in the different climatic conditions. In subtropical climatic conditions, such as Hong Kong, this decision factor is SHGC and therefore the best solution is a ventilated PV-DSF, with a low heat gain. Really, the flexibility of the management and the variation of configuration can be crucial points of strength.

Shakouri *et al*. [17] investigated the effectiveness of a building integrated photovoltaic thermal double-skin façade (BIPVT-DSF), applying the system to a five-story building located in Tehran (Iran). The cavity depth was of 0.3 m. The PV modules used are characterized by an efficiency of 15% and the total installation power was of 10.6 kW. The photovoltaic system produced approximately 18,064 kWh per year. The thermal load is scarcely influenced by the system, it is reduced by about 3.2%. As for the cooling load there were days in which the energy produced by the photovoltaic system is higher than that required. Globally, the building's energy performance index increased by 34.3%.

In [18], the energy performance of six different types of semi-transparent photovoltaics was assessed. The six modules differed for what concerns: surface area, efficiency (3.32% - 8.02%), SHGC (0.123- 0.413), U-value (1.67 W/m²K – 5.10 W/m²K), visible-light transmittance (1.84% -9.17%), photovoltaic technology, construction assembly and appearance (standard, red, golden, dark blue). As regards the construction assembly two modules were double glazed and four single glazed. All six modules were made of thin-film solar cell. To assess how much a module can be efficient, the authors introduced the net electricity benefit (NEB) indicator defined as “the sum of photovoltaic electricity production and energy savings for lighting minus the increase/decrease of energy demand for space conditioning (heating and cooling) in comparison to a building with 0% WWR” [18]. Therefore, when the NEB value is positive, the use of the photovoltaic modules is energetically convenient, as the production from photovoltaic technology exceeds the increase in HVAC consumption. The building under study was a typical office building and it was modeled and simulated in EnergyPlus. From a first analysis, conducted by varying the WWR, from 10% to 100%, and the orientations of the modules investigated, three of them showed a positive NEB value (with a growing trend with WWR).

Two of these were the double-glazed BIPVs, with a U-value of 1.67 W/m²K and 2.14 W/m²K and a photovoltaic efficiency of 5.01% and 4.75%. The other best case, with very similar performance to the other two, was a single glass that featured 37-40% higher efficiency and 20-24% higher visible light transmission (VLT) compared to a double-glazed window. The semi-transparent BIPVs performed an energy benefit to the building for any orientation, even for those that do not have a better sun exposure. This is due to Singapore's characteristic of diffuse light conditions; indeed, similar results are not achieved under different boundary and climate conditions. Moreover, semi-transparent BIPVs were compared with traditional glazed components (both single and double glazing and with low emissivity characteristics). With the conventional window glazing types, there was a negative linear dependence between the WWR and the total annual electricity consumption, i.e., as WWR increases, annual energy consumption increases. With the semi-transparent BIPV modules the trend was the opposite, i.e., the annual consumption is reduced by about 0.15- 2.14 kWh/m²year, and the savings obtainable with the semi-transparent BIPV modules increased as the WWR increased.

Wang *et al*. [19] presented a study on two types of dynamic façades, one with double envelope integrated with photovoltaic modules (PV-DSF) and the other with single photovoltaic insulating glazing systems (PV-IGU). The PV-DSF consisted of semi-transparent panel with air intakes on the upper and lower parts, an internal 400 mm air cavity and a last internal layer formed by single glass. The PV-IGU module consisted of a semi-transparent panel and a double tempered glass. The simulation models were built on the basis of a series of data collected by sensors. PV modules are characterized by an efficiency of 6.3% and a transmittance of 20%. Geometrically, they are characterized by a different area for the two applications, which resulted in a different maximum output power (51 Wp for the PV-DSF and 88 Wp for the PV-IGU). The two dynamic facades were applied on a typical office room and their performance were evaluated compared to traditional windows, in five different climatic conditions. The two systems obtained the maximum energy saving in the same city, with moderate climate. The energy saving was of 46.9% for the PV-DSF and of 44.8% for the PV-IGU. Generally, the energy performance of PV-IGU is slightly better than the PV-DSF. If ventilation is created inside the cavity of the PV-DSF system, the performance of the latter improves and exceeds that of the PV-IGU system in cold climates. Due to the high initial cost of these photovoltaic systems, there was a rather long payback time of approximately 15.5 years for PV-DSF and 12 years for PV-IGU. Especially for this reason there has not yet been a high diffusion of such systems.

Now, some summarizing remarks. The studies analyzed in this section were conducted in countries belonging to different continents, mainly Asia (China, Korea, Singapore) and Europe (Germany, Italy, Spain). In most of the analyzed cases, the intended use of the building was offices, both as a single zone and as a multi-story building dedicated to office activities. The technologies, DSF and BIPV, have shown energy benefits in different climatic conditions. This is clearly due to the diversification of the applied solutions in the different climates. For example, the energy saving in cooling season in Hong Kong [9] is comparable to that obtained in Turin and Munich [10], but in the first case the DSF presented a double absorptive glass as the outer layer while, in the second case, the DSF involved a thermal mass in the cavity. In Korea [11], a reduction in energy consumption is obtained by reducing the cavity thickness while, in Portugal [12], the reduction is obtained through an increase of the cavity thickness. In Spain [14], on the other hand, the same solution showed a greater benefit in the hottest area.

Table 4.1 reports a schematic overview of the discussed studies in matter of double-skin façades including the integration with solar cells.

Table 4.1: Studies concerning double-skin façades and Building-integrated photovoltaics: applied system and/or technology, type of investigation, cities and seasons of analysis, type of building and main findings

Year of the study	Authors	Applied System and/or Technology	Type of investigation	Cities and Seasons of Analysis	Type of building	Main findings and results
2009	Baldinelli [7]	DSF coupled with movable shading devices	Simulation	Central Italy Heating and cooling season	Office	In winter, the high air temperature in the cavity reduces heat losses and preheats the ventilation air. In summer, by adopting an open cavity configuration, the overheating effect is reduced.
2009	Chan *et al.* [9]	DSF	Simulation	Hong Kong Cooling season	Office	The maximum reduction in cooling energy is 26.6%, and this is achieved with the internal and external glass, both of the double-glazed type, respectively absorbing and reflecting.
2010	Fallahi *et al.* [10]	DSF with a thermal mass	Simulation	Theoretical, with validation in Turin (Italy) and Munich (Germany) Heating and cooling seasons	Test room	Compared to the conventional DSFs, the integration of thermal mass allows an energy savings of between 21% and 26% in cooling period and between 41% and 59% in heating period.

Year of the study	Authors	Applied System and/or Technology	Type of investigation	Cities and Seasons of Analysis	Type of building	Main findings and results
2014	Joe *et al.* [11]	DSF	Simulation	Seoul, Korea Heating and cooling season	Multi-story	Reduction in energy consumption of 5.62% is achieved by reducing the thickness of the cavity, from 780 mm to 430 mm.
2017	Alberto *et al.* [12]	DSF	Simulation	Porto, Portugual Summer and winter day	Office	The best configuration provides a cavity of 100 cm, with reduction in energy demand of a 9.5% compared to a cavity of 25 cm.
2019	Scorpio *et al.* [13]	DSF with plastic materials	Simulation	Naples, Italy Heating and cooling season	Sample room	The use of plastic materials has led to a reduction in the cooling energy demand (between 34.9% and 45.1%), and an increase on visual comfort both for the winter and summer periods.
2016	Blanco *et al.* [14]	DSF in perforated sheet metal	Simulation	Spain, various climates Heating and cooling seasons	Theoric al model	The greatest energy saving, of about 45%, was obtained in the hottest areas, with a percentage of the perforated sheet surface equal to 25%
2019	Yoon *et al.* [15]	DSF	Simulation	Seoul, Korea Heating season	25-story apartme nt	Heating energy savings of 30% at the upper floor (21th) are achieved. Results revelaed a good performance as retrofit technology.
2013	Peng *et al.* [16]	DSF-BIPV	Experimental	Hong Kong Heating and cooling season	—	The best solution is the ventilated PV-DSF, which guaranteed an SHGC value of 0.1.
2020	Shakouri *et al.* [17]	DSF-BIPVT	Experimental and Simulation	Tehran, Iran Heating and cooling season	Five-story	PV system, that produced approximately 18,064 kWh per year, can reduce the thermal load of about 3.2%. Globally it can improve the building performance of 34.3%.
2013	Ng *et al.* [18]	Semitransparent PV modules	Simulation	Singapore Heating and cooling season	Office	Compared to traditional windows, the semi-transparent photovoltaic modules allow a reduction in annual consumption. For the climatic conditions of Singapore, the energy benefit is obtained for any orientation.
2017	Wang *et al.* [19]	DSF-PV vs IGU-PV	Experimental	Five different climates of China Heating and cooling season	Office room	The best performances are obtained in moderate climatic conditions with an energy saving of 46.9% and 44.8% for PV-DSF and PV-IGU, respectively. From an economic point of view these systems are not convenient.

4.3.2 Responsive building elements for the adaptation to variable conditions

The terms “responsive” and “adaptable elements” indicate building components whose thermophysical behavior can vary over time and can adapt to the different needs of the building and occupants, taking into account the different boundary conditions that can occur along the seasons and during the days (for instance, the day-night cycles). Thus, an adaptive building envelope can be seen as an envelope capable to change its properties and control the different indoor parameters, heat transfer and energy conversion. These changes are applied to answer to load variation, changed indoor or outdoor conditions, with the aim of improving comfort and/or energy efficiency, according to several ways. Indeed, the changing can be obtained through the shift of the elements, the chemical change of the material or by exploiting an air flow. Among the definitions of responsive building envelopes, provided in the literature, the most used was given by Loonen *et al*. [20]: “An adaptive building shell has the ability to repeatedly and reversibly change some of its functions, features or behavior over time in response to changing performance requirements and variable boundary conditions, and does this with the aim of improving overall building performance”.

Responsive building elements can be utilized both in the transparent and opaque envelopes, and recent progress and investigations are proposed below.

<u>Responsive systems for the transparent building envelope</u>

Baetens *et al*. [21] analyzed four different prototypes of smart windows. The first are the electrochromic devices, that have a base in glass or plastic, coated by a clear conductive layer, usually Indium tin oxide, followed by one or more cathodic electroactive layers. The subsequent layers consist of an ionic conductor, an ion accumulation film, one or more layers of anodic electroactive elements, and a transparent conductive film. The second are the gasochromic devices, they are considered cheaper as only one electrochromic layer is sufficient. The dynamism of these elements is given by the modulation of the transmittance, achieved by a managed gas exchange. The third are the liquid crystals. For these smart windows, the switching is obtained through the application of an electric field that causes a movement of molecules, which allows a variation of transmittance. These devices present critical aspects, as the high cost and the need of a continuous power. The fourth analyzed prototype are the suspended-particle devices. They are composed of 3 to 5 layers and thus, for instance, two transparent conductors between which the adsorbent particles are present, suspended in an organic fluid. Even for this type of intelligent windows, as happens for liquid crystals, the application of an electric field generates a displacement of the particles (which align or not according to the intensity of the field) causing a variation in the value of the transmittance. The electrochromic windows, the most common on market, can reduce up to 26% of lighting energy and 20% of cooling loads in climates such as the Californian ones. Further research is however needed to evaluate their use and achievable performance in colder climates.

Perino *et al.* [22] studied "intelligent glass systems" (SMARTGlass), integrated with phase change materials (PCM). The configurations analyzed are two: a) a double glass with a paraffin wax inside with a melting point of 35°C; b) a triple glass with the coupling of a PCM and a thermo-tropic (TT) layer. With the first configuration, the input energy is reduced by about 20% compared to a traditional double glass. On days with high solar radiation the paraffin melting process ends too early (early afternoon) causing an increase in the internal surface temperature which in turn is responsible for thermal discomfort for the occupants. Regarding the second case, two cases were examined, that differs for the PCM position. In the first case, the PCM is located in the outward facing cavity in the second it occupies the inward facing cavity. When the PCM-filled cavity is facing inwards, PCM fails to finish the phase change and the heat flux exchanged by convection is reduced until a value of 35 W/m^2. When the PCM-filled cavity is facing outwards, the phenomenon is limited and the heat flux is reduced to twice the value of the previous case, as the entire PCM melts. Despite this positive result, the tested PCMs (RT35HC) were characterized by a too high melting temperature which makes them unsuitable during the winter period (*i.e.,* the heating season). According to the authors, a possible solution and improvement may be the adoption of electrochromic devices or the matching of two PCMs.

Favoino and Overend [23] evaluated the efficiency of an electrochromic smart glass, analyzing its impact on energy consumption and occupant comfort. The study was conducted through an inverse method, i.e., the thermo-optical characteristics of the envelope were assigned based on the required energy and thermal comfort. This was achieved by combining the software EnergyPlus, GenOpt and MATLAB®, which act as evaluation (with the Energy Management System), optimization, and control modules, respectively. The building under study is a typical office room located in London. The building has a south-facing façade, equipped with electrochromic intelligent glazing for the 40%, while the other 60% is opaque. The smart glazing can modulate the visible transmission, Tvis (0.01-0.6), and the solar heat gain coefficient, SHGC (0.005-0.27). The simulations were carried out during the hottest week of July (23-30 July). The electrochromic glazing (EC) was compared with different types of traditional double glazing (which are distinguished by the Tvis and SHGC parameters and by the presence of internal shading). The use of an EC glazing implied a cooling energy reduction of 80% compared the traditional solution, and 76% compared to the traditional glazing coupled with internal shading system. The primary energy consumption is reduced of 29% and 62%, respectively. In addition, instead of reactive control, an optimal receding horizon control can be even adopted: in this case, the energy consumption could be reduced by an additional 9-11%. Furthermore, with EC glazing, better indoor environmental quality – with a lower predicted percentage of dissatisfied (PPD) (9.3% compared to 12.8% of the traditional double glazing) – higher daylight autonomy (DA) (52.3% compared to the 33.7% of the traditional double glazing) and absence of glare are achieved.

Bui *et al*. [24] developed a computational optimization approach to investigate the performance of an adaptive façade system that can change its thermal and structural functions over time. The responsiveness of the single glass analysed is given by the variation of the parameters Tvis and U, respectively in the ranges 0.05–0.9 and 0.1–10 W / m²K. The investigation focused on the analysis of two case studies, both located in Melbourne, Australia: a) an office room, b) a three-floors office building. The analysis was performed in both a summer and a winter week. The adaptive system was compared to a traditional one, in both case studies. In case a), the system allowed energy savings in cooling demand in the range 18.8-29%, and in heating demand in the range 14.9-22.7%. In case b), the cooling energy saving is between 14.2% and 15.4% and the heating energy saving is between 18.1% and 22.3%. Obviously, the optimal U-value and Tvis are influenced by the dynamic climatic conditions.

Responsive systems for the opaque building envelope

Adaptive building coatings and shells concern also the opaque envelope, with reference to both vertical perimeters and roof slabs. A classic example is the Trombe wall. Here the most innovative technologies are presented. Recently, Kirkegaard [25] proposed the development of a new adaptive envelope system, composed of a primary structure that allows to form a double curvature thanks to a series of tetrahedral elements, and a secondary surface structure which can open and close allowing the passage of air flow and sunlight, this implies a change in the shape of the building. A prototype of this system was built at Aalborg University. The change can occur through different control strategies.

Favoino *et al*. [26], in the cold winter climate of Turin (north Italy) analyzed the characteristics of multifunctional façades' module, identified as "ACTRESS" (ACTive, RESponsive and Solar). The study was conducted on a prototype, built in Turin and tested for 35 days. The module consists of two main parts, one opaque and one transparent. The opaque module consists of an external part made up of glass laminated photovoltaic panels, an internal part made up of five layers, two of which are phase change materials with a melting temperature of 23°C and 27°C. Between the two PCM layers there is an electric heating sheet to activate them, allowing thermal energy storage. The external and internal parts are divided by a ventilated air cavity of 120 mm. The transparent module covering 50% of the façade has a lower part consisting of a triple low-emissivity glass, with gas argon in the cavity and in the external space there is a curtain (venetian), covered with highly reflective low-emissivity glass; the upper part consists of a triple glass, with aerogel in the external cavity. The results obtained confirmed the expectations and agree with those of other studies, such as [16]. In winter, the ventilation air was preheated, the hot air in the cavity created thermal buffer zone with a consequent increasing the thermal insulation and reducing the heat losses, as in [7] and [15]. In summer, the hot air in the cavity was expelled avoiding the overheating effect, guaranteeing an adequate temperature of the PV panels. To these benefits was added the heat recovery function when the solar radiation is high.

This experimental campaign enabled to verify that, with the use of this module, there is a significant reduction in heat losses and a better exploitation of solar energy. Thanks to this energy benefits the ACTRESS module was defined by the authors “energy positive". The upper part of the transparent module, with aerogel, showed the best energy performance with a U-value of 0.58 W/m²K. However, there are some negative aspects related to the use of aerogel (because of the high cost), the possibility of exploiting stored energy only between 20% and 70%, the need to develop a complex and automated management system to benefit of the ACTRESS potentials.

Figure 4.5: The ACTRESS façade module (source: Favoino et al. [26])

Matheou et al. [27] described two kinetic mechanisms of responsive facade systems. The first reactive system presented a design based on “origami”, i.e., the art of folding the paper. The structural unit is made of an aluminum frame that includes 8 triangular shaped units. Each unit can be folded six times. Through a system of cables, the unit can assume different configurations. A facade based on this mechanism was installed in a four-story building in Cyprus. A second system acted as a membrane made up of lightweight textile surface. Also in this case, the membrane can assume different configurations by means of cables. The objective in both cases is to control the daylight by ensuring adequate visual comfort for the occupants.

Gallo *et al*. [28] presented three innovative responsive systems called "SELFIE" (Smart and Efficient Layers for Innovative Envelope The first responsive system (SELFIE 1) is an opaque module (0.2 W/m²K) with louvers in the internal and external surfaces. It is formed by a double-glazed layer where, in the medium, there is a PVB (polyvinyl butyral) film combined with nanomaterials, capable of transmitting the visible light and reflecting in the IR zone. The next four layers consist of: a permeable ceramic honeycomb panel loaded with TiO2, a mesoporous glass foam filled with PCM, a surface consisting of sealing material and a closing panel. The second system (SELFIE 2) is an opaque module (0.2 W/m²K) consisting of an external layer in dye-sensitized solar cell (DSSC) photovoltaic panels, an insulating layer with PCM (phase change material), a system for the heat exchange and a closing panel.

The third system (SELFIE 3) is a transparent module consisting of a first stratified glass with PVB and nanomaterials (characterized by a U-value of 1.2 W / m²K), then a cavity with an electric shading system and finally a low-emissive glass with U-value of 1.2 W/m²K. The aim is to analyze these prototypes and compare their performance in different geographical areas. Really, these targets are future development of the conceived technology. In addition, even a combination of these systems is proposed (see Figure 4.6). The results of the developed configurations, not yet available, will be calculated in the Italian climates of Milan, Florence and Palermo and these will concern the cooling and heating energy request, the primary energy consumption and savings, implications on indoor thermal comfort, lifecycle issues and environmental footprint.

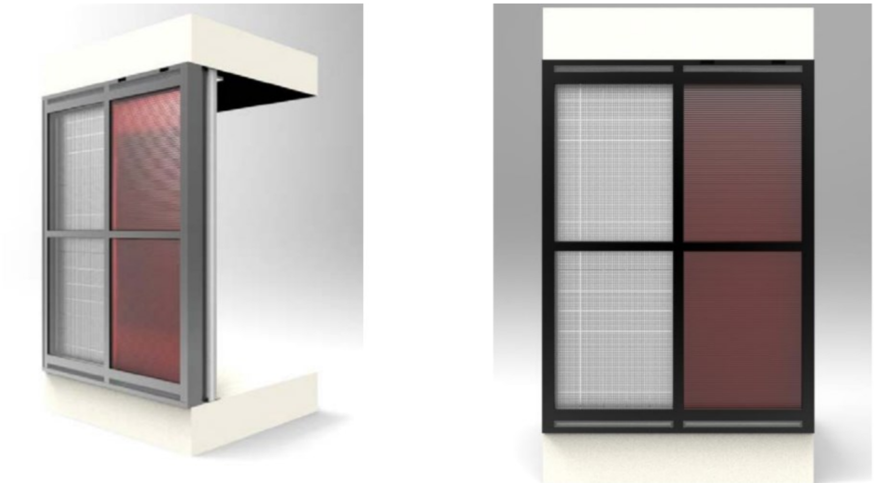

Figure 4.6: Combination of Responsive Façades, SELFIE 1 and SELFIE 2 (source: Gallo et al. [28])

Some researchers have dealt with real cases of using responsive elements on buildings. Radwan and Osama [29] studied the application of a biomimetic approach to the façade design. The case of greatest interest is a 10-storey building with a system of façades inspired by the bark of trees (The Council House 2, Melbourne, Australia) and which has, as main objective, the reduction of energy consumption by improving the comfort of the occupants at the same time. The façade facing west, and those facing north and south, are made in such a way as to imitate the epidermis and bronchi of trees, respectively. In addition, the facades facing north and south are provided with ventilation pipes joined to the air ducts towards the outside. The east façade, inspired by the bark, has an outer protective layer and an inner one that filter the light and the air respectively. Furthermore, perforated metal layers are added to the façade. The materials used for these façades are recycled wood, steel and concrete. The results obtained from an analysis based on the satisfaction of a series of parameters – such as air filtering, visual comfort, solar tracking systems, thermal protection or for example the use of photovoltaic panels – provided very interesting findings. Indeed, the proposed configuration, compared to two additional façade systems inspired by the natural formation of soap bubbles and by tropical durian fruits (biology analogy), respectively, allowed the highest energy efficiency, with an energy saving of 82%. In addition, the system allowed a saving of 65% for natural lighting and ventilation.

Barozzi *et al*. [30] investigated and compared different types of innovative shading systems applied to buildings. These shading systems were included in two macro-categories, the "kinematic systems" (*e.g.,* Al Bahr towers in Abu Dhabi, Figure 4.7a), and the "elastic kinetic systems" (*e.g.,* Thematic Pavilion in Yeosu, Figure 4.7b), respectively.

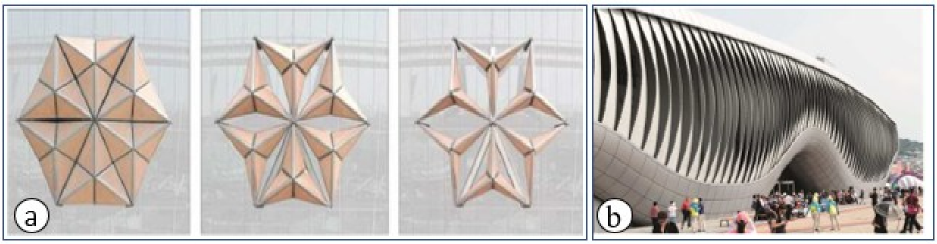

Figure 4.7: Configurations of solar shading in the Al Bahr tower (a) (source: Barozzi et al. [30]); Thematic Pavilion Yeosu (b) (source: Barozzi et al. [30])

Classic shading devices have a mechanism limited by planar surfaces and even if they are very simple and cheap, they are not suitable in a context dominated by the concepts of adaptation and dynamic response. In the

Al-Bahr tower there is an example of adaptive solar shading, which according to the project data leads to a saving in the cooling demand of about 1/4. The mechanism that makes this shading system responsive is inspired by the mashrabiya (a window protection system typically used in Arabic architecture) and allows five different configurations. For what concerns the second systems' type, "elastic kinetic systems", an example is the Flectofin®. The dynamicity of the elements is realized inspirating to the reversible deformations of plants. It is a hinge-less flapping mechanism. In the case of Pavilion at the EXPO 2012, the louvers are made of glass-filament supported polymer. The actuators, positioned at the top and at the bottom, can generate an elastic deformation to allow the passage of sun rays, improving the natural lighting.

Shahin [31] addressed three further design strategies, that adopted the adaptive building elements for multi-story buildings (see Figure 4.8). The first (Media-ICT building, Barcelona) uses an ethylene-tetrafluoroethylene (ETFE) polymer coating system with recessed lamellar fins operated with pneumatic mechanisms by sunlight sensors, capable of leading to an energy saving of about 20%. The second (again referred to the Al Bahr towers, Abu Dhabi) uses a shading system consisting of triangular panels in polytetrafluoroethylene (PTFE), covered with a micro-perforated layer of fiberglass, mechanically activated, and positioned on a façade structure located at 2 m. The solar gain is reduced of about 50% resulting in a reduction in HVAC energy consumption. It is also possible to obtain a reduction in lighting consumption with glasses that allow a greater passage of sunlight. The third model (*i.e.,* the Terrence Donnelly Center for Cellular and Biomolecular Research, Toronto) consists of a façade formed by a double-glazed casing, with an internal air gap with a thickness of 800 mm. Thanks to the natural ventilation that is generated in the façade, the cooling loads are reduced, while the perforated aluminum slats improve also the thermal quality of the rooms and the exploitation of natural lighting.

Figure 4.8: Media-ICT building, Barcelona (a) (source: Shahin [31]); Al Bahr towers, Abu Dhabi (b) (source: Shahin [31]); Terrence Donnelly, Toronto (c) (source: Shahin [31])

In the same vein, an innovative system was described by Park *et al.* [32], namely a dynamic façade that uses a wind turbine integrated in the building envelope (BIWT). The envelope presents compartments to collect, increase the speed and direct the wind on the turbine blades.

Preliminary studies have resulted in a prototype of a wind turbine, with a capacity of 200 W. The rotor, made of Aluminum 5052, was tested in a small-scale wind tunnel. The performance of the system was evaluated by installing it on the southwest direction of a multi-story building dedicated to residential spaces, in Busan (South Korea) consisting of 51 floors. This area is chosen because it is densely occupied by skyscrapers, among which strong air currents are created. The building daily electricity consumption was of 3860 kWh. In particular, a module with an area of 1 m² converted 0.248 kWh/day as average yearly value. The facade system is characterized by a daily electricity production of 241 kWh, which represents approximately 6.3% of the building's daily electricity consumption. From these results, the proposed system, a wind turbine integrated into the building envelope, appears to be a valid energy requalification measure for buildings located in urban areas.

As previously said, coming back to the premise of this review study, a large part of the existing building stock worldwide is not energy efficient. In this regard, for instance, at EU level, around 3/4 of the building stock is energy-intensive [33]. This means that a significant share of the energy used is wasted. Therefore, the concept of responsive elements must be applied to the existing buildings.

Cascone et al. [34] conducted a multi-objective optimization analysis using phase change materials (PCM) for energy enhancement of the opaque envelope component. Two layers of PCMs were selected, PCM1 with a melting temperature between 15.5°c and 23°C and PCM2 with a melting temperature between 23.5°C and 39°C, and different positions inside the wall of PCM were analyzed. The type of office chosen for the study was based on the model of the typical Italian building construction of the years 1946-1970, and thus in reinforced concrete with scarce, often zero, levels of insulation. The study was conducted on the third floor of a building consisting of a total of five floors. The choice of the third floor derives from the need to have a high solar radiation without neglecting the impact of the surrounding buildings. To evaluate the overall characteristics, simulations were conducted in two different Italian cities, characterized by different geographic and climatic conditions, Turin (north) and Palermo (south). The objective functions (to minimize) are divided into two groups, in-series analysis.

- primary energy consumption and global cost,
- energy demand for space conditioning and investment costs.

Regardless of the objective function to be minimized, a lower energy request for space conditioning is obtained compared to the baseline, without the PCM. As regards the primary energy consumption, in Palermo the system determines a reduction between 16% -24% while in Turin the reduction is between 25% and 33%. In particular, in Palermo, the system provides a reduction in heating energy request between 35% and 73% and in cooling energy request between 18% and 31%. In Turin, the saving in heating energy demand is limited in a range of 28-38%, while the cooling energy demand is reduced in the range of 28%-33%. For both climatic conditions the minimization of the primary energy consumption and of the global cost was obtained with the retrofit intervention on the internal layer (RTi). In general, the better position for the PCM is the closest to the indoor environment: the maximum saving is achieved with the PCM layer positioned between the existing wall and the external insulation or as an internal layer for the RTe and RTi options, respectively. Between the two PCMs investigated, the maximum reduction in primary energy consumption was obtained with PCM1, characterized by a peak melting temperature of 23.5 °C. The primary energy consumption decreases linearly as the thickness of the PCM increases. As regards the global cost minimization, this was never achieved with the insertion of the PCM layer. Therefore, if the economic aspect is of primary interest, the PCM would never be used.

Basso *et al*. [35] presented an innovative adaptive ventilated façade modules: the system “E2VENT”. This innovative module is made up of two parts: 1) a waste energy recovery unit (SMHRU) and a latent heat thermal energy system (LHTES). The first allows a free heating of the ventilation air in winter and obtaining free cooling in summer, the second system, composed of phase change materials, allows free cooling. The energy performance of this system was investigated in five cities

Stockholm, Gdansk, Paris, Madrid, and Athens which correspond to five different characteristic climatic conditions: Baltic climate with cold winters and mild summers, temperate continental climate, continental climate with hot summers and winters rigid, semi-arid climate with moderately cold winters and hot summers and hot Mediterranean climate with very hot and muggy summers and mild but rainy winters. The two units, SMHRU and LHTES, are complementary and both integrated into the façade cavity. The authors developed the module by using the TRNSYS® software, and thus the energy saving of the system was assessed on a winter and a summer day, January 1st and August 1st. The results highlighted an improvement in thermal and hygrometric conditions for all climatic zones, with a greater impact in hot climates, Athens. The E2VENT system involved a reduction of the number of discomfort hours that is dependent to the climatic conditions. The proposed system ensures a reduction of heating load in the range of 18%-43%, with maximum performance in Athens. Conversely, the reduction of cooling load is in the range of 13%-100%, with maximum in Gdansk. Despite a high reduction of energy from fossil fuels compared to a traditional energy renovation, the E2VENT system is characterized by a greater electricity usage. For this reason, future developments will be focused to reduce it. More information about this system and the Horizon Project in which it is developed can be found in [35],[36],[37] and at: http://www.e2vent.eu/.

An interesting solution is the one proposed by Elarga *et al*. [38], who investigated the performances of a PV-PCM combined with a double-skin façade, applying it in the west direction of a virtual office room. The PV implemented into the facade is a semi-transparent module (a-Si) with a nominal peak power of 140 W and a reference efficiency of 15%. The effectiveness of this technology was evaluated in three different climatic conditions, Helsinki (Finland), Venice (Italy) and Abu Dhabi (United Arab

Emirates), and two different PCMs were selected, as it is necessary that the phase change takes place in an adequate temperature range. In particular, for Helsinki and Venice, the nominal melting temperature is 41°C, while for the hot climate of Abu Dhabi is higher, *i.e.,* 55°C. In Venice, the cooling loads are reduced by 29% thanks to the implementation of PCM technology, whereas the heating energy demand is not influenced by PCM. Likewise, in Helsinki the PCM allows a reduction in cooling loads in the range of 20%-23%. The best potentialities of the PCM are obtained in Abu Dhabi, with an energy saving of average 22%, with reference to the whole year. The use of PCM influenced the surface temperature of the PV module, in particular the average surface temperature suffered a reduction. For the PCM material suitable charging and discharging cycles have to be allowed. In detail, when using a PCM layer, the cooling phase is important, during non-operation periods, which prepares the material to stock energy again, for this purpose the mechanical ventilation of the cavity is essential.

Hu et al. [39] investigated the application of: a thermochromic coating (TC), a phase change material (PCM) and the coupling of these two on a roof. The TC pigment is characterized by the change of its properties and color for a temperature value of about 31°C: below and above this value, it has a dark or light color, respectively. The operation of the TC coating is the following: during the summer period it shows a high solar reflectance while the opposite, (i.e., a high solar absorptance) occurs in the winter period. The PCM material is made of 60% paraffin microcapsules with a thermal conductivity that varies between 0.18 and 0.23 W/mK and a melting temperature of 21.7°C. As regards the operation of the PCM layer, during the night it liberates the energy accumulated during the day towards the surrounding environments, both internal and external. The energy performance of these elements was evaluated with reference to a

typical office building. When the TC and the PCM layers are both inserted, the roof has a TC coating as the outermost layer, while the PCM layer represents the fourth layer. The second, third and fifth (innermost) layers are asphalt shingles, an insulation and concrete layer respectively. The investigations were performed for five cities which correspond to five different climatic conditions of China: Beijing, Heilongjiang, Nanjing, Guangzhou, and Kunming.
Concerning cooling loads, TC, PCM and the coupling of these two integrated into the roof, led to a maximum saving of 16%, 4% and 18%, respectively. All solution yield larger energy savings in cities with milder climates, i.e., in Kunming, as the temperatures are closer to the temperatures that allow for a transformation of the TC and PCM materials. As regard the heating loads, TC, PCM and the coupling of these two integrated into the roof, led to a maximum saving of 2%, 14% and 19%, respectively. The highest savings are achieved in the warm climate region, as the temperature is higher than the melting temperature of the PCM. These results show that the application of the TC coating alone has a low influence on the heating demand, with a maximum energy saving of 2% in Beijing, while the application of the PCM alone has a low influence on the cooling demand, with a maximum energy saving of 4% in Kunming. Finally, with reference to the annual total energy consumption, TC roof, PCM roof and TC/PCM roof led to a maximum saving of 13%, 6% and 17%, respectively. These maximum energy savings are all achieved in Kunming, characterized by a mild climate. A sensitivity analysis was conducted as regards the thickness of the TC and PCM layers. In detail, the thickness of the PCM layer was increased up to 25 mm (with an initial value of 5mm), obtaining an increase in energy savings of about 10%, while the thickness of the TC coating was increased up to 50 mm (with an initial value of 10mm), obtaining an increase in energy savings of about

12%. This analysis also identified that the positioning of the PCM layer in the roof insulation allows for the highest energy savings. Really, the accurate design of PCM is quite complicated and it requires specific studies.
For instance, a deep investigation about the suitable selection of PCM quantity and peculiarities, for the application to the opaque building envelope, was proposed by Mastellone et al. in [40], for what concerns an educational building, located in the south Italy, on the Adriatic coastline. It should be noted that, for exploiting at the best the PCM features during the warm season, a significant night ventilation must be guaranteed to discharge the latent heat and thus for the solidification of the melted material in order to allow that, in the next day, this will be ready again to store energy by means of a new melting process [41]. This technology was also reviewed by Ascione [42], together with other traditional and innovative ones, passive and active, useful for upgrading the global performance of buildings, also by means of the thermal storage.
As seen in the previous lines, this section has proposed some real cases [30],[31] located in UAE, in particular in Abu Dhabi, famous for its skyscrapers with responsive façades. The other studies, experimental or prototype, were conducted in numerous countries, Australia, California, China, Iceland, Italy, Sweden, obtaining reductions in energy consumption ranging from a minimum of 17% [39] to a maximum of 82% [29]. Each alternative produces energy benefits as it is designed for the different climates. In California [21], the reduction of cooling loads is comparable to that of Abu Dhabi [30] but in the first case smart windows were adopted while in the second external adaptive solar shading was adopted. In [38], a DSF cavity that integrated a PV-PCM system showed a reduction of cooling loads in Venice higher than that of Helsinki.

In [39], the same intervention was adopted for the different climates of China with the best benefits in the mild climate.

With reference to both the opaque and transparent building envelope, a summary scheme of recent studies and findings in the matter of responsive building components and façades is proposed in Table 4.2.

Table 4.2: Studies concerning Responsive building elements: applied system and/or technology, type of investigation, cities and season of analysis, type of building and main findings

Year of the study	Authors	Applied System and/or Technology	Type of investigation	Cities and Seasons of Analysis	Type of building	Main findings and results
2010	Baetens *et al*. [21]	Smart windows	Simulation	Californian climate. Cooling season	——	The lighting consumption is reduced of about 26%.
2015	Perino *et al*. [22]	Intelligent glass systems	Simulation	Turin, Italy. Heating and cooling season	Test room	Reduction of daily net energy and total heat flux are obtained by using PCM coupled with a thermo-tropic layer.
2015	Favoino *et al*. [23]	Electrochromic intelligent glass	Simulation	London, U.K. Cooling season	Office	Cooling energy reduction of 80% compared to the traditional glazing, and 76% compared to the traditional glazing with internal shading device. Moreover, a better indoor environmental quality is achieved.
2020	Bui *et al*. [24]	Adaptive façades	Experimental	Melbourne, Australia. Summer and winter week	Three-story office	A maximum energy saving of the cooling demand,of about 29%, is obtained.
2011	Kirkegaard *et al*. [25]	Adaptive kinetic structure	Prototype	——	——	The prototype allowed to modify the shape of the structure and allows the passage of air flow and sunlight, through the opening and closing of an external surface.

Year of the study	Authors	Applied System and/or Technology	Type of investigation	Cities and Seasons of Analysis	Type of building	Main findings and results
2014	Favoino *et al.* [26]	Prototype ACTRESS (ACtive, RESponsive and Solar)	Prototype	Turin, Italy. Winter and summer season	___	In winter, the ventilation air was preheated, and the thermal buffer zone increased thermal insulation. In summer, the overheating effect is avoided by expelling the hot air.
2020	Matheou *et al.* [27]	Prototype of a reactive system based on the folding techniques of “origami”	Prototype	___	___	The prototypes allowed to control the daylight.
2017	Gallo *et al.* [28]	A new prototype "SELFIE" (Smart and Efficient Layers for Innovative Envelope)	Prototype	Milan, Florence and Palermo, Italy Heating and cooling season	Theroretical and experiemtal set-up	The prototype is developed and investigations will concern impacts on energy need for the space heating, space cooling, primary energy demands, the impact on indoor thermal comfort, and environmental footprint.
2016	Radwan *et al.* [29]	System façade inspired by the bark of trees	Real case	Melbourne, Australia Heating and cooling season	10-storey	Energy savings of 82% are achieved by means of a biomimetic approach.
2016	Barozzi *et al.* [30]	Adaptive façades	Real case	Abu Dhabi, U.A.E. Cooling season	Multi-storey	Adaptive solar shading involves a reduction of the cooling loads and improve natural lighting.
2019	Shahin *et al.* [31]	Various adaptive building envelopes are described	Real case	Barcellona, Spain Abu Dhabi, U.A.E. Toronto, Canada. Heating and cooling season	Multi-storey	Energy savings of about 20% are achieved in the building of Barcelona (EFTE material), solar gain limitation of 50% are obtained in Abu Dhabi (responsive façades with PTFE panels), better ventilation and air circulation are verified in Toronto.

Year of the study	Authors	Applied System and/or Technology	Type of investigation	Cities and Seasons of Analysis	Type of building	Main findings and results
2015	Park *et al.* [32]	Wind turbine integrated in the building envelope	Experimental	Busan, South Korea. Heating and cooling season	Multi-story residential	A 200W turbine can cover 6.3% of the daily electricity energy demand. This contribution is significant.
2018	Cascone *et al.* [34]	Phase change materials for opaque envelope	Simulation	Turin – Palermo, Italy. Heating and cooling season	Office	Regardless of the climate, the proposed system ensures a lower primary energy consumption of about 18%-33%.
2017	Basso *et al.* [35]	Adaptive ventilated façade named E2VENT	Experimental	Stockholm, Sweden Gdansk, Poland Paris, France Madrid, Spain, Athens, Greece. Winter and summer day	Residential	The system can save a maximum of 43% of heating loads in warm climate, and the 100% of cooling loads in cold climate.
2016	Elarga *et al.* [38]	PV-PCM combined with a double-skin façade	Simulation	Helsinki, Island Venice, Italy Abu Dhabi, U.A.E. Heating and cooling season	Office	Reductions of 29% of energy demands during summer season are achieved.
2020	Hu *et al.* [39]	Adaptive building roof that integrates thermochromic (TC) coating, phase change material (PCM) layer and the coupling of these two.	Simulation	Beijing, Heilongjiang, Nanjing, Guangzhou, and Kunming, in China. Heating and cooling season	Office	Energy saving of 17% under mild climate are obtained, by experiments.

4.3.3 Discussion about effectiveness of transparent novel technologies of the building envelope

The proposed review focuses on the building envelope by proposing and analyzing different energy efficiency measures for transparent and opaque envelopes, with the integration of high-technologies: double-skin façades, building integrated photovoltaic panels, responsive building elements. It is clear, from the performed investigations and review, that these solutions can determine an increase in the efficiency of buildings, an improved thermal behavior, a reduction in energy consumption and, consequently, in polluting emissions with important benefits also in terms of global and local warming. However, each strategy has limitations and possible future developments to be investigated.

In detail, double skin façades (DSFs) can provide a thermal buffer zone, energy savings and other benefits. Regarding this solution, several studies and results are available in the literature. With a simple DSF a reduction up to 90% of heating loads and 30% of cooling loads is obtainable [1], and there is the possibility of increasing these savings with the interposition of shading devices. Other researchers have analyzed the correlation between the thickness of the cavity and the consequent energy saving [11],[12], others have proposed the use of different materials, such as plastic, for the transparent component of the DSF [23].

From the literature review, the benefits due to DSFs are evident, but in the warm season, even an indoor overheating phenomenon can be generated, as a side effect; indeed, the inhabited environment is subjected to heat exchange with the cavity, which is at a temperature higher than that of the outside air, and this implies an increase in the use of mechanical cooling to ensure acceptable comfort conditions. One of the possible solutions is to make the façade ventilated. The natural ventilation, although free and activated by solar radiation by means of the stack effect, is difficult to control. Moreover, with the simulation tools available, it is difficult to model it, and in the scientific literature there is a gap in this regard. The available studies are exclusively of measurements on the existing façades. Instead, the regulation of the flow rates with mechanical ventilation allows precise control of the conditions inside the façade, by avoiding internal recirculation conditions and incorrect air expulsions. Obviously, this introduces the disadvantage of consumption for ventilation. The glazed cavity thus becomes a real plant (system) component, spread over the entire envelope. Furthermore, it is possible to use movable shading devices.

Building Integrated Photovoltaic (BIPV) systems, as well as being a way to generate electricity, can protect the building from atmospheric agents, and can provide thermal insulation and shading. Solar energy conversion is one of the technologies of generation from renewable sources with the greatest potential and suitable for being implemented in the building envelope. This provides a valid solution to reduce the energy taken from the urban grids. Really, the transition towards electricity is based on the intense exploitation of renewables. On the other hand, the diffusion of transparent photovoltaics is still limited by the low yields guaranteed by this technology (even 1/3 compared to panels with traditional opaque cells). This solution can be coupled to double skin façades obtaining a further reduction in energy consumption.

Regarding building responsive elements, there are several possibilities. The most widespread are phase change materials, non-conventional glass, materials with variable optical properties. The achievable energy savings range from values of 29%, with windows able to modulate the visible transmission and the solar gain coefficient [23], to values between 18% -73% for cooling and heating depending on the climate [34]. Other studies investigated cases in which the building has the possibility of changing shape inspired by the technique of "origami" or by the bark of trees [27],[29]. The development of variable thermo-physical-property of buildings (VTPBs) play a key role in the necessary refurbishment of the building stock. Definitely, many open issues and progressions are necessary. Only as a mere example, an issue connected to the PCM use is the melting temperature. The optimal value can vary between the heating and cooling periods. Accordingly, it is well-known that PCMs that have a good performance during the warm-up period can only have a minimal impact in the cool-down period and vice versa. For this reason, the employment of two PCMs can be useful for improving energy efficiency throughout the year. Furthermore, it is necessary to control the appropriate "charge-discharge" phase of the PCM to avoid a high temperature increase, which can cause undesired effects both in the heating and cooling periods: heat dispersions and gains, respectively.

In addition, a non-negligible issue concerns the required investment costs for materials, for implementation, for maintenance. In this regard, some studies showed that these interventions are not always selected, compared to traditional retrofit measures, because the costs are a barrier, and the cause long payback times [9],[19].

Furthermore, current building energy simulation tools often do not always allow perfect modeling and simulation of such novel technologies (especially as concerns the operation phase), limiting the ability to evaluate their potential, and this is a further challenge that the scientific research, also in terms of the development of new numerical models, has to face. For instance, Do and Chan [43] proposed a comprehensive study that outlines the complex modeling of multi-sectional façades, in which operable shading systems, fenestrations and controls have to be optimized in order to allow views, visual comfort, daylight and avoiding of uncomfortable glare. Analogously, a complex simulation framework, based on computational fluid dynamics applied to an opaque ventilated façade in comparison to an unventilated one, both during the heating and cooling seasons and under dynamic conditions, was proposed by [44]. The authors evaluated surface temperatures and thermal fields in the different façade layers, the airflow trends and thermal fluxes as well. Even in this case, the need of reliable energy models and trustworthy simulations is underlined by the authors, for testing, comparing and developing such complex systems.

4.4 Double-skin façades: deepening of characteristic parameters

From the investigated up-to-date scientific literature, it is deduced that the design of double-skin façade is extremely complex, as it is necessary to optimize:

- the configuration which can be window box, shaft box, corridor box or multi-storey [1];
- the depth of the cavity (that can vary from 0.2 m to 2 m [1]);
- the characteristics of the external glass, i.e., the thermal transmittance of the component;
- the shading systems;
- the ventilation in the cavity (natural, mechanical or non-ventilated).

All these parameters can represent decision-making variables in optimizing the energy consumption of a building that has a double-skin façade. The optimal combination depends on the place where the building is located both in terms of urban context and climatic conditions. From the state of the art, it can be deduced that different combinations of the characteristic parameters can produce energy benefits in any climate.

In the following section, the influence of the characteristic parameters of a DSF on the energy performance of a building located in a Mediterranean area is investigated.

4.4.1 Methods

Typically, an accurate energy audit involving the collection of data on the opaque and transparent envelope, on the systems installed, and general data in reference to the climate, occupancy profiles, electrical equipment - precedes the modeling phase of the complex system building/plant, as discussed in Chapters 2 and 3. In this case, the building investigated is representative of the Mediterranean urban context built between the 60ies and the 80ies, characterized by tuff bricks (or hollow blocks) to fill a structural frame in reinforced concrete. The graphical software DesignBuilder® is used to model the building geometry and the HVAC (heating, ventilating and air conditioning) systems, while the building energy performance is evaluated through a dynamic simulation using the EnergyPlus software. The energy outputs, obtained through the dynamic thermo-energy simulation, are validated, to make the model reliable and thus predictive of the reliable behaviour. The validation will be conducted by comparing the simulation results with the typical energy consumption of office buildings, in the same region and with reference to the same construction periods, that is predictive of the technological level [45]. A transparent double-skin façade is proposed as energy efficiency measure. This is created only on the facade of the building most exposed to the sun, i.e., the south facade. The cavity created is an unoccupied zone, and the HVAC and lighting systems are switched off. To assess the influence of the characteristic parameters of a DSF a sensitivity analysis with respect to the primary energy consumption is carried out. The coupling between EnergyPlus and Matlab® software is exploited. The EnergyPlus ".idf" input file has been parameterized. The parametrization allows to the Matlab® numerical computing environment to automatically run the EnergyPlus simulations, by varying the parameters, and to post-process its outputs.

The sensitivity analysis [46], [47] performed aims to identify the influence that the various parameters have on the chosen objective functions, which in this case are the primary energy consumption for heating, cooling and the total. Through a MATLAB® code, a sensitivity index was assessed,

i.e., the standardized rank regression coefficient (SRRC). This index can vary between -1 and 1, where 1 indicates a strong dependence between the objective and the parameter and 0 indicates that the objective and parameter are independent, while the sign indicates a growing monotonic dependence (positive sign) or a decreasing one (negative sign).
The investigated parameters are: the thickness of the cavity, the type of external glass, the position of the shading systems, the type of shading control and the setpoint for its activation. The configuration is fixed and is for a single floor and the cavity is not ventilated.

4.4.2 Case study

The case study under investigation is a building of the University Federico II, in Naples Figure 4.9.

Figure 4.9: The Engineering Campus, partial view, with the building and some envelope details

The city is in Italy, southern part of the peninsula, Tyrrhenian coastline, Climatic Zone C [48], classified "Csa" according to the Köppen-Geiger scheme. The climate is typical Mediterranean, the rated design outdoor temperatures, for the space heating and cooling, are = 2°C and 32 °C,

respectively. The building is occupied by offices, and it consists of 5 floors with a height of 4.5 m each. It has a rectangular floor plan (length of 20.8 m and width of 14.5 m), and the longest facades are oriented to north and south. The conditioned area is 947.4 m². The building, representative of Mediterranean constructions in reinforced concrete, built between 1960 and 1980, is characterized by very poor energy performance. In particular, there is no thermal insulation, with quite old energy systems.
The opaque envelope has the following composition:

- the external walls consist of a 2 cm layer of internal plaster, a 35 cm thick tuff core, and an external 3 cm solid brick cladding. The transmittance of the wall is U = 1.56 W/m²K.
- internal walls have a thickness of 10 cm. They are composed of plaster coatings on both the sides, 1 cm, and a core of 8 cm of hollow brick. The U-value is of 1.54 W/m²K.
- the flat roof is composed of five layers. The most external one is a 1 cm thick layer of asphalt, used to make the roof waterproof. Then there is 21 cm of lightweight concrete, 20 cm of mixed layer of concrete and bricks, and a 2 cm of internal plaster. The U-value is of 1.01 W/m²K.
- the floor slab on the ground is composed of four layers. The first one, in direct contact with the ground, is a 5 mm sheet of bitumen, used as waterproofing. Then, there's a 20 cm layer of hollow bricks and concrete, followed by 8 cm layer of reinforced concrete. The last layer is made of 15 mm of tiles. The U-value is of 1.265 W/m²K.
- the inter-storey slab has a composition similar to the floor on the ground: tiles, reinforced concrete, hollow bricks and concrete, 1.5 cm internal plaster. The U-value is of 1.17 W/m²K.

The transparent building envelope consists in a double glazing, without thermal break, with a U-value of 3.16 W/m²K.

As regards the heating, ventilating and air conditioning (HVAC) systems, the building is served by a centralized gas boiler, that has a nominal efficiency – estimated – of 0.89 and a thermal capacity of about 82 kW, and a chiller, that has a nominal thermal capacity of about 107 kW with an air to water heat pump. The terminal units are fan coils and are in each zone. An air change rate, quite high, of about 0.75 h^{-1} is due to infiltration and natural ventilation; this value is the default one for building in which the opening of fenestrations is occasional and the airtight is poor. The indoor environmental conditions control is based on the temperature:

- heating period begins on November 15th and ends on March 31st, with a maximum activation time of ten hours per day. This fulfils the Italian Decree D.P.R. 26/93 [48] which divides the Italian territory into six climatic zones, defining for each the heating period and the number of working hours. The heating setpoint is 20°C, according to the Italian D.P.R. 74/2013 [49];
- the cooling period begins on May 16th and ends on September 15th and a maximum activation time of ten hours per day is considered. The cooling set point is 26°C.

Once the model has been created, the energy needs are validated through a comparison of the simulations energy results with the energy needs characteristic of this type of building, i.e., the office building in the same climatic conditions (Mediterranean climate). In detail, once arranged some boundary conditions concerning the indoor systems and equipment and endogenous gains, the annual building gas demand is equal to 24985 kWh. Considering a cost of 0.09 €/kWh (during the 2021 these prices are the common ones) the annual operating cost is around 240 €/100 m^2, and thus quite reliable and common for similar edifices. It has to be underlined that the punctual calibration of the model from billings is not possible, given the absence of gas meters for each individual building of the

Campus. Moreover, meters of demands for different uses (heating, laboratories, mechanical equipment, testing of systems) are not available: finally, the statistical reliability is the only one validation possibility. It should be noted that the low energy demands is due to the important solar gains. The annual baseline primary energy consumption, by considering as primary energy factor 1.05 for the natural gas, and 1.95 for the electricity, are:

- primary energy consumption for the heating system: 27720.4 kWh_p, or 29.3 kWh_p/m^2;
- primary energy consumption for the cooling system: 24401.1 kWh_p, or 25.7 kWh_p/m^2;
- primary energy consumption for lighting system: 21792.6 kWh_p, or 23 kWh_p/m^2;

primary energy consumption for equipment: 47461.4 kWh_p, or 50.1 kWh_p/m^2.

4.4.3 Sensitivity analysis: values of the parameters and results

The parameters investigated and the possible values they can assume are shown below:

- Cavity thickness varies from 0.6 m to 2 m with a step of 0.2 m;
- Type of external glass, i.e., the thermal transmittance value of the glass. Different types of glasses are selected from those used in literature. The values implemented are shown in Table 4.3;
- Shading position: internal and external position;
- Shading control: the shading system can be activated by solar radiation [W/m²] and by temperature [°C]. About temperature, the setpoint value is 27 ºC, which means that when the temperature is reached inside the cavity, the shading systems are activated;

- Setpoint for shading activation in case of solar control: the considered values are 150, 300, 450 and 2000 W/m² (the value of 2000 W/m² means that the shading is not activated.)

Table 4.3: U-value for external glass

Option	Thermal transmittance value [W/m²K]
1	5.45
2	3.16
3	2.55
4	1.76
5	1.30
6	0.78

Figure 4.10 shows the values of the SRRC assessed for all the investigated parameters in respect to the primary energy consumption for heating, cooling and total.

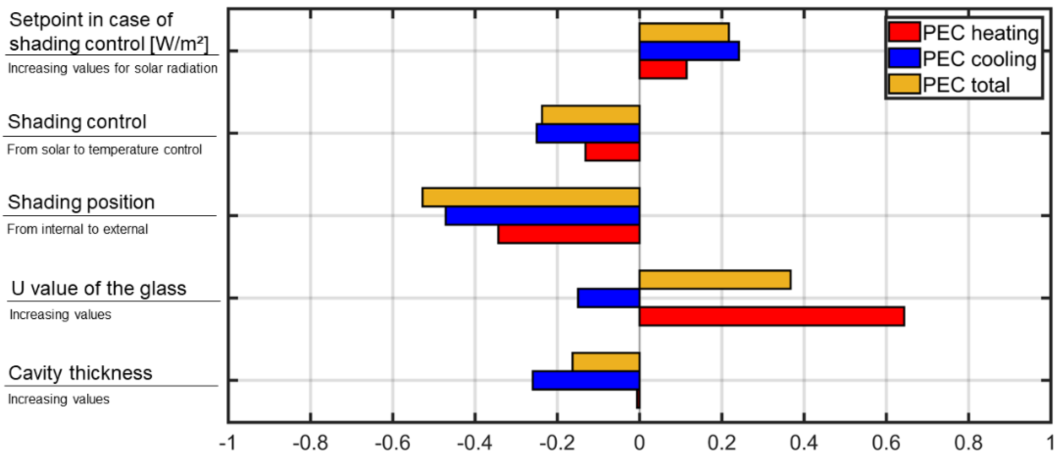

Figure 4.10: Sensitivity Analysis

Therefore, the results that emerge from this analysis are the following:

- cavity thickness: the influence on primary energy consumption for heating (PEC_h) is negligible, while it has a slight decreasing influence on primary energy consumption for cooling (PEC_c). PEC_c is decreased as the cavity's thickness is increased since this speeds up air circulation in the cavity, which mitigates the overheating effects. As regard the total primary energy consumption (PEC_t) there is a slight reduction as the thickness of the cavity increases due to the effect on PEC_c.

- thermal transmittance of transparent building component: as the thermal transmittance value of the glazed component of the outer layer of the DSF increases, there is an increase in the PEC_h (therefore there is an increasing monotonous trend, quite accentuated), vice versa the PEC_c undergoes a slight reduction. A glazed element characterized by high thermal transmittances determines a greater dispersion of heat with the external environment (there is a reduction in the thermal insulation capacity). The advantage of the DSF in the winter regime consists in the thermal buffer zone that is created in the cavity zone, it is therefore clear that if this zone has a glazed component that increases the thermal dispersion, this advantage is lost. In the summer regime the opposite effect occurs. The greater dispersion of heat with the outdoor environment reduces the overheating effect and this causes a reduction in PEC_c. As for the PEC_t, it follows the trend of the PEC_h with a less accentuated influence, due to the effect on the PEC_c.
- position of the shading systems: the external positioning of these systems determines a reduction on all the functions investigated. The effect is greater on the PEC_c compared to the PEC_h as there is greater protection with respect to the phenomenon of overheating.

- type of shading control: shading control using temperature is more effective than solar control. Thus, a greater reduction in the primary energy consumption (for heating, cooling, and total) is achieved.
- setpoint for shading activation in case of solar shading control. The influence on the PEC_h is low and can be neglected, the influence on the PECh is equally low although greater than that on the PEC_h. In particular, as the activation value of the shading device increases, there is an increase in the PEC_c. In fact, if the shading is activated at a higher value, the building, and the cavity of the DSF are exposed to greater solar radiation which determines an increase in consumption of the PEC_c.

Finally, it emerges that the primary energy consumption for heating is significantly influenced by the thermal transmittance value of the glass implemented in the outer layer of the DSF and by the position of the shading systems. Instead, it is slightly influenced by the type of control on the shading systems. Regarding the primary energy consumption for cooling, the parameter that has the greatest influence is the position of the shading systems followed by the thickness of the cavity, the type of control for the shading activation and the U-value of the window component in the external layer.

In the following sections, the effects on the energy performance of buildings located in the Mediterranean area will be investigated following the application of a double skin facade, designed taking into account the results of the sensitivity analysis.

4.5 Passive façade

In this section the retrofit measure proposed consists of the creation of a "structural exoskeleton" which allows to get two benefits, giving a better structural stability to the building and ensuring an energy improvement. Then, the realization of a glazed system to cover the exoskeleton formed by panels installed in the frame geometry of this structure determines the creation of the double skin façade (Figure 4.11). The cavity that is formed between the previous external envelope and the new fully glazed one is completely closed and therefore acts as a thermal buffer, and therefore the facade is passive.

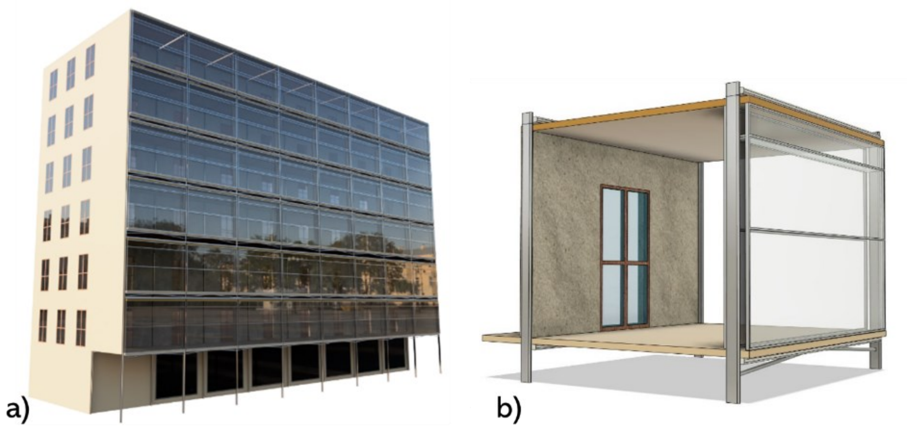

Figure 4.11: Design of a double skin façade (a), detail of the cavity (b)

This energy retrofit measure will be investigated for two office buildings. The first building, which will be called building A from now on, is the one described in section 4.4.2, the second building, called building B, is the one described in section 3.1.2 (see Figure 4.12).

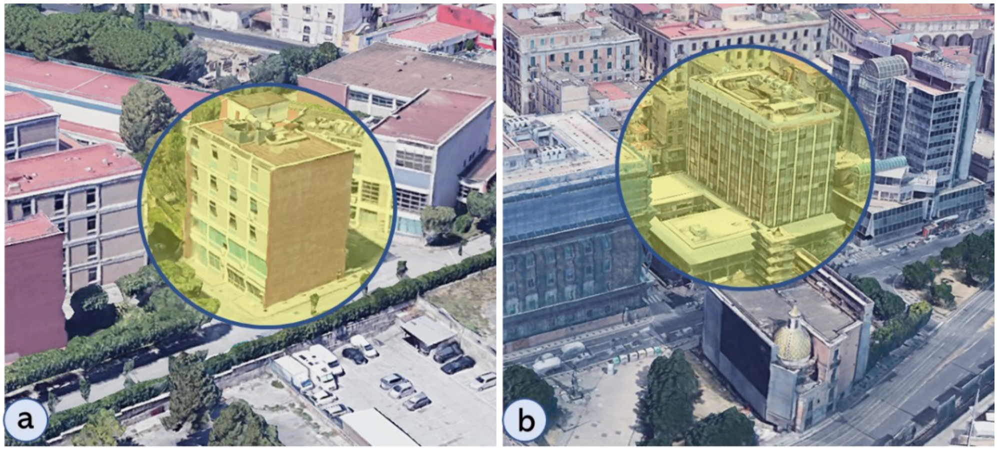

Figure 4.12: Building A (a), building B (b)

4.5.1 Application of a passive DSF to the office building A

The first application is realized on the building (Building A) described in the section 4.4.2, so the thermophysical properties, the installed systems and the validation of the model are described in detail in this section.
The proposed retrofit consists in the creation of a “structural exoskeleton”, the existing structure is flanked by a self-supporting structure (usually made of steel, highly performing in terms of rigidity and dissipative capacity) that allows an anti-seismic improvement of the building. A glazed system, formed by panels installed in the frame geometry of the structure, cover the exoskeleton. The system is applied to the south facade of the building from the first to the last floor (i.e., excluding the ground floor). This results in the Double Skin Facade (DSF) system because it forms a second skin (transparent) of the building that replaces the previous outer one. The DSF configuration chosen is the one for a single floor, while ensuring communication between the air in the cavity zones of the individual DSFs.

In this application the shading systems are not implemented, while as regards the thickness of the cavity and the choice of the external glass, the results obtained from the sensitivity analysis are taken into account.
As regards the thickness of the cavity, a value equal to 1 meter was chosen. This allows to avoid excessive encumbrance in the realization of the DSF but does not allow to reach the maximum saving on the PEC_c, which is reached for greater depths. The external layer is composed of modules with a 1 m² area. As for the thermal transmittance value of the glass of the outer layer, to balance the effects on PEC_h and PEC_c, bearing in mind that the influence is more marked on the PEC_h, the choice was a low-emissivity double glass with U-value of 1.96 W/m²K (Figure 4.13).

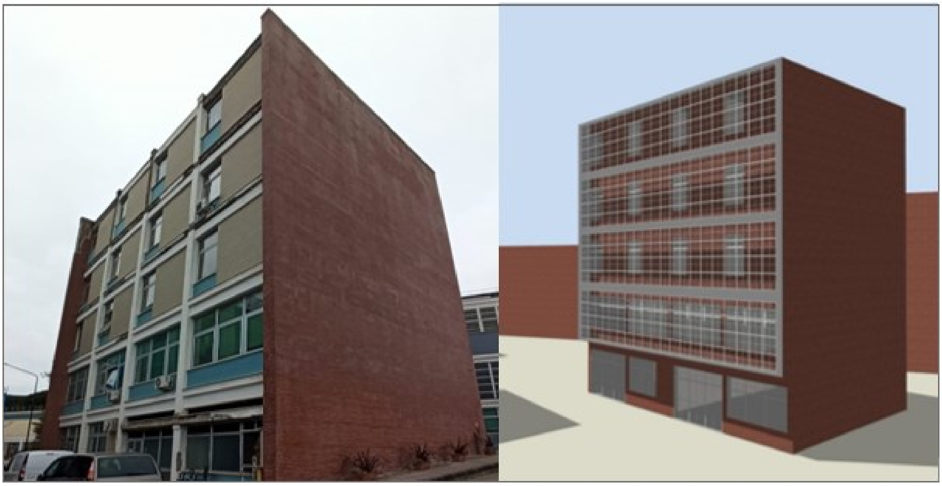

Figure 4.13: Real building (on the left) and model of double skin façade (on the right)

With the DSF, the indoor environments are no longer subject to external environmental conditions, but they are in contact with the cavity area.
The effects obtained through this application are two, according to the season:

- in winter: the temperature in the cavity zone, thanks to solar radiation, is higher than that of the outside air (Figure 4.14). The temperature difference between the internal and the current external environment (represented by the cavity zones) is reduced, resulting in lower heat exchange. In terms of energy consumption, a reduction for heating load is achieved by approximately 37%, i.e., approximately 10000 kWh_p saved. The mean and maximum temperatures reached in the cavity zone are 24°C and 48°C, respectively.

- in summer: the same phenomenon occurs. The high temperature reached in the cavity (Figure 4.15) determines a condition of overheating (greenhouse effect), and this is a higher heat gain to the building which represents an additional load for the cooling system. Moreover, 37°C and 52°C are the mean and maximum temperatures in the cavity. In terms of energy consumption, an increase for cooling load is achieved by approximately 6%, i.e., around 1500 kWh_p.

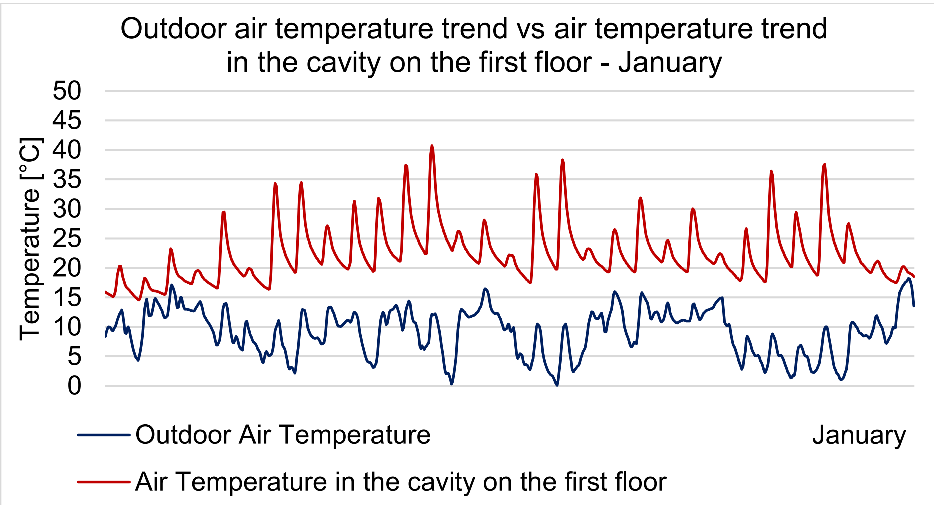

Figure 4.14: Outdoor air temperature trend vs air temperature trend in the cavity on the first floor in January

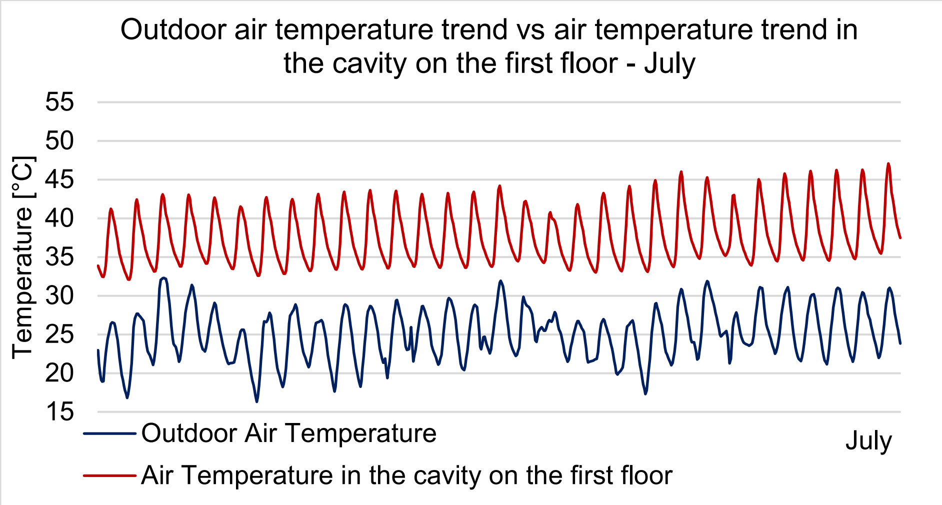

Figure 4.15: Outdoor air temperature trend vs air temperature trend in the cavity on the first floor in July

In summary, in the winter period, a saving on energy consumption for heating of about 37% is obtained, while in summer, due to the overheating effect of the cavity, which occurs when it is completely closed, there is an effect of increasing energy consumption for cooling by about 6%. The results obtained in this first phase are entirely in line with those of the studies in the literature. Reduction in heating consumption, with percentages ranging from 20% [5] to 40% [50] depending on the climatic location and the parameters that characterize the DSF. Increased cooling consumption[5], high temperature in the cavity and the need to ventilate the cavity[4].

4.5.2 Application of a passive DSF to the office building B

The second application is realized on the building (building B) described in the Section 3.1.2, so the thermophysical properties, the installed systems and the validation of the model are described in detail in this section.

Only the rectangular block that constitutes the examined building was analyzed (see Figure 4.16*). Therefore, the zones on the ground floor and on the first floor that do not belong to the vertical block have been excluded.*

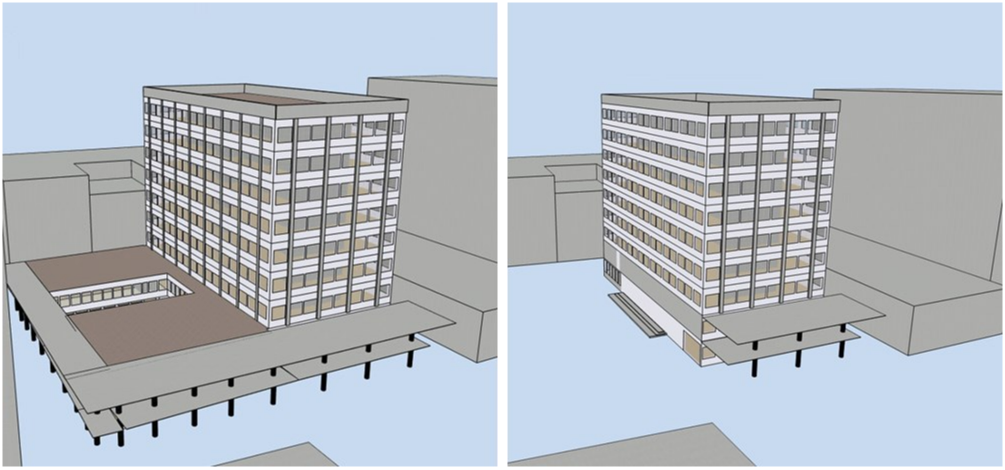

Figure 4.16: Building B (left side), rectangular block of building B (right side)

The primary energy consumptions of the rectangular block alone are:

- primary energy consumption for the heating system: 489795 kWh_p, or 79.5 kWh_p/m^2;
- primary energy consumption for the cooling system: 296072 kWh_p, or 48.1 kWh_p/m^2.

In this case study, the double skin facade will be applied first on the South-West facade and then also on the South-East side of the building.

The configuration is the same of the previous case (Section 4.5.1), so a corridor one with an interspace of 1 m between the external and the internal layer is created. The double skin façade, completely transparent, consists of modules of 1 m² area with double low-e glass with a thermal transmittance U=1.96 W/m²K.

Application on the South-West façade of the building

Figure 4.17 shows the application for the South-West facade of the building.

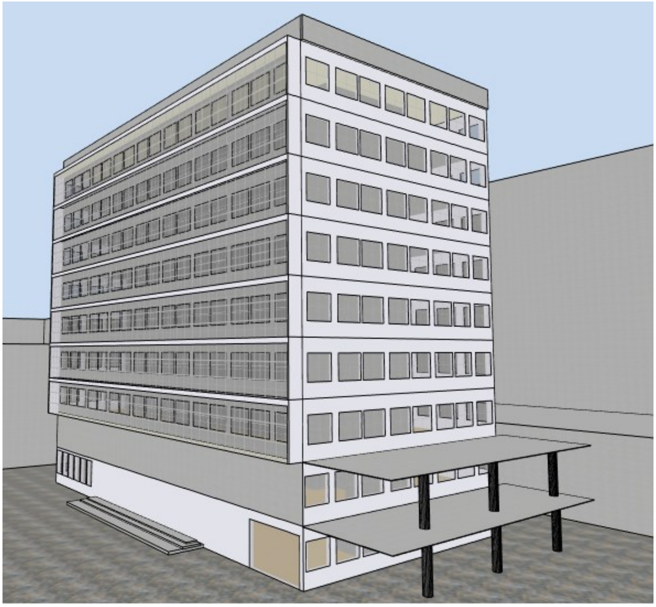

Figure 4.17: Double skin façade on the Sout-West side of the building

With the application of the double skin façade, a closed cavity is created. In this cavity, thanks to solar radiation, a thermal buffer zone is obtained, in which the air temperature is higher than the external one. The effects on energy consumption are different in the two seasons:

- in winter the energy consumption of the heating system is reduced by about 17.8%. The increase in the temperature of the cavity (and thus this novel thermal buffer zone) has a beneficial effect as the internal environments are no longer subject to cold external conditions, and the heat losses are reduced.
- in summer the temperature increase in the cavity involves an overheating effect which negatively affects the energy

consumption of the cooling system, which increases by approximately 1.2%.

Application on the South-East façade of the building

At this point the same facade, i.e., with the same characteristics, is applied to the South-East side of the building Figure 4.18.

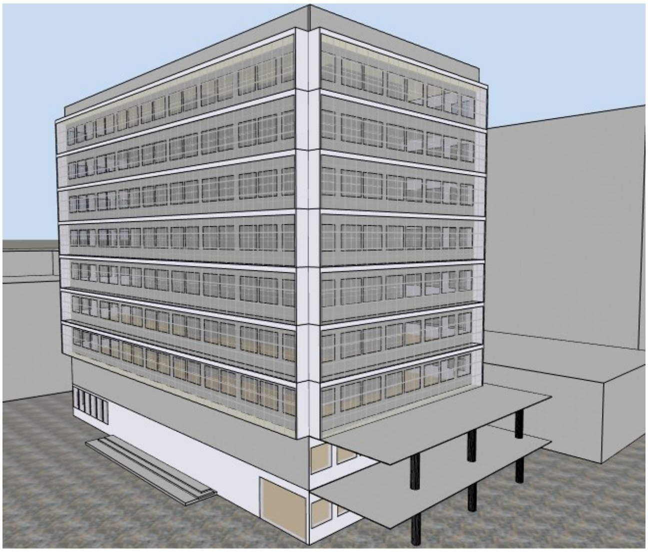

Figure 4.18: Double skin façade on the South-West and South-East sides of the building

With the installation of the double skin facade on the short side of the building, South-East, in addition to the DSF on the long side, South-West, the following results are obtained:

- in the winter period (i.e., cold season), an energy saving of about 28.7% is achieved compared to the base case.
- in the summer period (i.e., warm season), an energy increase of about 1.7% is achieved compared to the base case.

The energy demand variations (- = saving, + = increase), achieved with the application of the double skin façade on the South-West side and on both it and the South-East sides, are summarized in the following table.

Table 4.4: Energy savings compared to the base case

	Energy saving in winter period [%]	Energy saving in summer period [%]
Passive DSF on S-W side	-17.8%	+1.2%
Passive DSF on S-W and S-E sides	-28.7%	+1.7%

4.5.3 Analysis and comparison of the results for the two cases analyzed – passive façade

By comparing the results of these two applications, it is shown that the energy saving in the winter period with the passive DSF, only on the S-W side of the building B is lower compared to the saving achieved for the building A (17.8% vs 37%). There are two reasons for this lower impact of the DSF:

- the facade on which the DSF is installed is exposed to the South-West in the building B and not completely to the South as happens in the building A;
- the analyzed façade in the building B is subject to a shading effect, from the surrounding building, that limits the temperature increase in the cavity area. This phenomenon limits the potential of the DSF in the winter season but determines a beneficial effect in the summer season. Indeed, the energy increase in summer period is lower in building B compared to the building A (1.2% vs 6%).

In a second step for the building B, the double skin façade is also installed on the South-East façade. From this side, the building has a lower shading effect. In this way, a saving for winter air conditioning of about 28.7% is achieved, even if a slight increase of cooling energy for the summer air conditioning. The increase in energy consumption for cooling is obviously an undesirable and negative effect for this system. To counteract it and at the same time to increase the energy advantage obtained in the winter season, the double skin facade is made dynamic through the modeling of a network of air flows.

4.6 Active façade

The choice to make the double skin façade dynamic arises from the necessity to counteract the negative effect in summer season, and so to allow the expulsion of the hot air from the cavity towards the external environment. At the same time, however, it is possible to exploit the hot air, that is established in the cavity in winter, to heat the internal environments for free.

4.6.1 Modeling of the airflow network

The aim is to establish an airflow from the cavity to the indoor or outdoor environment. The fields needed to model the Airflow Network (AFN), in EnergyPlus environment, are as follows:

- Simulation Control: in which the general data for the airflow network method are defined. In this field, the method for the wind pressure coefficients calculation and the initialization method for the evaluation of the air pressures are defined;
- Zone: the areas between which the airflow is established are defined. These elements constitute the nodes of the airflow and the variable associated with the node is the pressure. In this field, the type of control for the natural ventilation is modeled. It can be constant, or regulated by temperature or specific enthalpy, or on the basis of thermal comfort conditions;
- Surface: the surfaces through which the airflow occurs are here defined. These elements are the connections of the airflow; the variable associated with the connection is the airflow rate.

By adopting this model, the equation for the evaluation of the indoor temperature (2.11) is modified as follow, namely equation (4.1):

$$T_z = \frac{\sum_{i=1}^{N_{sl}} \dot{Q}_i + \sum_{i=1}^{N_{surface}} h_i A_i T_{si} + MCPT_{air\,flow} + QADS_z + \dot{m}_{syst} C_p T_{supply} - \frac{C_z}{\delta t}\left(-3T_z^{t-\delta t} + \frac{3}{2}T_z^{t-2\delta t} - \frac{1}{3}T_z^{t-3\delta t}\right)}{\frac{11}{6}\frac{C_z}{\delta t} + \sum_{i=1}^{N_{surface}} h_i A_i + MCPT_{air\,flow} + \dot{m}_{syst} C_p}$$

(4.1)

Where:

- $MCPT_{air\,flow} = \dot{m}_{inf} C_p T_{amb} + \sum(\dot{m}_{mix} C_p T_{zone})$;
- $\dot{m}_{inf}$ is the mass flow rate from the external environment;
- $\dot{m}_{mix}$ is the mass flow rate from adjacent zones;
- $QADS_z = \sum_j Q_{cond(i,j)} + \sum_j Q_{leak(i,j)}$ is the sum of the conduction loss of the duct wall and the sensible loss of power through the linkage.

Two different managements of the airflow are provided in this application, according to the season:

- the airflow between the cavity and the outside environment, in summer;
- the airflow between the cavity and the indoor environment, in winter.

The airflow is managed through a control logic (CL) for the opening of the inner and outer layer windows of DSF.

4.6.2 Application of active DSF to the office building A

The network is based on the definition of nodes, represented by the zones between which the flow has to take place, and of connections, represented by the surface through which the flow is established. In the summer season, the nodes are the cavity zones and the outside environment, while the linkages are the windows of the outside layer of the DSF. The variable that allows the management of the airflow, and the

opening of the windows, is the temperature. In detail, when the air temperature in the cavity is higher than 26°C (summer comfort temperature for indoor environments) and is higher than the external air temperature, the windows of the outer layer of the double-skin open, and an airflow is established from the cavity to the outside environment.
From Figure 4.19, it is observed the reduction of the air temperature in the cavity, achieved by the opening of the windows.

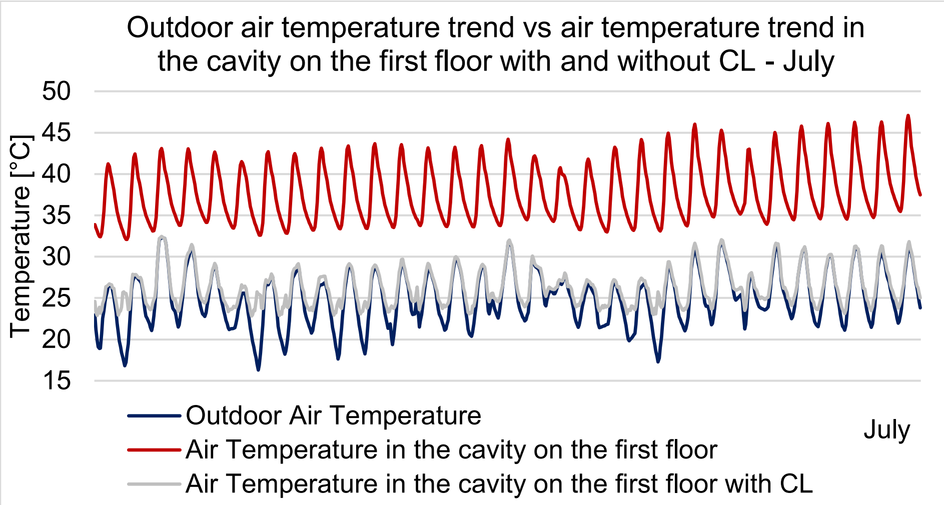

Figure 4.19: Outdoor air temperature trend vs air temperature trend in the cavity of the first floor in July, with and without CL

This involves a reduction of the heat gain to the building and saving for the cooling system load, of about 13% compared to the case with DSF completely closed and of about 8% compared to the basic configuration; these values correspond respectively to approximately 3500 and 2000 kWh_p saved. Furthermore, 26°C and 36°C are the mean and maximum temperatures reached by the air inside the cavity, therefore lower than the 37 ° C and 52 ° C of the passive configuration.

As regards the winter regime, an energy-saving is obtained with the application of the double-skin alone. However, observing the high temperatures reached by air inside the cavity, Figure 4.14, an airflow network is defined also in this season. The goal is to take advantage of hot air to heat the indoor environments. In this case, the nodes of the network are the cavity zones and the adjacent indoor environments, while the connections are the windows of the inner layer of DSF. The temperature is the variable that allows the management of the airflow and therefore the opening of the windows. In detail, when the air temperature in the cavity is higher than 21°C and is higher than the external air temperature, the windows open, and airflow is established from the cavity to the inside environments. This strategy results in a reduction of the consumption of the heating system by about 11% compared to the case in which the control logic is not adopted, and therefore the cavity is completely closed. Compared to the basic case, i.e., without the double-skin façade, the saving is around 42%, and about 11.000 kWhp of primary energy are saved. The issue of summer overheating is typically addressed with the use of shading systems [50], natural ventilation [51] or mechanical ventilation systems [52]. However, if the system is unable to adapt to climatic conditions, the summer benefit could come at the expense of the winter one. For example, in [51] the introduction of shading systems reduces the savings related to the thermal load from 40% to 10% and with the configuration that implements natural ventilation it reaches 7%, while for the cooling load a reduction of about 45% is obtained. With the approach presented in this study, the dynamism of the system allows to maximize savings in both seasons.

4.6.3 Application of active DSF to the office building B

An airflow is modeled between the cavity area and the internal zones or the external environment according to the season, also in this second case study. The variable that controls the air flows, also in this case, is the temperature. In detail:

- in the winter season an airflow is modeled between the cavity and the internal environments, so the airflow is established through the internal windows of the DSF. The airflow between the cavity environment and the internal one is established if the air temperature in the cavity is higher than both the external air temperature and a set point value, set at 22°C;
- in the summer season an airflow is modelled between the cavity and the outside environment, so the airflow is established through the external windows of the DSF. The airflow between the cavity environment and the external one is established if the air temperature in the cavity is higher than both the external air temperature and a set point value, set at 25°C.

South-West façade of the building

An increase in winter energy saving is expected because when the air in the cavity reaches a temperature higher than 22°C, that is the set point required in the indoor environment, it is introduced into the rooms through the windows of the inner layer of the DSF. In the summer season, it is expected to reduce the overheating effect by allowing the hot air in the cavity to flow out through the windows of the outer layer of the DSF. The results obtained with this solution are the following:

- an energy saving in winter period of about 18% compared to the base case;

- an energy saving in summer period of about 1.5% compared to the base case.

The adoption of a dynamic façade determines a slight increase in the energy saving for the winter heating service (18% for the active configuration compared to 17.8% of the passive one) and, at the same time, contrasts the increase in consumption for the cooling system in summer, also resulting in a small saving.

South-West and South-East façade of the building

Thanks to the dynamism of both facades the following savings are achieved:

- 29.3% in winter regime compared to the base case;
- 1.2% in summer regime compared to the base case.

Also in this case, through the active façade a slight increase in the energy saving in winter season is achieved (29.3% compared to 28.7% of the passive façade). Furthermore, as concern the energy consumption of summer season a saving of 1.2% is achieved compared to an increase of 1.7% obtained with the passive configuration.

4.6.4 Analysis and comparison of the results for the two cases analyzed – active façade

The dynamic facade provides a different impact on the two buildings. In particular, it seems to be more efficient for the building A, for which it allows a saving for the PEC_h of about 42% compared to the 37% achievable with the passive façade, and a saving for the PEC_c of about 8% compared to an increase of 6% obtained with the passive configuration. Instead, for building B, we go from a saving for the PEC_h of 28.7% to one of 29.3%, and to a saving for the PEC_c of 1.2% compared to an increase of 1.7% (when the intervention is carried out on both do South-West and South-East side of the building).

The slight impact of the active façade on the energy consumption of the building B is due to the use of air conditioning systems, and in particular at the temperatures required inside the rooms. In winter mode, the setpoint is 22 °C. Due to both the shading effect of the surrounding buildings and the exposure of the analyzed facade, the air temperature in the cavity, higher than that of the outside air, exceeds 22°C in a few hours (Figure 4.20). Therefore, the hours in which it is possible to exploit the hot air of the cavity for space heating are few and consequently the impact on energy consumption is slight, about 1%. This phenomenon also occurs for the facade facing south-east. Therefore, the high set point value and the shading effect limit the use of the dynamic facade.

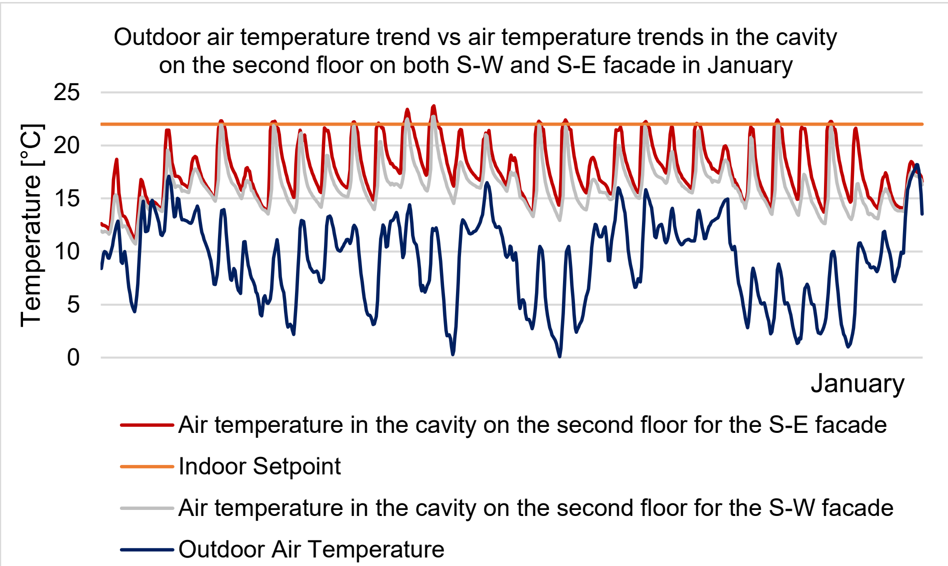

Figure 4.20: Outdoor air temperature trend vs air temperature trends in the cavity on the second floor on both S-W and S-E façade in January

For building A, the setpoint inside the rooms is equal to 20 ° C and from Figure 4.14 it is possible to observe how there is a wide time interval in which the temperature in the cavity is higher than the setpoint value. Furthermore, the façade on which the double skin façade is applied is not subject to shading effects from the surrounding buildings.

In the summer season, the shading to which the double skin facade in building B is subjected limits the increase of the PEC_c and temperature inside the cavity. When the façade is made dynamic, the natural circulation motion that is established has a lower effect than that which occurs in building A.

4.7 Integration of semi-transparent a-Si Photovoltaic modules – Application to building A

As previously mentioned, the double-skin façade offers the possibility of hosting photovoltaic (PV) modules. In this case, two different semi-transparent photovoltaic modules are integrated into the outer layer of the DSF, by replacing the outer glasses in different percentages. In particular, 20% to 80% of the total glazed surface is replaced, with steps of 20%. The two types of photovoltaic glasses, selected following an analysis of the systems available on the market, have the same U-value of 1.6 W/m²K, but they vary for the following characteristics:

- photovoltaic glass 1 (indicated as PV1 below) has an efficiency of 4% and a solar heat gain coefficient (SHGC) of 9%;
- photovoltaic glass 2 (indicated as PV2 below) has an efficiency of 2.8% and a SHGC of 17%.

The direct consequence of the integration of photovoltaic modules is the production of electricity that covers part of the building's demand. This production increases proportionally to the increase in the percentage PV introduced. Furthermore, since the PV1 modules are more performing, with higher efficiency, the electricity conversion obtained with these modules is higher than that the one obtained with the PV2 modules. In

Figure 4.21, it is shown the percentage of total electricity saved in the different cases. Further results in terms of primary energy savings of the building are shown in Table 4.5.

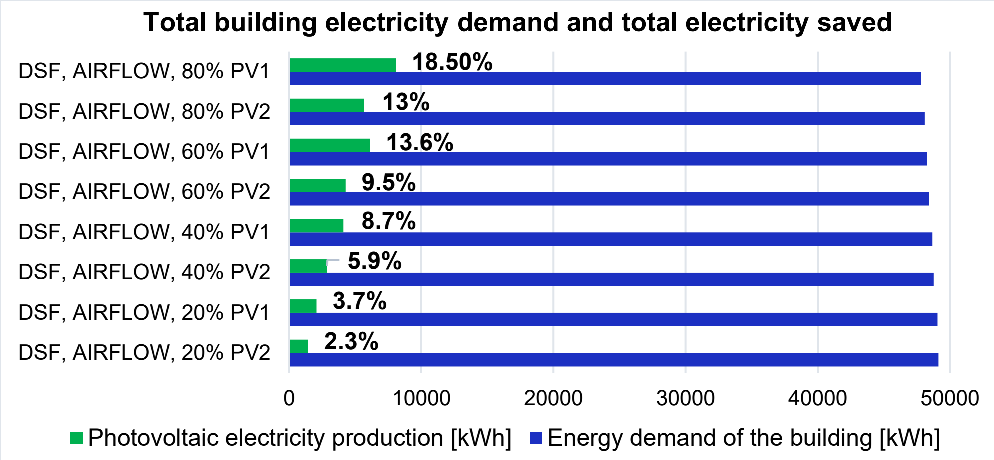

Figure 4.21: Total electricity demand of the building and total electricity saved thanks to PV generation

Table 4.5: Primary energy savings compared to the baseline case

	PEC_h		PEC_c	
	PV1	**PV2**	**PV1**	**PV2**
DSF	-37.3%		6.2%	
DSF with AFN	-44.5%		-8.4%	
DSF, AFN, 20%PV	-38.7%	-39.6%	-11.4%	-10.9%
DSF, AFN, 40%PV	-32.2%	-34.3%	-14.5%	-13.7%
DSF, AFN, 60%PV	-24.9%	-28.6%	-17.2%	-16.2%
DSF, AFN, 80%PV	-17.9%	-22.8%	-20.5%	-18.6%

From Table 4.5, it is noted that the production of electricity is not the only consequence. The replacement of the external glasses, with PV modules, modifies the solar heat gain for the building. The PV1 and PV2 modules have a different SHGC (between them and with respect to the double glass initially present), therefore, the amount of solar energy they let through is different. PV1, with a lower SHGC, protects the indoor environments more from external heat, letting a smaller amount of solar energy pass through. This effect is advantageous in the summer season.

The implementation of the active facade was necessary to reduce the overheating effect of the cavity in the summer period. With the integration of PV glazed systems, characterized by a lower SHGC which therefore allows a reduction of solar heat gain, the air temperature in the cavity is reduced. This effect is added to that obtained by controlling the opening of the windows, resulting in a further reduction in PEC_c. The maximum energy saving, for cooling, is about 20.5% and has been achieved with PV1 modules and with a percentage of coverage of the external facade of 80%. In the winter period, the reduction in solar energy gain contrasts with the objective of the active facade, which is to exploit the hot air in the cavity to heat the indoor environments. For this reason, the primary energy saving for heating is reduced, while it remains a saving compared to the base case (without retrofit measures). The last performed analysis compares passive and active facades, both with the integration of PV modules, in terms of primary energy consumption for space conditioning (PECsc) and total primary energy consumption (TPEC).

In Figure 4.22, it is investigated the PECsc, without considering the electricity production by photovoltaic.

The DSF, alone, implies a reduction of PECsc of 28% and 17% compared to the baseline, for the active and passive façade respectively. The influence of PV percentage introduced is not significant, especially for the passive façade, because the contrasting effects – namely, an increase in the heating demand and a decrease in the cooling demand - compensate for each other. As regards the active façade, as the percentage of PVs introduced increases, the PECsc approaches that of the passive façade. This happens because the increasing shading effect, provided by the modules, reduces the risk of summer overheating inside the cavity, and so the positive effect of the airflow network and the control logic for the opening of the windows are less efficient, as previously discussed.

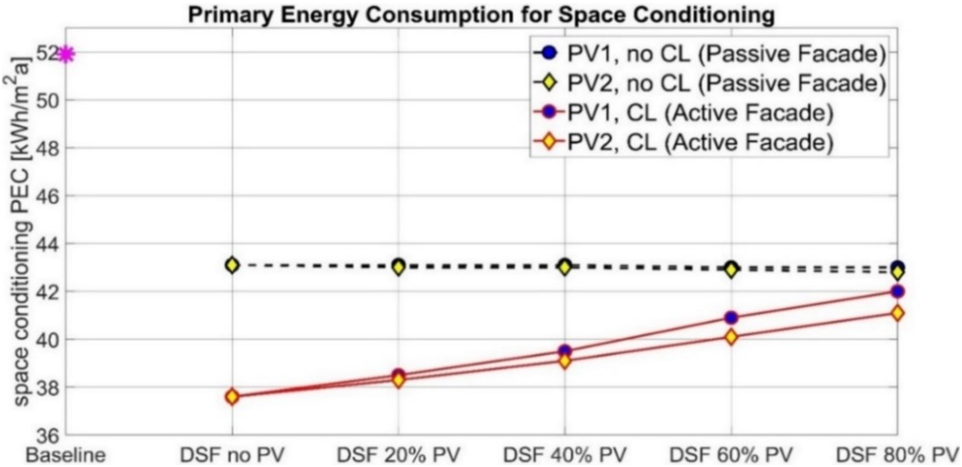

Figure 4.22: Primary energy consumption for space conditioning

For the passive façade, the performance of the modules PV1 and PV2 is quite the same, while for the active façade, PV2 has a better performance. This happens because, being PV2 characterized by a higher SHGC than PV1, it allows a greater amount of heat to pass through and it is possible to better exploit the potential of the airflow network. The best solution is the active façade without the integration of photovoltaics. Different results are achieved if the electricity production of PV is considered. In Figure 4.23, it is investigated the total primary energy consumption of the building.

In this case, PV1 has always a better performance due to its higher efficiency, 4% compared to 2.8% of PV2. As the percentage of PV modules introduced increases, the gap between active and passive façade is reduced because the risk of summer overheating is once again reduced by reducing the beneficial effect of implementing the control logic for opening windows. The best solution is the active façade with the maximum percentage of PV modules integrated into the façade, i.e., 80%, which allows a reduction of total primary energy consumption up to 18%.

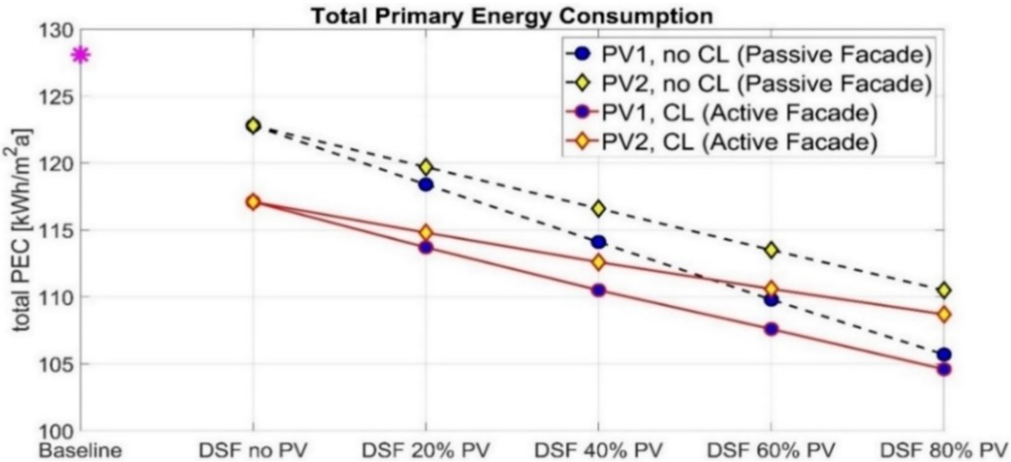

Figure 4.23: Total primary energy consumption of the building

4.8 Integration of shading systems – Application to building A

A further characteristic parameter, discussed in section 4.4, concerns the possibility of installing shading devices on the outermost layer of the double skin facade. Taking into account the results obtained from the sensitivity analysis, the shading systems are arranged externally to the outer layer of the DSF, and the temperature is chosen as the control variable for their activation.

In the previous sections, it was discussed how that in the winter season the energy advantage of using the DSF is given by the thermal buffer zone that is created in the cavity, an advantage that is further increased by exploiting the dynamism of the facade. To avoid compromising this advantage, the activation of the shading devices is programmed only in the summer period, in order to further limit the overheating effect, and obtain a greater energy benefit in the cooling season.

Therefore, an external shading system is proposed, active only in the summer season with temperature control. The shading systems are implemented on the external facade of the double skin system and are activated if the temperature in the cavity is higher than 27°C. Thanks to the implementation of shading systems it is possible to obtain a saving on energy consumption for cooling of about 20% compared to the base case (with the dynamic facade the saving on energy consumption for cooling was about 8%). Therefore, as already highlighted by the sensitivity analysis, the implementation of shading systems has a positive effect on energy consumption in the summer season. However, the use of shading systems could lead to an increase in energy consumption for lighting especially if automatic internal lighting control strategies are implemented. Therefore, like all design cases, it is necessary to take into account all the variables involved. When an energy refurbishment is carried out, a multi-objective problem is incurred, and the intent is to find the best trade-off between these conflicting aspects.

4.9 Further considerations on energy renewal process

Nowadays, in the energy refurbishment activities of buildings, it has become important to consider not only the operational energy and CO_2-eq emissions but also those embodied in materials and technologies [53]. In general, it is possible to identify three phases that characterize the life of a building:

- construction that starts from the extraction of raw materials, passing through the production of materials, their transport and the construction of the building in situ;
- operational, therefore, the use phase of the building, any maintenance and replacements of building components;

- end of life, with the demolition and eventual disposal or recycling of the materials used. This phase has an impact on the total energy in the life cycle of a building of less than 1% and for this reason it will not be mentioned below [54].

What has also shifted attention to the construction phase is a consequence of the objectives set at an international level with regard to increasing energy efficiency in the building sector. The energy renovation of a building determines a reduction in energy consumption in the operational phase and this involves a change in the relationship between the energy associated with the construction and operational phases. In particular, from a 20% - 80% between the energy embodied in the materials and the energy used in the operational phase [54], we are moving to a 40% - 60% [55]. For this reason, it is important to choose the materials implemented both in a new building and especially in an energy efficiency intervention. In the literature it is possible to find studies related to the implementation of recycled materials [56], as well as studies comparing the performance of different materials [57], in order to reduce the impact associated with embodied energy.

To assess the energy and environmental impact of an asset (in this case the building) during its entire life cycle, the life cycle assessment (LCA) method is used. This method is regulated by UNI EN ISO 14040 and 14044. It consists of four main phases:

- definition of the objectives and scope of the analysis;
- life cycle inventory (LCI);
- life cycle impact assessment (LCIA);
- interpretation of the results.

Depending on the phases of the life cycle of a product that are studied, different approaches of LCA are defined:

- cradle to grave from the extraction of raw materials to demolition (therefore the end of the useful life of the product);
- cradle to gate from the extraction of raw materials to the production of the product;
- cradle to cradle from the extraction of raw materials to their recycling for the production of a new product.

The cradle to gate approach (stage A1 to A3) with the integration for the transport stage (stage A4) and the use stage (stage B6) has been used to evaluate how much the embodied energy and emissions account in the energy refurbishment of a building located in a Mediterranean area (the investigated energy retrofit measures concern only the building envelope, both opaque and transparent). The building in question is described in [58], and therefore the thermophysical and plant characteristics, and the modeling through the DesignBuilder software are reported there.
The analyzed energy retrofit measures concerned first the insulation of external vertical walls and the roof (by selecting different type of insulating and plaster materials) and then the replacement of the transparent components. Environmental product declarations (EPDs) have been used to take into account the environmental footprint of these materials. This environmental label is defined by ISO 14025 as type III or that "quantifies environmental information on the life cycle of a product to enable comparisons between products fulfilling the same function", and its definition is based on the LCA tool. EPDs are publicly known for the employed materials. All materials are manufactured in Italy, in this way the energy mix of the country - where the building under investigation is located - is considered. The data obtained from EPDs refer to A1-A3 stages, cradle to gate. The data for phase A4 - i.e., the transport from the manufacturer to the building site - are calculated using the SimaPro software. For this calculation, the tons of materials used, and the km of

transportation are required. The data for phase B6, i.e., building use, are calculated through EnergyPlus software (dynamic energy simulation). The investigated indicators are: NRPEC (non-renewable primary energy consumption) for the energy impact and GWP for the environmental impact.

4.9.1 Energy retrofit of the external vertical walls

For the intervention on the vertical walls, different insulating materials and plasters were considered, which are then combined with each other. In particular, the following insulating materials:

- cork panels: λ=0.043 W/mK, thickness in the range [2-10] cm;
- Rock wool panels: λ=0.032 W/mK, thickness in the range [4-10 cm];
- Glass wool panels: λ=0.031-0.032-0.034-0.035 W/mK, thickness in the range [4-10 cm].

For the plaster layer a natural and a cement mortar material were considered. By coupling the different insulating materials and plasters selected, 162 scenarios are obtained.

The primary energy saving ranges between 4.8% and 12.9%. The lowest energy saving, 4.8%, is obtained with the minimum thickness of the insulating material, i.e., 2 cm, and with the less performing material in terms of thermal conductivity, i.e., the cork panel with a λ=0.043 W/mK. The thermal transmittance value in this scenario is 0.67 W/m²K (scenario S1). The CO_2 emissions saving is 4.9%. The maximum energy savings, 12.9%, is obtained with the maximum thickness of the insulating material, i.e., 10 cm, and with the most performing material in terms of thermal conductivity, i.e., the glass wool panel with a λ=0.031 W/mK. The thermal transmittance value in this scenario is 0.24 W/m²K (scenario S2). The CO_2 emissions saving is 13.2%. In both extreme solutions, the plaster is a cement mortar. These results are summarized in the following table.

Table 4.6: Energy and CO_2 emissions savings with the energy retrofit of the vertical walls

Scenario	U-value of the wall [W/m²K]	Insulating materials	Primary energy saving [%]	CO_2 emissions saving [%]
S1	0.67	2 cm of Cork panel: λ=0.043 W/mK	4.8	4.9
S2	0.24	10 cm of Glass wool panel: λ=0.031 W/mK	12.9	13.2

But how much does embodied energy account for these solutions? For scenario S1, characterized by both the minimum savings for the primary energy consumption and CO_2 emissions, the total embodied energy associated with the stages A1/3+A4 is 159 MWh. Considering an analysis over 30 years, the embodied energy is 5.3 MWh, which has a very slow weight on the total annual primary energy consumption of about 1%.

For scenario S2, characterized by both the maximum savings for the primary energy consumption and CO_2 emissions, the total embodied energy associated with the stages A1/3+A4 is 330 MWh. Considering an analysis over 30 years, the embodied energy is 11 MWh, which has yet a slow weight on the total annual primary energy consumption of about 2.2%. Analyzing all the scenarios, the weight of the embodied energy on the total annual primary energy consumption ranges between 0.6% and 4.1%. What emerges from these first analyses is that the energy refurbishment on the external vertical walls, alone, allows a low energy saving, which is expected, and that the incidence of embodied energy is negligible.

According to the Italian requirements provided by the Inter-Ministerial Decree June 26, 2015, the thermal transmittance limit for the external vertical walls of an existing building undergoing energy redevelopment is 0.36 W/m²K for climatic zone C, to which the city of Naples belongs (1034 HDD, baseline 20°C). The scenarios that do not respect this limit will be excluded from the following analysis.

4.9.2 Energy retrofit of the roof combined with the energy retrofit of the external vertical walls

The energy retrofit measure for the roof includes a layer of 8 cm of glass wool (0.035 W/mK) and a waterproof layer of 6 mm. The thermal transmittance value is 0.306 W/m²K, which respect the limit of 0.32 W/m²K provided by the Italian requirements.

Considering the energy requalification interventions on the external vertical walls that respect the limit on the U value, 44 scenarios are analysed in this sub-section.

The primary energy saving ranges between 12.3% and 15%. The lowest energy saving, 12.3%, is obtained with 6 cm of glass wool, λ=0.034 W/mK. The thermal transmittance value in this scenario is 0.36 W/m²K (scenario S3). The CO_2 emissions saving is 12.7%. The maximum energy savings, 12.9%, is obtained with 10 cm of glass wool panel, λ=0.031 W/mK. The thermal transmittance value in this scenario is 0.225 W/m²K (scenario S4). The CO_2 emissions saving is 15.5%. These results are summarized in the following table.

Table 4.7: Energy and CO_2 emissions savings with energy retrofit of roof and vertical walls

Scenario	U-value of the wall [W/m²K]	Insulating material for wall	Primary energy saving [%]	CO_2 emissions saving [%]	U-value of the roof [W/m²K]
S3	0.358	6 cm of glass wool: λ=0.034 W/mK	12.3	12.7	0.306
S4	0.225	10 cm of glass wool λ=0.031 W/mK	15	15.5	0.306

For scenario S3, the total embodied energy associated with stages A1/3+A4 is 280 MWh. Considering an analysis over 30 years, the embodied energy is 9.3 MWh, which has a slow weight on the total annual primary energy consumption of about 1.9%.

For scenario S4, the total embodied energy associated with stages A1/3+A4 is 308 MWh. Considering an analysis over 30 years, the embodied energy is 10.3 MWh, which has yet a negligible weight on the total annual primary energy consumption of about 2.1%.

4.9.3 Energy retrofit of transparent building envelope coupling with the energy retrofit of the opaque building envelope

The replacement component for the transparent building envelope is a low-emissivity triple glazing system, with a thermal break aluminum frame, with a U-value of 1.1 W/m²K, which respect the limit of 2W/m²K provided by the Italian requirements. The energy savings ranges between 37.2% and 39.4% and the extreme solutions are the same as in the previous sub-section (S3 and S4) with the replacement of the window components (S3W and S4W). In this case, for the scenario S3W, the embodied energy associated with the stages A1/3+A4 is 25 MWh per year and, the weight on the total annual primary energy consumption is of about 6.7%.

For scenario S4W, the embodied energy associated with the stages A1/3+A4 is 26 MWh per year, which has a weight on the total annual primary energy consumption of about 7.1%. By investigating all scenarios, the weight of the embodied energy on the total annual primary energy consumption ranges between 5.5% and 9.2%, and, the weight of the embodied emissions ranges between 6.1% and 9.7%.

4.9.4 Analysis of the results

What emerges is that - with the energy refurbishment of both opaque and transparent building envelopes - the achievable energy savings are increased, which is expected, and the incidence of the embodied energy also increases.

Therefore, it results that the lower the energy consumption of the building, the higher the incidence of energy and embedded emissions. Since the future of buildings is nZEB, with zero or very low energy consumption, the weight of the embodied energy and emissions will increase, and therefore the choice of materials must be carried out carefully.

CHAPTER 4 - Nomenclature

Acronyms		
ACTRESS	ACTive, RESponsive and Solar	
AFN	Airflow network	
BIPV	Building-integrated photovoltaic	
BIWT	Building-integrated wind turbine	
CO_2	Carbon Dioxide	
DA	Daylight autonomy	
DSF	Double skin facade	
EPD	Environmental product declaration	
EU	European	
ETFE	ethylene-tetrafluoroethylene	
HVAC	Heating, ventilating and air conditioning	
IGU	Insulating glass unit	
LCA	life cycle assessment	
LCI	life cycle inventory	
LCIA	life cycle impact assessment	
NEB	Net electricity benefit	
nZEB	nearly Zero Energy Building	
PCM	Phase change material	
PEC	Primary energy consumption	
PPD	Predicted percentage of dissatisfied	%
PV	photovoltaic	
SELFIE	Smart and Efficient Layers for Innovative Envelope	
SHGC	Solar heat gain coefficient	
SRRC	standardized rank regression coefficient	

UDI	Useful daylight illuminance	
VLT	Visible light transmission	
WWR	Window to wall ratio	
<u>Symbols</u>		
CL	Control logic	
EC	Electrochromic	
RTi	Retrofit on the internal layer	
RTe	Retrofit on the external layer	
TC	Thermocromic coating	
Tvis	Visible trasnmittance	
U-value	Thermal transmittance	W/m^2K
<u>Subscripts</u>		
c	referred to space cooling	
eq	equivalent	
h	referred to space heating	
p	referred to primary energy	
t	referred to total energy	
sc	Space conditioning	

CHAPTER 4 - References

[1] Pomponi, F., Piroozfar, P. A., Southall, R., Ashton, P., & Farr, E. R. (2016). Energy performance of Double-Skin Façades in temperate climates: A systematic review and meta-analysis. Renewable and Sustainable Energy Reviews, 54, 1525-1536.

[2] Saelens, D., Roels, S., & Hens, H. (2008). Strategies to improve the energy performance of multiple-skin façades. Building and environment, 43(4), 638-650.

[3] Shameri, M. A., Alghoul, M. A., Sopian, K., Zain, M. F. M., & Elayeb, O. (2011). Perspectives of double skin façade systems in buildings and energy saving. Renewable and Sustainable Energy Reviews, 15(3), 1468-1475.

[4] Anđelković, A. S., Gvozdenac-Urošević, B., Kljajić, M., & Ignjatović, M. G. (2015). Experimental research of the thermal characteristics of a multi-storey naturally ventilated double skin façade. Energy and Buildings, 86, 766-781.

[5] Gratia, E., & De Herde, A. (2007). Are energy consumptions decreased with the addition of a double-skin?. Energy and Buildings, 39(5), 605-619.

[6] Barbosa, S., & Ip, K. (2014). Perspectives of double skin façades for naturally ventilated buildings: A review. Renewable and Sustainable Energy Reviews, 40, 1019-1029.

[7] Baldinelli, G. (2009). Double skin façades for warm climate regions: Analysis of a solution with an integrated movable shading system. Building and environment, 44(6), 1107-1118.

[8] Ghaffarianhoseini, A., Ghaffarianhoseini, A., Berardi, U., Tookey, J., Li, D. H. W., & Kariminia, S. (2016). Exploring the advantages and challenges of double-skin façades (DSFs). Renewable and Sustainable Energy Reviews, 60, 1052-1065.

[9] Chan, A. L. S., Chow, T. T., Fong, K. F., & Lin, Z. (2009). Investigation on energy performance of double skin façade in Hong Kong. Energy and buildings, 41(11), 1135-1142.

[10] Fallahi, A., Haghighat, F., & Elsadi, H. (2010). Energy performance assessment of double-skin façade with thermal mass. Energy and Buildings, 42(9), 1499-1509.

[11] Joe, J., Choi, W., Kwak, Y., & Huh, J. H. (2014). Optimal design of a multi-story double skin façade. Energy and Buildings, 76, 143-150.

[12] Alberto, A., Ramos, N. M., & Almeida, R. M. (2017). Parametric study of double-skin façades performance in mild climate countries. Journal of Building Engineering, 12, 87-98.

[13] Scorpio, M., Ciampi, G., Spanodimitriou, Y., Laffi, R., Rosato, A., & Sibilio, S. (2019). Double-Skin Façades with Semi-Transparent Modules for Building Retrofit Actions: Energy and Visual Performances. In 16th IBPSA Conference (pp. 464-471).

[14] Blanco, J. M., Buruaga, A., Rojí, E., Cuadrado, J., & Pelaz, B. (2016). Energy assessment and optimization of perforated metal sheet double skin façades through Design Builder; A case study in Spain. Energy and Buildings, 111, 326-336.

[15] Yoon, Y. B., Seo, B., Koh, B. B., & Cho, S. (2019). Performance analysis of a double-skin façade system installed at different floor levels of high-rise apartment building. Journal of Building Engineering, 26, 100900.

[16] Peng, J., Lu, L., & Yang, H. (2013). An experimental study of the thermal performance of a novel photovoltaic double-skin façade in Hong Kong. Solar Energy, 97, 293-304.

[17] Shakouri, M., Ghadamian, H., & Noorpoor, A. (2020). Quasi-dynamic energy performance analysis of building integrated photovoltaic thermal double skin façade for middle eastern climate case. Applied Thermal Engineering, 179, 115724.

[18] Ng, P. K., Mithraratne, N., & Kua, H. W. (2013). Energy analysis of semi-transparent BIPV in Singapore buildings. Energy and buildings, 66, 274-281.

[19] Wang, M., Peng, J., Li, N., Yang, H., Wang, C., Li, X., & Lu, T. (2017). Comparison of energy performance between PV double skin façades and PV insulating glass units. Applied Energy, 194, 148-160.

[20] Loonen, R. C., Trčka, M., Cóstola, D., & Hensen, J. L. (2013). Climate adaptive building shells: State-of-the-art and future challenges. Renewable and sustainable energy reviews, 25, 483-493.

[21] Baetens, R., Jelle, B. P., & Gustavsen, A. (2010). Properties, requirements and possibilities of smart windows for dynamic daylight and solar energy control in buildings: A state-of-the-art review. Solar energy materials and solar cells, 94(2), 87-105.

[22] Perino, M., & Serra, V. (2015). Switching from static to adaptable and dynamic building envelopes: A paradigm shift for the energy efficiency in buildings. Journal of Façade Design and Engineering, 3(2), 143-163.

[23] Favoino, F., & Overend, M. (2015). A simulation framework for the evaluation of next generation Responsive Building Envelope technologies. Energy Procedia, 78, 2602-2607.

[24] Bui, D. K., Nguyen, T. N., Ghazlan, A., Ngo, N. T., & Ngo, T. D. (2020). Enhancing building energy efficiency by adaptive façade: A computational optimization approach. Applied Energy, 265, 114797.

[25] Kirkegaard, P. H., & Foged, I. W. (2011, March). Development and evaluation of a responsive building envelope. In Adaptive Architecture-An International Conference at the Building Centre.
[26] Favoino, F., Goia, F., Perino, M., & Serra, V. (2014). Experimental assessment of the energy performance of an advanced responsive multifunctional façade module. Energy and buildings, 68, 647-659.
[27] Matheou, M., Couvelas, A., & Phocas, M. C. (2020). Transformable building envelope design in architectural education. Procedia Manufacturing, 44, 116-123.
[28] Gallo, P., & Romano, R. (2017). Adaptive façades, developed with innovative nanomaterials, for a sustainable architecture in the Mediterranean area. Procedia engineering, 180, 1274-1283.
[29] Radwan, G. A., & Osama, N. (2016). Biomimicry, an approach, for energy efficient building skin design. Procedia Environmental Sciences, 34, 178-189.
[30] Barozzi, M., Lienhard, J., Zanelli, A., & Monticelli, C. (2016). The sustainability of adaptive envelopes: developments of kinetic architecture. Procedia Engineering, 155(275-284).
[31] Shahin, H. S. M. (2019). Adaptive building envelopes of multistory buildings as an example of high-performance building skins. Alexandria Engineering Journal, 58(1), 345-352.
[32] Park, J., Jung, H. J., Lee, S. W., & Park, J. (2015). A new building-integrated wind turbine system utilizing the building. Energies, 8(10), 11846-11870.
[33] News of EU Commission of 5 April 2019, Energy (2019). New rules for greener and smarter buildings will increase quality of life for all Europeans, Brussels 2019, Available online at: https://ec.europa.eu/info/news/new-rules-greener-and-smarter-buildings-will-increase-quality-life-all-europeans-2019-apr-15_en (Last accessed on 16/12/2020)
[34] Cascone, Y., Capozzoli, A., & Perino, M. (2018). Optimisation analysis of PCM-enhanced opaque building envelope components for the energy retrofitting of office buildings in Mediterranean climates. Applied energy, 211, 929-953.
[35] Basso, P., Mililli, M., Herrero, F. J., Sanz, R., & Casaldiga, P. (2017). E2VENT–design and integration of an adaptable module for residential building renovation. Journal of Façade Design and Engineering, 5(2), 7-23.
[36] Diallo, T. M., Zhao, X., Dugue, A., Bonnamy, P., Miguel, F. J., Martinez, A., ... & Brown, N. (2017). Numerical investigation of the energy performance of an Opaque Ventilated Façade system employing a smart modular heat

recovery unit and a latent heat thermal energy system. Applied energy, 205, 130-152.
[37] Dugué, A., Raji, S., Bonnamy, P., & Bruneau, D. (2017). E2VENT: an energy efficient ventilated façade retrofitting system. Presentation of the embedded LHTES system. Procedia Environmental Sciences, 38, 121-129.
[38] Elarga, H., Goia, F., Zarrella, A., Dal Monte, A., & Benini, E. (2016). Thermal and electrical performance of an integrated PV-PCM system in double skin façades: A numerical study. Solar Energy, 136, 112-124.
[39] Hu, J., & Yu, X. B. (2020). Adaptive building roof by coupling thermochromic material and phase change material: Energy performance under different climate conditions. Construction and Building Materials, 262, 120481.
[40] Ascione, F., Bianco, N., De Masi, R.F., Mastellone, M., Vanoli, G.P. (2019). Phase change materials for reducing cooling energy demand and improving indoor comfort: A step-by-step retrofit of a Mediterranean educational building. Energies, 2019, 12(19), 3661.
[41] Ascione, F., Bianco, N., De Masi, R.F., de Rossi, F., Vanoli, G.P. (2014). Energy refurbishment of existing buildings through the use of phase change materials: Energy savings and indoor comfort in the cooling season. Applied Energy, 2019, 113, pp. 990-1007.
[42] Ascione, F. (2017). Energy conservation and renewable technologies for buildings to face the impact of the climate change and minimize the use of cooling, Solar Energy, Volume 154, 2017, 34-100.https://doi.org/10.1016/j.solener.2017.01.022.
[43] Do, C. T., & Chan, Y. C. (2020). Evaluation of the effectiveness of a multi-sectional façade with Venetian blinds and roller shades with automated shading control strategies. Solar Energy, 212, 241-257.
[44] Gagliano, A., & Aneli, S. (2020). Analysis of the energy performance of an Opaque Ventilated Façade under winter and summer weather conditions. Solar Energy, 205, 531-544.
[45] Ascione, F., Bianco, N., Iovane, T., Mastellone, M., & Mauro, G. M. (2020). Is it fundamental to model the inter-building effect for reliable building energy simulations? Interaction with shading systems. Building and Environment, 183, 107161.
[46] K. Menberg (2016). Sensitivity analysis methods for building energy models: Comparing computational costs and extractable information
[47] R.M. Leicht (2014). A Sensitivity Analysis of Energy Modeling Input Parameters for Energy Retrofit Projects
[48] D.P.R. (Decree of the President of the Republic) 26 agosto 1993 n. 412. [in Italian]

[49] D.P.R. (Decree of the President of the Republic) 16/04/ 2013 n. 74. [in Italian]
[50] KIM, Dongsu, et al. Comparative investigation on building energy performance of double skin façade (DSF) with interior or exterior slat blinds. Journal of Building Engineering, 2018, 20: 411-423.
[51] Wang, Yanjin, Youming Chen, and Cong Li. "Airflow modeling based on zonal method for natural ventilated double skin façade with Venetian blinds." Energy and Buildings 191 (2019): 211-223.
[52] Ioannidis, Zisis, et al. "Double skin façade integrating semi-transparent photovoltaics: Experimental study on forced convection and heat recovery." Applied Energy 278 (2020): 115647.
[53] Almeida, M., Ferreira, M., & Barbosa, R. (2018). Relevance of embodied energy and carbon emissions on assessing cost effectiveness in building renovation—Contribution from the analysis of case studies in six European countries. Buildings, 8(8), 103.
[54] Bragança, L., & Mateus, R. (2012). Life-cycle analysis of buildings: envirnonmental impact of building elements.
[55] Vilches, A., Garcia-Martinez, A., & Sanchez-Montanes, B. (2017). Life cycle assessment (LCA) of building refurbishment: A literature review. Energy and Buildings, 135, 286-301.
[56] Ingrao, C., Scrucca, F., Tricase, C., & Asdrubali, F. (2016). A comparative Life Cycle Assessment of external wall-compositions for cleaner construction solutions in buildings. Journal of Cleaner Production, 124, 283-298.
[57] Llantoy, N., Chafer, M., & Cabeza, L. F. (2020). A comparative life cycle assessment (LCA) of different insulation materials for buildings in the continental Mediterranean climate. Energy and Buildings, 225, 110323.
[58] Ascione, F., Bianco, N., De Masi, R. F., Mastellone, M., Mauro, G. M., & Vanoli, G. P. (2020). The role of the occupant behavior in affecting the feasibility of energy refurbishment of residential buildings: Typical effective retrofits compromised by typical wrong habits. Energy and Buildings, 223, 110217.
[59] Streicher, W., Heimrath, R., Hengsberger, H., Mach, T., Waldner, R., Flammant, G., ... & Blomquist, C. (2006, November). State of the Art of Double Skin Facades in Europe: The results of WP1 of the BESTFAÇADE Project. In Proceedings of the AIVC 27th Conference, Lyon, France (pp. 20-22).

Conclusions

This Thesis work, entitled " Energy efficiency of the building envelope: modeling, simulation, and performance of passive-active technologies for double skin and responsive components", presents the research work carried out in the three years of PhD activity.

The concerns of energy poverty, climate change, and sustainable development are interconnected and urgent in our society, necessitating a concrete effort to address their grave and irreversibility effects. Nowadays, it is recognized that the construction sector, including building industry and building operations, is a key area of intervention, responsible for an important amount of World energy consumption and greenhouse gas emissions. A large part of the existing building stock, worldwide, is inefficient and inadequate from the thermal and energy point of view, as well as concerning the current needs of thermal, hygrometric, visual, and acoustic comfort, healthiness, and accessibility. Thus, a large-scale deep retrofit and re-development of buildings is a must. Chapter 1 describes the evolution of environmental legislation, highlighting the role of the construction sector and the related legislation in the field of energy efficiency. From this, two main conclusions are achieved:

- new buildings must be almost zero energy, therefore highly efficient;
- existing buildings must necessarily be energy efficient.

The research activity developed in the last three years is focused on the built environment by proposing and analyzing different strategies for improving energy performance.

To this end, a description of the modeling and simulation methods is initially provided in Chapter 2, while in Chapter 3 they are applied to buildings with different intended uses. The modeling phase requires an accurate knowledge of data relating to the thermophysical characteristics of the building, information on the systems installed, the use profile of the building itself (occupation, lights, equipment), information on the urban context, on climatic conditions. All this makes this phase extremely complex and to simplify the process some factors are often overlooked, or tools based on stationary/semi-stationary analysis are used, reducing the accuracy of the results. The modeling phase and the subsequent simulation phase are therefore characterized by two aspects: complexity for the data collection and the realization of the model and reliability of the results obtained from the dynamic simulation. The search for the best compromise between these two functions is investigated in Chapter 3 by analyzing the inter-building effect and developing a user-friendly tool for modeling and simulation. In both analysis the aim of simplifying the modeling phase without compromising the accuracy of the results.

The influence of the urban context, i.e., the interbuilding effect (IBE), is investigated with the purpose to determine if its modeling is necessary to achieve accurate energy simulations. In addition, the influence of shading devices is investigated. The findings demonstrate that the interbuilding effect (IBE) modeling is not essential when:

- the building is partially surrounded by other structures;
- the building is equipped with externally positioned shading systems characterized by low solar transmittance values and medium/high values for solar reflectance;
- the solar setpoint value that causes the activation of shading is not very high.

Under these conditions, using a simplified model, calculation times are reduced by up to 50%, with errors in the estimation of the building's energy needs of about 1.5%. The use of models that require less computational effort can be an advantage in the energy optimization phases, allowing to

investigate a greater number of scenarios without excessive computational effort.
A tool, called EMAR, is then developed for the modeling and simulation of residential buildings, which although based on complex and accurate software such as EnergyPlus and Matlab®, requires only 63 inputs. The inputs relate to the geometry of the building, the characteristics of the envelope and systems, and any PV systems. It has been validated against an ASHRAE test building and two European buildings, providing discrepancies for the building's energy needs of less than 10%, often 5%. The simplicity of the modeling and the consequent reduction of the computational load, makes EMAR an ideal tool for professionals in the sector, allowing to obtain accurate results. In addition, EMAR can provide outputs at dwellings' level, thereby enabling deep investigations of energy demands, thermal comfort and heating/cooling loads for different stakeholders. Future research will focus on the development of open-source graphical user interfaces (free of MATLAB®) and the incorporation of EMAR into the building energy optimization process, large-scale analysis of the stock of buildings to meet public energy policy, building information modeling (BIM), design of HVAC system, etc.

Chapter 4 is entirely dedicated to the proposal and the analysis of passive and active technologies for the energy renovation of the existing building stock. The focus is on the building envelope and in particular, the performance of the double skin façade (DSF) technology, its eventual dynamism, and the integration of renewable energy sources are proposed and investigated. This technology, in addition to benefits on the energy performance of the building, provides the building with a new aesthetic aspect and an increase in structural safety and therefore is suitable for the recovery of existing buildings. After a review and a discussion of the most recent research, in order to identify the greatest potential but also the limits, this technology was proposed for the energy renovation of buildings located in the Mediterranean area.

The study is developed in several phases, and has led to the following results:

1. Application of a DSF (passive, i.e., completely closed) for two office buildings with different sun exposure. In both cases, a reduction in energy consumption for heating is obtained, albeit different in absolute terms, due to the exposure of the double-skin façade and the urban context in which the investigated building is located. The energy advantage in the winter season is obtained thanks to a heat storage area between the inner and outer layers of the DSF. If this area is not completely exposed to the sun (i.e., southern exposure) or is partially shaded by the surrounding environment, the benefits are reduced. In the summer period, on the other hand, there is an increase in energy consumption. In this season, the exposure of the DSF not completely to the South, and the shading effect represent positive factors, limiting the increase in energy consumption. Both effects, reduction and increase in winter and summer energy consumption respectively, are due to the solar heat gain, which in winter represents a positive factor that allows a reduction of heat losses, while in summer it represents an additional load for the cooling system. The increase in energy consumption for cooling is obviously an undesirable and negative effect. To counteract it and at the same time to increase the energy advantage obtained in the winter season, the double skin facade is made dynamic through the modeling of a network of air flows.
2. Modelling of airflow through a control logic for the opening of the windows (active facade). The control is achieved through the temperature variable. That is, if the temperature inside the cavity

exceeds both the external temperature and a set point temperature, the windows open allowing air to circulate between the cavity and the external environment in the summer regime, and between the cavity and the internal environment in the winter regime. This innovative approach combines the potential of the DSF system with the concept of dynamism. The interaction of the air in the cavity with the external environment determines a reduction of the cooling energy consumption compared to the increase obtained with the passive configuration. In addition, the interaction of the air in the cavity with the internal environment allowed a further reduction of heating energy consumption.

3. Integration of transparent PV modules, in different percentages, in the external layer of the DSF. To the benefits provided by the DSF, passive or active, is added that of the production of energy from renewable sources. Furthermore, the presence of PV modules reduces the risk of summer overheating in the cavity by reducing the difference between the passive and active configurations.

The application of these technologies as a retrofit intervention appears to be an aspect worthy of investigation, both from the analysis of the proposed revision and from the benefits obtained in the case studies analyzed. The results suggest that these technologies, today not widespread in the construction market, will be a future opportunity to investigate, also in combination with structural reinforcement (by means of new materials or structure, for instance, external exoskeletons), and thus their capabilities in upgrading the global performance of buildings have to be deeply explored. At the same time attention must be paid to increasing efficiency and materials' optimal selection to reduce energy demands, without underestimating the issue of polluting emissions related to the entire life cycle of a building (from the realization of the materials to its demolition). This aspect was investigated at the end of Chapter 4, and the results obtained showed that with the reduction of the energy consumption (CO_2 emissions) of the buildings obtained through energy efficiency solutions of the building envelope, there is a greater incidence of the energy (CO_2 emissions) incorporated in the materials. Therefore, the choice of materials must be made carefully. Implementing eco-sustainable solutions is one of the most important challenges for the future.

Final remarks and future developments

To date, there is a progressive, albeit slow, increase in the installation of double skin facade technology. The main limits of its greater diffusion consist in the higher costs of construction, maintenance, in the intrinsic characteristics of the technology in terms of occupation of a space for its realization. As for the costs, these fall in a range between 560 and 1000 €/m² [59] depending on the chosen configuration, the possible presence of shading systems without considering the possible integration of photovoltaic systems for energy production. The need to occupy a new space and the complexity of the realization, in addition to the high costs, make it preferable to use more classic retrofit measures.

On the other hand, however, considering the structural, as well as energy, criticalities of the buildings of the existing building stock, in anticipation of a spread of external exoskeletons as a structural reinforcement system, the double skin facade technology lends itself to being combined with such exoskeletons through their covering with a glazed system. In this way, the benefits obtainable through this application would be multiple: energetic, structural, aesthetic, protective against external agents, without neglecting that the surface of the facade is suitable for hosting photovoltaic technology. Therefore, in addition to the passive use of solar radiation, the DSF technology can provide for an active use of the same thanks to semi-transparent photovoltaic technology. To date, the latter has a very low efficiency, but scientific research gives hope that there will be huge developments and improvements in the future. The enhancement and innovation of a highly-efficient transparent photovoltaic system is a great challenge, capable in opening this kind of new technology to the solar market, also for achieving new chances of installation in buildings, and this is suitable to significantly offset the consumption of fossil fuels worldwide.

Furthermore, there is the possibility of making the DSF technology dynamic, through the management of air flows in the cavity - as investigated in the context of this thesis - or even through the implementation of electrochromic glasses, and therefore to make resilient design.

The potential benefits of the investigated technologies are huge, even if different barriers and limits need to be overcome. A wider spread of these technologies globally would trigger a reduction in prices over time, as happened with other technologies, making these more accessible and convenient. A crucial aspect worthy of investigation is the application of these technologies as a retrofit intervention, and thus it is necessary to conduct studies to obtain results in this direction.

Due to the relatively low turnover rate of the buildings, we must address the issue of upgrading the current inefficient stock's energy and environmental performance. The solutions presented in this Thesis can represent a concrete possibility in overcoming this challenge, allowing to regenerate the building stock making it technological, innovative, and ecological. The reduction of heating consumption and the conversion goes in the direction of the energy transition towards electric, and therefore contributes to the creation of renewable energy communities in which each sector (primarily construction and transport) is seen as nodes of the same energy network, in which each subject is both consumer and prosumer.

Index of figures

Chapter 1

Chapter 2.

Chapter 3

Chapter 4

Index of Tables

Chapter 3

Chapter 4